FINAL SCIENTIFIC/TECHNICAL REPORT FOR "NANITE" FOR BETTER WELL-BORE INTEGRITY AND ZONAL ISOLATION CONTRACT NO: DE-FE0014144

Submission Date: May 30, 2017
Project Period: October 1, 2013 – February 28, 2017

SUBMITTED TO:
U.S. Department of Energy
National Energy Technology Laboratory
Pittsburgh, PA 15236-0940
Attn: Dr. William Fincham, NETL Project Manager

PREPARED BY:
OCEANIT
Oceanit Building
828 Fort Street Mall, Suite 600
Honolulu, HI 96813
DUNS #: 14454082

Principle Investigator: Vinod P. Veedu, Oceanit
Phone: 808-531-3017 x170
Fax Number: 808-531-3177
E-Mail: vinod@oceanit.com

Submitting Official: Derek Ah Yo, Oceanit Program Manager
Phone: 808-531-3017 x110
Fax Number: 808-531-3177
E-Mail: dahyo@oceanit.com

Signature: dahyo@oceanit.com Digitally signed by dahyo@oceanit.com DN: cn=dahyo@oceanit.com Date: 2017.05.30 17:36:13 -10'00'

oceanit®

DISCLAIMER

ABSTRACT

Nanite™ is a cementitious material that contains a proprietary formulation of functionalized nanomaterial additive to transform conventional cement into a smart material responsive to pressure (or stress), temperature, and any intrinsic changes in composition. This project has identified optimal sensing modalities of smart well cement and demonstrated how real-time sensing of Nanite™ can improve long-term wellbore integrity and zonal isolation in shale gas and applicable oil and gas operations. Oceanit has explored Nanite's electrical sensing properties in depth and has advanced the technology from laboratory proof-of-concept to sub-scale testing in preparation for field trials.

TABLE OF CONTENTS

EXECUTIVE SUMMARY

PROJECT OBJECTIVES

Demonstrate the capability of real-time, smart sensing of Nanite for improving the long-term wellbore integrity and zonal isolation in unconventional resource development.

BENEFITS OF NANITE FOR WELL INTEGRITY

- Improve well integrity:
  - Isolation of hydrocarbon zones behind casing
  - Isolation of hydrocarbon zones in abandoned open holes
  - Protection of fresh water zones
- Evaluation and validation of wellbore barriers:
  - Improve evaluations of cement barriers
  - Increase options for cement barrier detection
- Possible secondary benefits:
  - Ability to identify and measure stress on casing, cement shrinkage and life of well
  - Reliable inspection of multiple casing strings for the life of the well
  - Ability to monitor and differentiate the infiltration of gas, mud and various fluids into the cement

MAJOR OUTCOMES

- Optimized admixture formulation for enhanced electrical response to mechanical loading.
- Designed, fabricated, and tested custom low-power, low-cost, and compact electrical resistivity tools for Nanite with high sample rates, multiple calibration modes, and direct connection to a single board computer.
- Demonstrated Nanite electrical response to temperature, curing, damage, contamination, and mechanical load.
- Nanite cement formulation was evaluated, in accordance with API recommended practices, by a certified third party lab service and the impact of Nanite admixture on cement properties was found to be minimal and within limits for field use.
- Translated Nanite technology from the laboratory cube form factors to downhole relevant form factors, such as concentric steel pipes.
- Demonstrated scale up of Nanite sensing capabilities using a 4 ½ inch diameter 30-inch long cemented pipe section pressurized up to 1400 psi.

NEXT STEPS

In collaboration with industry partners, Oceanit has identified future steps for the development and commercialization of Nanite for oil and gas cementing applications. Nanite has promising applications including top-of-cement/wait-on-cement verification, long term abandoned plug monitoring, and though multiple casing cement assurance. Outside of the oil and gas domain, Nanite has promising applications for infrastructure and traffic monitoring.

TABLE OF FIGURES

TABLE OF TABLES

PROJECT MANAGEMENT AND PLANNING

Risks to the project were minimized using detailed schedules, metrics and assignment of specific responsibilities. Weekly meetings were held by the Project team to assess progress, potential problems and to develop appropriate actions. Oceanit submitted a draft version of the project's Project Management Plan (PMP) to NETL on 13 November 2013 and a revised version on 27 November 2013.

Oceanit held the Project Kickoff Meeting on 23 January 2014 with the NETL program manager and staff reviewing project objectives, status and management procedures. Oceanit continued to provide periodic briefings at NETL as the project progressed, including yearly detailed project status briefings to explain project plans, progress, and results of the current technical effort as well to provide briefings at key project decision points and/or budget period transitions.

Finally, Oceanit held periodic technical interchange meetings with HESS and Shell to discuss technical status and develop strategies to successfully complete project milestones and with Saudi Aramco and ConocoPhillips Corp to establish them as additional JIP partners.

To accommodate the recommendations from the JIP partners to maximize the commercial outcome of the project and expedite field deployment, Oceanit requested to reorder some of the project tasks in Budget Period I and II. This request was submitted on 19 November 2014 to our Project Manager, William Fincham of the DoE NETL, along with revisions to the Statement of Project Objectives (SOPO) and the Project Management Plan, which reflected how the proposed reordered tasks prioritize the project objectives and how were to be managed.

Oceanit submitted the Budget Period 1 to Budget Period 2 Continuation Application to DoE NETL on 9 February 2015 and then presented the findings of Budget Period 1 to DoE NETL during the BPI to BPII Continuation Application Meeting on 3 March 2015. Oceanit received Modification No. 0003 to Award No. DE-FE0014144 authorizing Budget Period 2 to commence through period of performance 1 April 2015 – 30 September 2016. DoE obligated the remaining DoE award funds totaling $1,132,074.00 and Non-DoE Cost Share funds totaling $300,000.00.

The project was granted a three month no-cost extension by DOE executed on 19 September 2016. The new end date for the project was 31 December 2016. Oceanit used the project extension to further coordinate with oil industry partners on design and optimization of the Nanite system for subscale proof testing more relevant to current exploration, extraction and abandonment operations. The project had sufficient budget to fund the additional three months of effort.

The project was granted a two month no-cost extension by DOE NETL executed on 19 January 2017. The new end date for the project was 28 February 2017. The extended period of performance was used to complete currently underway testing of Nanite's electrical response to radial pressures exerted on subscale concentric wellbore casing strings cemented with Nanite and to prepare for the potential next field test and evaluation phase of the project by further coordinating with oil industry partners and developing a statement of work relevant to current exploration, extraction, and abandonment operations. The project had sufficient budget to fund the additional two months of effort.

EXPERIMENTAL METHODS

Overview of the Problem

Cementing is a crucial step in drilling safely for oil or natural gas; however, it is prone to frequent failures such as the one that led to the Deepwater Horizon disaster in the Gulf of Mexico, Figure 1. The accident involved a well-integrity failure, followed by a loss of hydrostatic control of the well. This was followed by a failure to control the flow from the well with the blowout preventer (BOP) equipment, which allowed the release and subsequent ignition of hydrocarbons. Ultimately, the BOP emergency functions failed to seal the well after the initial explosions. Three things could have contained those pressures: the cement at the bottom of the well, the mud in the well and in the riser, and the blowout preventer [1]. But mistakes and failures to appreciate risk compromised each of those potential barriers, steadily depriving the rig crew of safeguards until the blowout was inevitable and, at the very end, uncontrollable.

Figure 1: Deepwater Horizon explosion site. It was April 22—Earth Day (Oil Spill Commission, 2011).

US Minerals Management Service survey, reported 6,650 out of 14,927 active wells had sustained annular pressure in deep-water and shelf Gulf of Mexico [2]. Figure 2 shows how the percentage of wells that have developed cementing failures rises with the age of the well. In this figure, SCP means "sustained casing pressure". This is measured at the wellhead and is often called the Bradenhead pressure. These data, published in 2003, are from the 22,000 underwater wells in the Gulf of Mexico (GOM), but the failures have nothing to do with the fact that these are underwater wells. After 10 years about 40% of wells have cement failure. After 30 years about 60% of wells have cement failure.

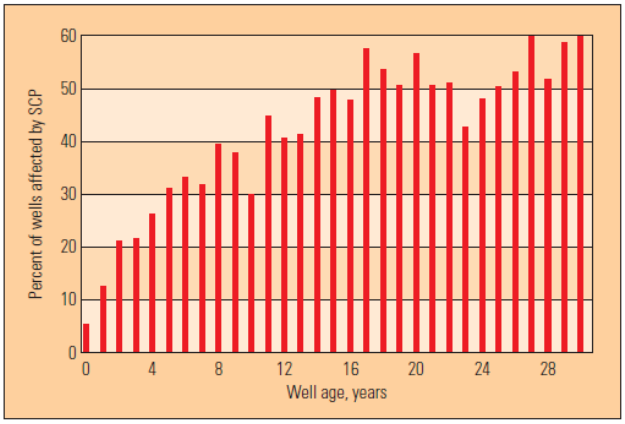

^ Wells with SCP by age. Statistics from the United States Mineral Management Service (MMS) show the percentage of wells with SCP for wells in the outer continental shelf (OCS) area of the Gulf of Mexico, grouped by age of the wells. These data do not include wells in state waters or land locations.

Figure 2: Data on frequency of occurrence of sustained casing pressure (SCP) in offshore wells. (Brufatto et al. 2003).

Well-integrity and performance failures occur due to different reasons. Data in Figure 3 shows relative distribution of failures affecting well performance encountered by survey participants **[3]**.

Cementing an oil well is an inherently uncertain process. Cement is generally required to extend to 150ft below the deepest water well in the area to protect aquifers from the fluids in the wellbore. Thus, the fracturing process is not supposed to begin until the wellbore is properly cased and cemented to ensure protection of fresh water aquifers. However, contractors often rush the casing and cementing to move on to the next job and what may appear to be a good cement job or casing connection at first ends up being degraded by the pressure exerted during the fracking process and in the end the casing fails at the connecting joints or the cement cracks. The cracked cement or failed casing then allows wellbore fluids (including fracking fluids and natural gas) to contaminate aquifers or the surface.

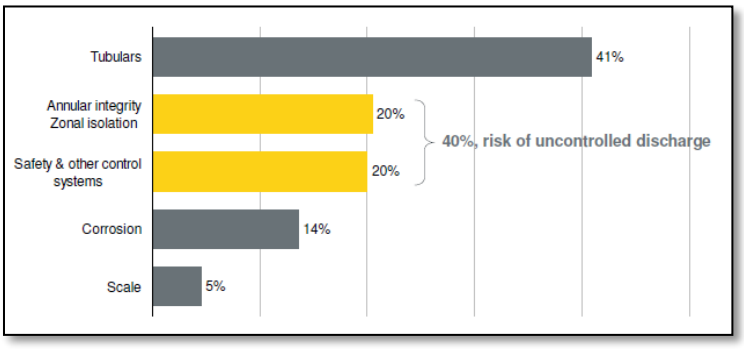

Figure 3: Failures affecting well integrity & performance.

Zonal Isolation: Cement barrier provides zonal isolation between geologic strata and structural support of the wellbore and casing. Figure 4 summarizes some of the primary cementing challenges. The cement prevents gas or fluids from moving between the pipe and the exposed rock. A poorly cemented well can create a path for contaminants to migrate upward and leech into shallow porous rocks that hold drinking water. Deepwater wells pose special challenges: severe pressures and temperatures, as well as the need for specialized equipment and lots of cement. Cement is inexpensive and abundant throughout the world but its mechanical and chemical properties are challenged to consistently ensure strength and durability for the typical 30+ year lifetime of a well.

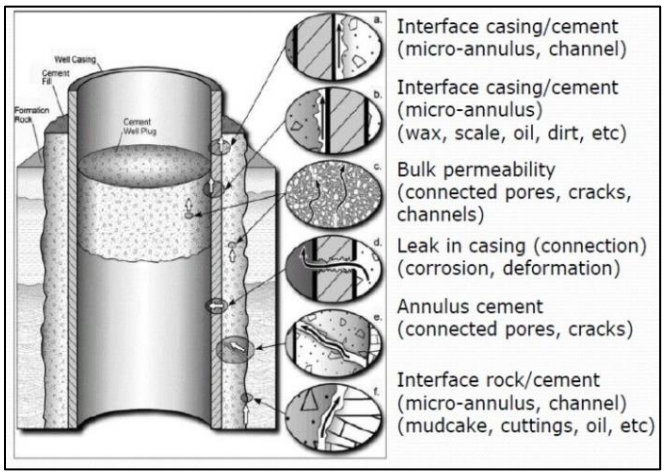

Figure 4: Typical zonal isolation problems.

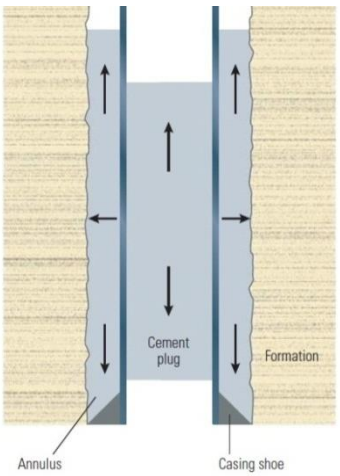

Figure 5: Basic Plug – P&A.

Plug & Abandonment (P&A): Another important operation where cement plays a major role is plug and abandonment (P&A) of unproductive wells that are sealed to permanently remove the potential environmental threats, Figure 5. Cement plugs are setup to prevent cross flow and production, isolate all flow and protect from pressures. The responsibility does not usually end with P&A activities, if leaks develop in the plugs the responsible party is mandated to repair and remediate the well and site. The only solution is to make sure that P&A operations are done right the first time. However, many cement plugs fail for the following reasons:

1. Cross flow cuts channels into the plug.
2. Cement is higher density than mud –cement falls through the mud. Mud contamination of the cement may keep it from setting.
3. The open-ended tubing produces a high momentum energy condition that the mud cannot stop – thus cement falls through the mud.

In summary, for oil and gas cementing, key challenges are:

- ***Conventional techniques (acoustic & ultrasonic) used to inspect the integrity of cementing behind multiple casing strings are inaccurate, insufficient and non-reliable.***
- ***Continuous monitoring of the integrity of cement plugs through their life-time using conventional approaches is not pragmatic.***

Hence, there is imminent need for new cement evaluation technologies and approaches to improve the effectiveness of existing technologies to assess the cement integrity.

Initially Intended Experimental Approach

Oceanit's advanced cementitious materials technology (Nanite™) has the potential and promise to address some of the key challenges in assuring, monitoring, mitigating methane emissions, long-term wellbore integrity and zonal isolation. The specific challenge areas that Oceanit's Nanite™ technology addresses are listed below:

- Cement formulation, additives and associated properties – for improving zonal isolation
- Monitoring, Sensors and Nanotechnology – for wellbore integrity

Oceanit proposes Nanite™ – a nanotechnology based smart concrete, as a candidate material to address some of the key challenges faced by Oil and Gas (O&G) cementing. Core to the development of Nanite™ is Oceanit's ability to modify the molecular level interfaces in cement by delivering functional nanomaterials at these interfaces, uniformly throughout the bulk matrix. This is achieved via an admixture based on nanomaterials which when added to the traditional cementitious material, transforms it into a highly durable, smart and multifunctional cement.

The technical basis for Nanite™ multifunctional properties is attributed to the physical and chemical nature of nanomaterial additive. The electrical, radiometric and piezometric functions of

Nanite™ can provide unique sensing capabilities. Nanite™ takes advantage of the conductive network formed by the nanomaterials for reversible sensing of load via electrical resistivity measurements. Essentially Nanite™ acts as an intrinsic structural sensor. Nanite™ can transform traditional cement used for wellbore zonal isolation into multifunctional material. Over the last 5 years, Oceanit has utilized Nanite's electrical properties for detection and classification of loads (e.g., human beings and vehicles). The sensitivity and accuracy of detection is adequate for outdoor and indoor security systems, where low profile, or integrated sensor technology is required.

Nanite™ based sensing cement technology can be customized to achieve the following key benefits to the cementing applications to the Oil and Gas industry:

- ***Reliable and long term inspection behind multiple casing strings for the life of the well. The conventional techniques (Acoustic & ultrasonic) to inspect the integrity of cementing behind multiple casing strings are inaccurate, insufficient and non-reliable.***
- ***On demand logging of the internal quality and performance of the cement through its life time***
- ***A tool to identify and measure the stress on casing, cement shrinkage and development of micro annulus throughout the life of the cementing***
- ***A tool to monitor the infiltration of various fluids, gas, mud, well bore fluids, micro fluids in to the cement and functional differentiation of infiltrates.***
- ***Secondary confirmation tool that could help manage well integrity during well operational phase.***
- ***A low cost long term monitoring tool for plug and abandonment (P&A) of unproductive wells that are sealed to permanently remove the potential environmental threats.***

Nanite™ Mechanical Properties

Nanite can potentially address the mechanical properties of cement, tensile strength, elasticity and ductility. The following are the attributes of Nanite™ compared to the traditional cementitious material.

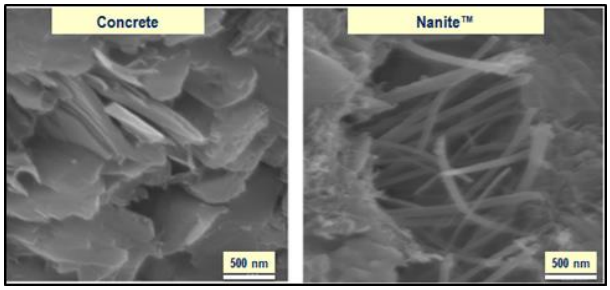

Figure 6: Scanning electron micrograph (SEM) showing failure mechanism and the crack bridging by nanomaterials based 'rebars' in Nanite™.

- Nanite™ material has demonstrated a 30-50% increase in compression strength (ASTM C39) and 40% increase in flexural strength (ASTM C78) compared to carbon fiber reinforced concrete.
- High strength and high aspect ratio of the nanomaterials at the interface provide improved compression strength and flexural strength.
- Nanomaterial acts as micro-rebar providing high tensile strength and elasticity to concrete. In addition, improve the fracture toughness of Nanite™ by bridging the crack at a micron scale (Figure 6).
- Chemical compatibility of nanomaterials with cement results in improved durability due to enhanced bonding with cement.

Nanite™ Cement Integrity Monitoring

Electrical, radiometric and piezometric properties provide different sensing capabilities to Nanite™. Nanite™ is responsive to pressure, internal changes, defects, foreign inclusions and self-sensing. Oceanit has utilized the electrical properties of Nanite™ to analyze the cement curing/hydration process (Figure 7). A relationship between interfacial response and compressive strength of Nanite™ was obtained and it was confirmed that rapid curing will reduce the risk of gas migration. The setting time of Nanite™ was monitored by capturing the physical/chemical changes at the interface. The interrogating mechanism could be acoustic, radio frequencies (RF) or electrical measurement.

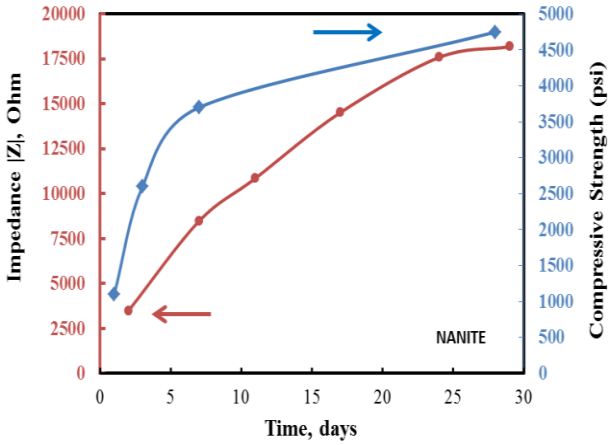

Figure 7: Impedance and compressive strength of Nanite™ as a function of curing time.

Figure 8 shows the concrete embedded between two concentric steel pipes replicating the cementing scenario used in oil and gas drilling. The impedance of concrete was measured using the concentric steel tubes as electrodes. The stable impedance signal (no noise) demonstrates that the steel pipes can be reliably used as electrodes impedance extraction and analysis. The impedance measurements can be used to estimate the following:

- Bonding between cement and steel casing
- Structural integrity of the cement
- Foreign species ingress into the cement

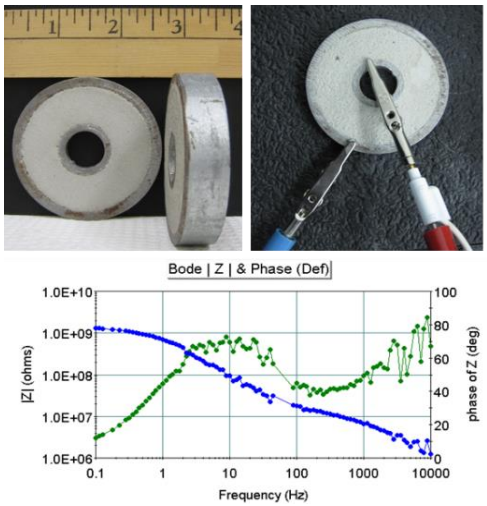

Figure 8: Impedance measurement of cement embedded between concentric steel pipes.

The above-mentioned sensing capabilities of Nanite™ will help provide *in-situ* monitoring of cement properties such as curing, strength development and sensing down hole for cement integrity (both short and long term).

Some of the specific advantages of Nanite™ cement for oil wells are:

- Currently, acoustic cement bond logging (CBL) device is used to analyze the cement-casing bond integrity. It involves evaluating the effect of the casing, the cement sheath, and the formation on the acoustic wave emanating from the acoustic cement bond. Cement evaluation relies on a contrast in the acoustic properties of the cement and liquid. The higher the contrast between liquid and hardened cement, the easier the log is to interpret. The acoustic properties of set lightweight cement are close to those of cement slurry, making it difficult to distinguish the two.
- Nanite's electrical impedance varies with the physical and chemical factors hence can be used as a signature for sensing. The impedance of Nanite can be correlated to (i) bonding between

cement and steel casing, (ii) structural integrity of the cement and (iii) foreign species ingress into the cement. Nanite can be used to supplement the conventional technologies for accurate and reliable inspection behind the casing.

- The continuous monitoring of integrity of cement used in cementing and P&A operations through its life-time using conventional technologies is not practical. However, Nanite can be used to continuously monitor the casing and cement plugs without the need of sophisticated technologies.

Nanite™ Thermal Conductivity:

Nanite™ has improved thermal properties due to high thermal conductivity of nanomaterials thoroughly dispersed in the matrix. This will lead to rapid temperature equilibration in cement resulting in uniform curing. More than 40% increase in thermal conductivity (ASTM E1530) compared to traditional cement was observed in Nanite™.

- Nanite™ with improved thermal conductivity will aid in cement curing time and relax thermal stresses in cement matrix.
- Nanite™ cement can dissipate the heat of hydration during cement setting process, preventing crack and micro-annulus development due to the build-up of tensile and compressive stresses from inhomogeneous heat distribution in the center of slurry column vs. the slurry adjacent to the casing and formation. Nanite™ could aid to reduce the thermal stress and strain in the cement casing due to hot fluids in the wellbore.
- Cement curing is a critical stage in wellbore cementing process. The setting and hardening of cement is predictable, uniform and relatively rapid. However, reducing the wait on cement (WOC) time which usually ranges from few hours to several days will have a significant impact on drilling operations. Nanite™ will reduce the cement curing time due to improved thermal conductivity of cement matrix which results in uniform setting throughout the matrix.
- Microwave radiation curing is often used for fast turnaround times in concrete structures. Microwaves have the potential to deeply penetrate a material, which enables heating from within the material; thereby concrete can be cured in less than six hours without the use of chemical accelerants. Nanomaterials interact with microwave radiation to further improve the curing process.

Nanite™ Stress Sensing:

Nanite™ has improved electrical properties due to high electrical conductivity of nanomaterials thoroughly dispersed in the matrix. Oceanit has already demonstrated the basic sensing capabilities of Nanite™. The Nanite™ specimen showed detectable, repeatable and consistent change in its electrical resistance with vehicular or pedestrian presence. To show the detection capabilities of the NANITE samples, electrical response was monitored over many cycles. The change in electrical resistance ($\Delta R/R_0$) of the samples with and without Oceanit's nano additive

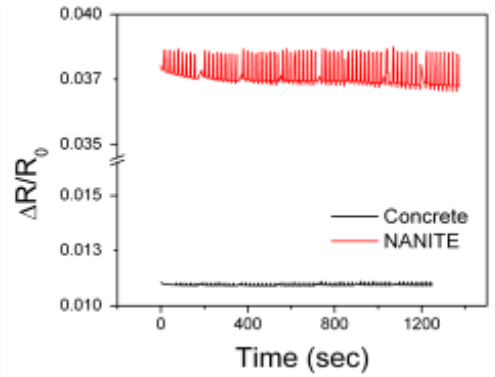

Figure 9: Variation of resistance vs. cyclic applied stimulation for Nanite™.

as a function of time under cyclic presentation of stimulus is illustrated in Figure 9. The change in resistance is significantly greater for Nanite™ compared to base concrete. The increase in the magnitude of the resistance change is important in that it provides proof that accumulated damage due to stress cycling can indeed be monitored via an electrical measurement, an added benefit of Nanite™.

Nanite™ has a network of electrically conducting nanomaterials. The electrical conductivity of Nanite™ is significantly higher than base concrete. Higher conductivity is attributed to the formation of continuous and dense network of nanomaterials in the concrete matrix and provides sensing capability. The electrical behavior of Nanite™ is reversible under dynamic cyclic loading, showing their capability to sense the external environment. The sensing data also revealed that Nanite™ is reliable over many compression cycles, like commercially available strain gauges.

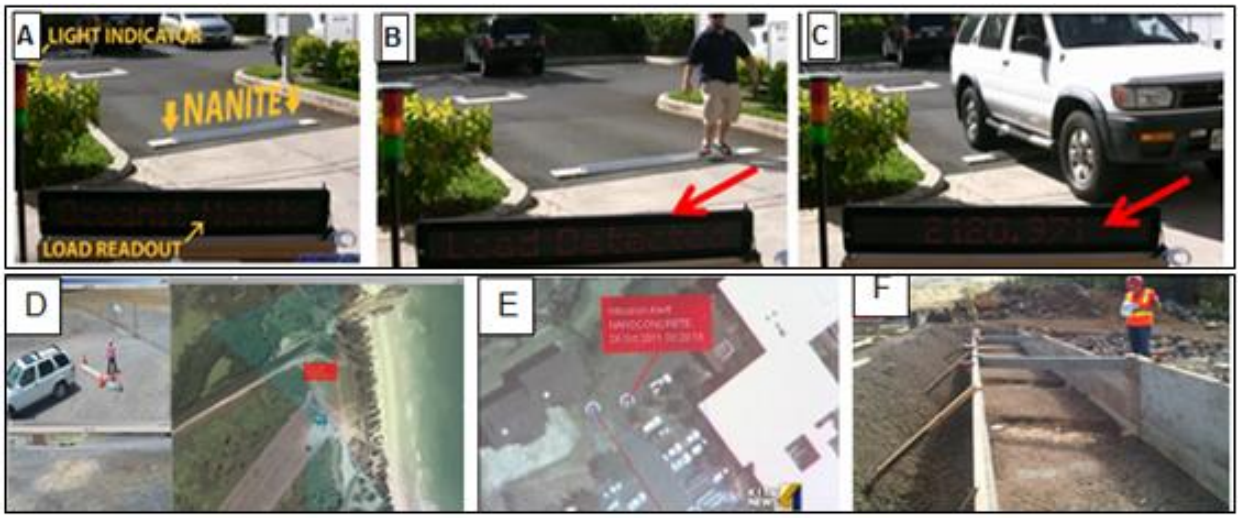

Figure 10: Screen Capture: (A) Set up of Nanite™ concrete for location, presence and weight demonstration outside the lab, (B) Presence detected (indicated by the red arrow) as a person steps on the Nanite™ speed bump, (C) Load detected as a vehicle goes over the Nanite™ speed bump (D) Fenceless perimeter demonstration using Nanite™ at the Marine Corps Training Area Bellows, (E) Nanite™ security application demonstration with multiple sensors and (F) Nanite™ concrete in the process of installation at a newly constructed bridge in Maui.

Oceanit Nanite™ shows significant promise as a self-sensing concrete for cementing application. Nanite's sensing capabilities have already been field demonstrated in different scenarios such as fenceless perimeter for the Department of Defense, self-monitoring bridge for the Dept. of Transportation etc (see Figure 10).

RESULTS AND DISCUSSIONS

This project was initiated in 2013 and progress has been documented in detail in the quarterly technical reports provided by Oceanit. The program has progressed over several Budget Periods with several no cost extensions (NCE) granted so that work on specific areas could be completed. As is often the case with projects of this magnitude; avenues of research and development were

initiated, pursued where successful and redirected when less so. As a result, this report, endeavoring to provide a full summary of project progress, is presented in a chronological format in order to preserve the logical progression of the research.

Quarter 1: Period End Date December 31, 2013

Oceanit's intention was to optimize Nanite cement slurries to ensure suitability for shale gas and oil & gas cementing applications. To this effect it was considered essential to evaluate and customize these slurries and then further evaluate the properties of set/cured Nanite cement.

Evaluate Properties of Nanite-Based Slurries

Cement sourcing

As recommended by API-10B2, class G and class H cement was used for this research. Cement samples were procured from Lafarge North America.

Determination of slurry density

A standard document "Recommended Practice for Testing Well Cements - API Recommended Practice 10B-2" was used as a guide to evaluate the physical and mechanical properties of cement slurries developed in the current study.

The preferred apparatus for measuring the density of a cement slurry is the pressurized fluid density balance. Density of sample slurries were measured per API 10B (Figure 11). The densities data is shown in Table 3.

Figure 11: Mud balance density meter and different steps involved in the measurement.

Table 1: Densities of sample slurries.

Sample Slurry (W/C ratio 2.68)	**Density (lb/gal)**
Portland cement	16.15±0.1

Class H cement	16.70±0.2
Nanite-Class H cement	16.25±0.2

Quarter 2: Period End Date March 31, 2014

Nanomaterials Quality Control

During this period Oceanit continued testing the quality of multi-wall carbon nanotubes (MWCNTs) from different suppliers and establishing testing protocols. The process involves characterizing the materials, including validation of the manufacturers' product specifications.

Acid dispersion test

50 mg of MWCNT sample was dispersed in 25 ml of 50% nitric acid solution. The dispersion was mixed for 2 hours on a shaker plate and allowed to settle for 5 days. Sustained suspension of the dispersion indicates the absence of amorphous carbon and residual catalyst impurities. Because the samples are not acid functionalized, their dispersion in acid solution is poor. Moreover, the settled sediments show that MWCNTs are aggregated and not well dispersed in the solution.

UV-Vis spectrometer analysis

UV-Vis spectrometer analysis of the samples was performed to determine residual catalyst content. From the preliminary baseline measurements, the spectral peak was identified as that of Fe^{+2} or Fe^{+3} using potassium ferrocyanide ($K_4[Fe(CN)_6]$) and potassium ferricyanide ($K_3[Fe(CN)_6]$). The analysis procedure for MWCNT samples dispersed in nitric acid (HNO_3) solution was:

1. MWCNT samples direct from manufacturer were dispersed at 0.1 mg/mL in 50% nitric acid solution
2. Sample dispersions were sonicated for 30 minutes and allowed to settle for 24 hours
3. Supernatant of the settled dispersion was diluted 10-fold in 50% nitric acid solution
4. 1 mL of sample was transferred to microfuge tubes and spun at 14,500 rpm for 5 minutes
5. The supernatant was diluted 5- and 25-fold in doubly deionized (DI) water
6. A standard curve of $K_3[Fe(CN)_6]$ was prepared for 1000, 500, 250, 125, 62.5, 31.25, and 15.625 ppm in DI water
7. 200 µL of standard and diluted sample were dispensed into duplicate wells
8. Absorbance at 305 nm was measured

Thermogravimetric analysis (TGA)

TGA was performed to estimate the impurity content of the samples. Samples were heated from room temperature to 800 °C at 10 °C/min in air. A typical weight loss profile is shown in Figure 12 and impurity residue after the experiment is shown in Figure 13.

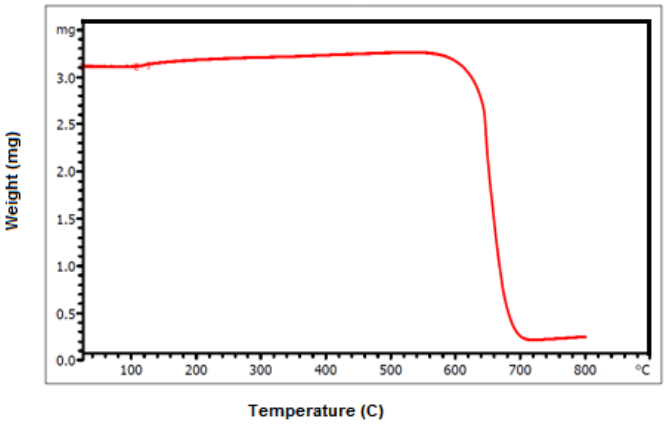

Figure 12: Residual impurity content determined using Thermogravimetric Analysis (TGA).

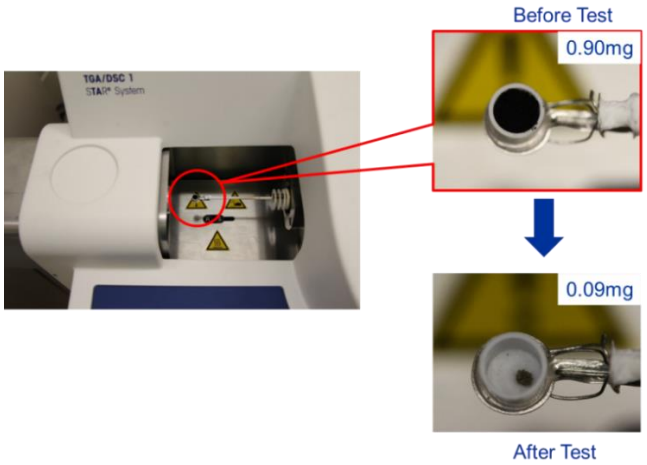

Figure 13: TGA experiment showing the impurity content after the test.

The residual catalyst content calculated from the UV-Vis and impurity content calculated from TGA mass loss are shown in Table I. High impurity content indicates that post-cleaning may be necessary to remove impurities and functionalization may improve dispersion. Samples have reasonably high purity and are suitable for Nanite application

Electrical impedance spectroscopy assessment of cement properties

Electrical impedance spectroscopic (EIS) techniques apply an alternating voltage (current) stimulus to a sample and measure the amplitude and phase response of the current (voltage). The frequency dependent impedance of the sample is obtained by sweeping the stimulus frequency[1]. Exploration of the AC impedance of a microcrystalline solid sample demonstrates three different regimes of electrical charge exchange interactions:

- within microcrystalline grains
- grain boundary interactions

[1] Evgenij Barsoukov, J. Ross Macdonald, Impedance Spectroscopy: Theory, Experiment, and Applications, 2nd Edition, March 2005, John Wiley & Sons, Inc.

- electrode surface boundary interactions (e.g. corrosion)

The electrical behavior may be modeled with a suitable equivalent circuit combination of R (resistive) and C (capacitive) components as shown in Figure 14

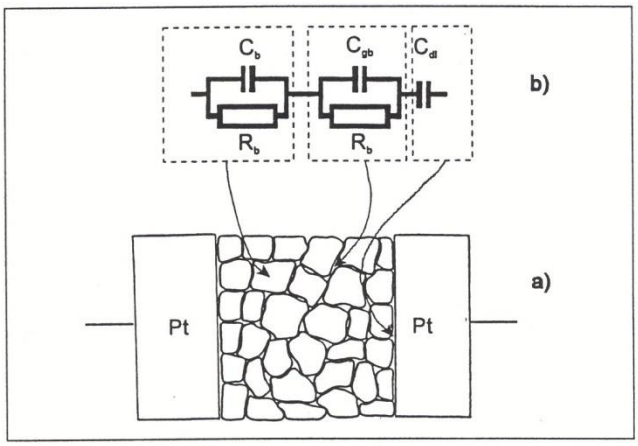

Figure 14: Equivalent circuit model for interpretation of cement microstructure using EIS.

Electrical impedance spectroscopy (EIS) has previously been used to study the microstructure of cement paste. It has been shown that the impedance spectra of cement pastes depend strongly on the amount of porosity in the microstructure, and perhaps more importantly, on the arrangement and connectivity of the pores. By studying the impedance spectra at different times during the curing reaction, upon mechanical loading, or after damage, information about the arrangement and interconnectivity of micro- and nanostructures can be obtained.

According to the equivalent circuit analysis (Figure 15), the low frequency arc (related with R_2 and C_2) represents the electrode–cement interface phenomenon and the high frequency arc (related with R_1 and C_1) is associated with bulk effects. Many impedance studies have reported an offset resistance (R_0) in cement hydration. However, the explanation of the offset resistance is still unclear.

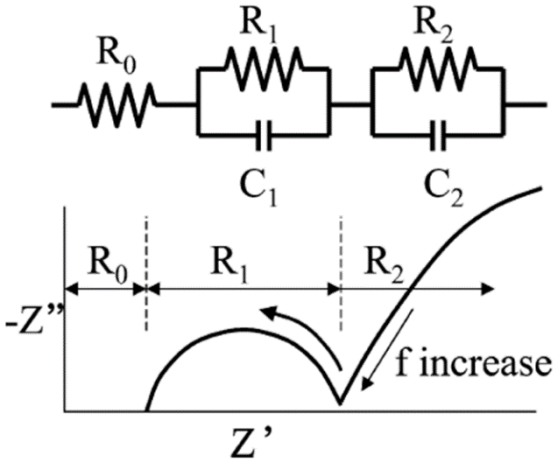

Figure 15: Equivalent circuit model for cement.

EIS measurements were performed on 2 inch cube test samples cast with two embedded mesh

electrodes (1.25 cm × 1.25 cm stainless steel gauze with strand width 0.25 cm) (Figure 16). EIS of Nanite and base cement (API Class H) samples was carried out at intervals through the curing period. The samples were cured in a saturated lime solution (non-API standard) and were dried for 30 min before the measurement.

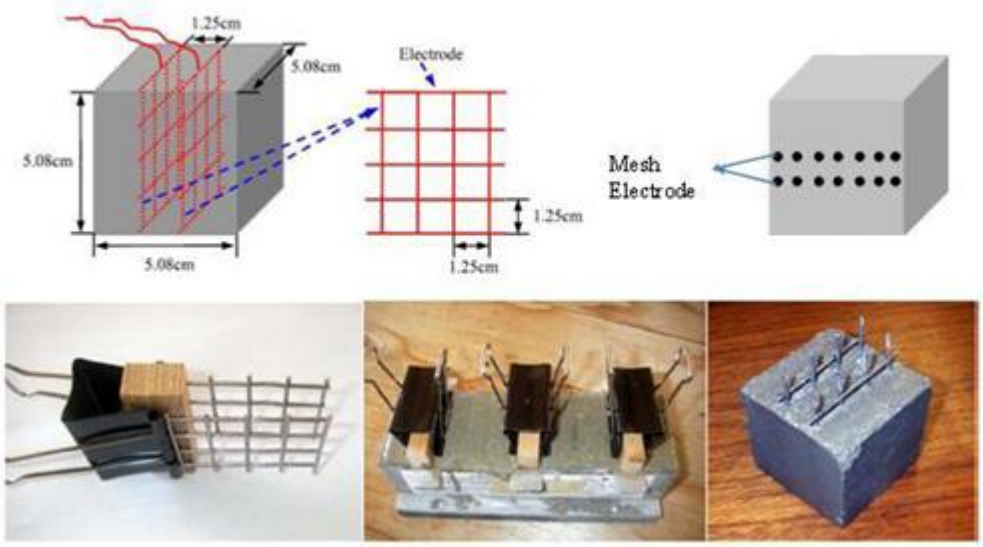

Figure 16: Schematic of cement sample with electrode configuration for electrical resistance measurement (top). Images of the concrete specimens fabricated with mesh electrodes (bottom).

An example Nyquist plot (negative imaginary versus real impedance) for the 36 day old cement samples exhibits characteristic capacitive loops (semicircles), although the left loop (high frequency) is not fully formed in both cases (base and Nanite) due to wiring impedance and the frequency limitation of the Bio-Logic VMP-3 potentiostat. The equivalent circuit model was used to fit the parameters. A better fit was obtained by using constant phase element (CPE) instead of capacitance. Clearly, the bulk resistance of Nanite is lower compared to base cement. Even the low frequency loop shows that the Nanite-electrode interface has lower resistance than the base cement-electrode interface. Additional tests are in progress to fully understand the microstructure of cement using impedance spectroscopy.

Four-wire electrical impedance measurements

Electrical impedance measurements made using two parallel steel mesh electrodes, described earlier, may suffer systematic errors due to variable contact resistance and corrosion potentials present at the electrode-cement interface. The Wenner technique depicted in Figure 17 utilizes an array of four uniformly placed electrodes where the outer pair is used to source current and the inner pair is used to sense the voltage drop in the material due to the bulk and surface resistivity of the material being tested.

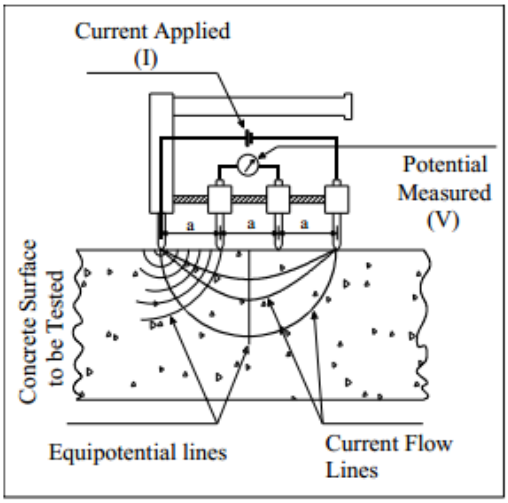

Figure 17: Four-point Wenner Array Probe Test Setup (Kessler et al., 2008).

When the Wenner probe technique is applied to a large concrete slab or soil in the earth where the electrode spacing is small relative to the material dimensions, the bulk resistivity is given by $\rho = \frac{2\pi aV}{I}$ where a is the electrode separation. Rather than making a surface measurement we cast steel wires in an array penetrating through each 2" cubic cement sample. Accounting for the additional degree of symmetry in an array of parallel wires through the sample, the resistivity is given by $\rho = \frac{\pi tV}{-(\ln 2)I}$, where t is the thickness of the sample penetrated by the electrodes. Note that although this expression is now independent of the electrode spacing, edge effects must be taken into consideration unless a << t. In all practical electrode configurations, the edge effects will be significant, thus requiring a geometric correction factor to determine the absolute resistivity. In the scope of this work, however, the uncorrected resistivity (or more simply V/I) serves as the required precision metric for comparison of the electric-mechanical characteristics of the various cement formulations under study. Compared with a traditional Wenner contact measurement, our technique has the advantage of current transmission through a larger volume of material, thus averaging over inhomogeneity that may be present (e.g. inclusions, liquid or air filled pores, etc.)

Initial samples were fabricated with a 4x4 grid array of electrodes. A variety of configurations including different electrode diameter and spacing were tried to identify an optimal geometry. This 16-electrode configuration allows different subsets of 4 electrodes (e.g. columns, rows, diagonals) to independently test different regions of the sample. Differences in impedance as a function of distance from the sample edge may be useful in studying curing behavior and electrical edge effects. Anisotropy of the impedance when the material is loaded under a particular axis can also be studied. The quasi-planar electrode effect of the original wire mesh electrodes can also be approximated by wiring the 16 electrodes in planes of four without acting as reinforcement in the sample and changing its mechanical properties substantially.

Electrode grid sample preparation

Disposable plastic 2" cube molds were prepared by drilling a 4x4 array of 0.035" holes 0.375" apart opposing sides with a reusable aluminum template. The holes were then de-burred and

covered externally with transparent vinyl tape. The tape serves to hold the electrodes in place and to keep water from leaking out from the unset cement slurry. 3" lengths of 0.033" diameter 304 stainless steel wire were cut and inserted through the holes in the molds, as shown in Figure 11.

Cement sample preparation

A sample preparation procedure was adapted from API Recommended Practice 10B, "Recommended Practice for Testing Well Cements", in order to establish a consistent mixing, casting, and curing protocol. For cement preparation, Class H cement from LaFarge (Joppa Plant, Grand Chain, Illinois) was added to water while mixing at 4,000 RPM over a time period of 15 and 30 seconds in a Fann Constant Speed Mixer Model 686CS (Halliburton). For each batch, water and cement are apportioned for a water-to-cement ratio and both dry materials and mixing fluid were at room temperature. After the dry cement was wetted into a slurry, the blender was covered and mixing was continued at 12,000 RPM for 35 seconds. The slurry was immediately poured into previously prepared molds. The molds either contained inserted electrodes, 4x4 array as shown in Figure 18, in which case the slurry was scraped to level the top of the mold, or electrodes were inserted into the slurry after scraping the top of the mold, 4-wire array as shown in Figure 19. The samples were then placed into air-tight containers cured for 24 hours at 60 ^{o}C. Beyond 24 hours, the samples were kept wet in the humid air-tight containers at room temperature until they were removed for testing.

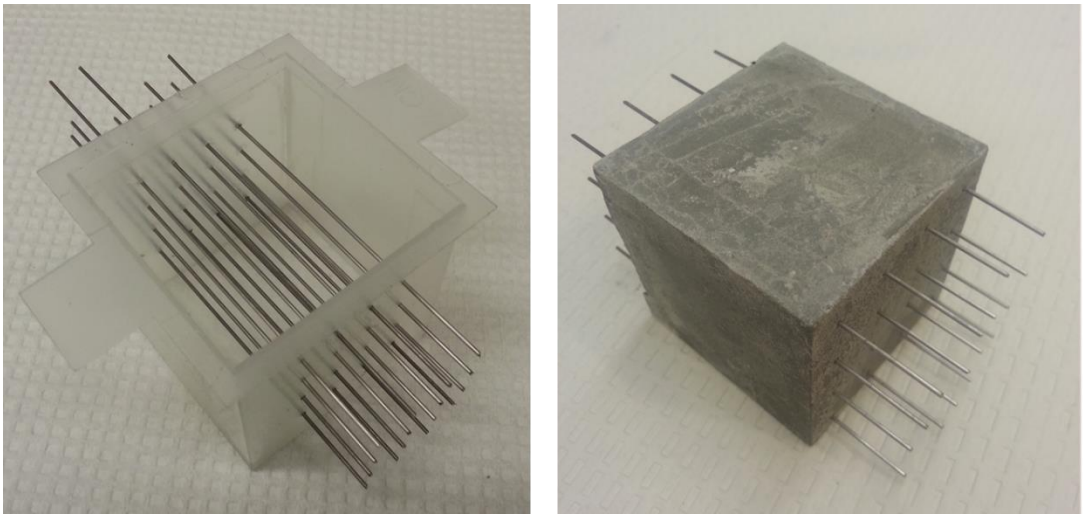

Figure 18: 4x4 array electrode configuration mold preparation (left) and cast and cured cement cube with embedded electrodes (right).

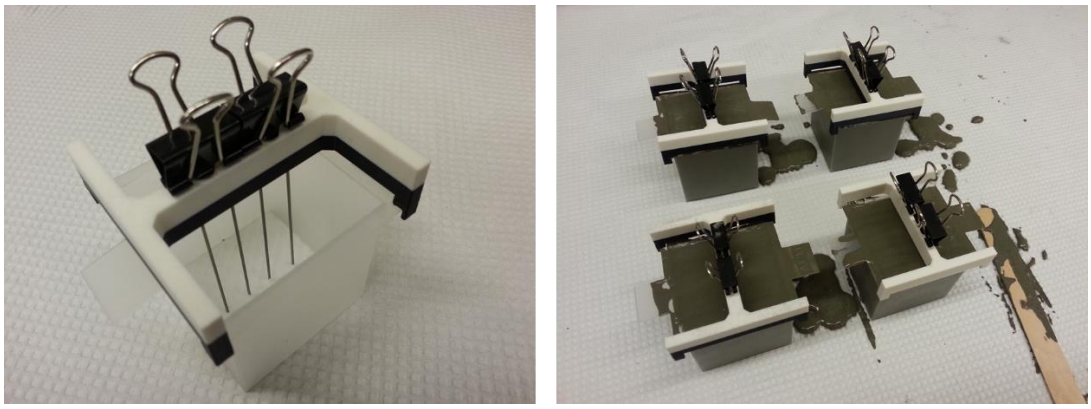

Figure 19: Four electrode configuration mold preparation (left) and sample casting (right).

For Nanite cement samples, nanomaterials were dispersed in water using a proprietary process before mixing with cement powder.

Quasi-DC impedance measurements

The DC impedance of the cement samples was measured using a Keithley 2400 Sourcemeter and Fluke 45 multimeter. Both instruments are controlled from a PC via RS232 and custom control software. The control software instructs the 2400 to act as a current source with a low frequency square wave with increasing amplitude on each cycle. The square wave period is approximately 3 seconds (167 mHz) and the inner sense electrode voltage is measured by the 2400 at the end of each cycle while the source electrode potential is measured with the Fluke 45, Figure 20. The application of a constant current the source electrodes results in previously described charging behavior with significant hysteresis such that the DC voltage offset on both the source and sense electrode pairs in unpredictable. By measuring the peak-to-peak voltage for alternating current polarity the resistive voltage drop of the material can be inferred.

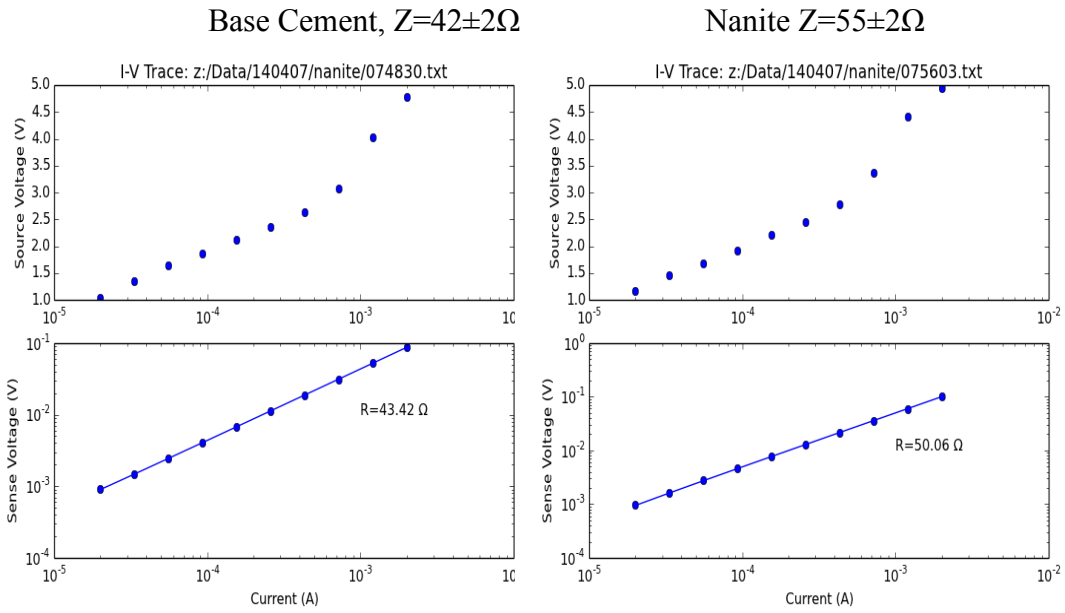

Figure 20: Quasi-DC electrical impedance testing using 167 mHz square wave excitation.

We observe that while the source voltage compliance is nonlinear and roughly logarithmic with current, the sense voltage is linear over two decades of current. I-V characteristics were measured for both CNT Nanite and base cement samples using all available electrode configurations. The resulting effective cement resistance was consistent with batches to within 2Ω. Note that the effective DC resistance computed from the source voltage was highly variable and drifts widely over time while the 4-wire results were quite consistent.

We have determined from these tests that the 4-wire measurements are an effective means of suppressing the electrode charging behavior that affected previous tests, however, due to steady electrochemical potential drifts in the material, AC measurements are a practical option for future analysis. Since the Keithley 2400 is limited to low speed analyses, other instrumentation must be used for thorough AC analysis.

AC impedance spectroscopy

Both a Bio-logic VMP3 potentiostat and a PARSTAT 2273 were used to perform galvano electrical impedance spectroscopy (GEIS) on MWCNT Nanite test cubes. In the galvano mode of operation the excitation current amplitude is held constant as opposed to the voltage for potential electrical impedance spectroscopy (PEIS). The galvano mode is more appropriate for analysis at high frequencies since the PEIS current can become excessive when the impedance becomes very small.

Care must be taken in the analysis of AC impedance spectra. Calibration data was taken using the PARSTAT and all 4 channels of the VMP3 for a 4-wire measurement of a precision test circuit (Bio-logic Test Box 1) consisting of a two stage Randall's cell shown in Figure 6. Comparison of the data from both sources in Figure 21 shows agreement of results in the low frequency regime (rightmost arc on Nyquist plot), however, above 1 kHz the PARSTAT and VMP3 diverge from each other and the theoretical Randall's cell. Furthermore, the high frequency arcs for each of the four VMP3 channels are quite different from one another. In order to understand data collected

from these instruments in the high frequency regime an appropriate equivalent circuit model must be developed to isolate this source of systematic error.

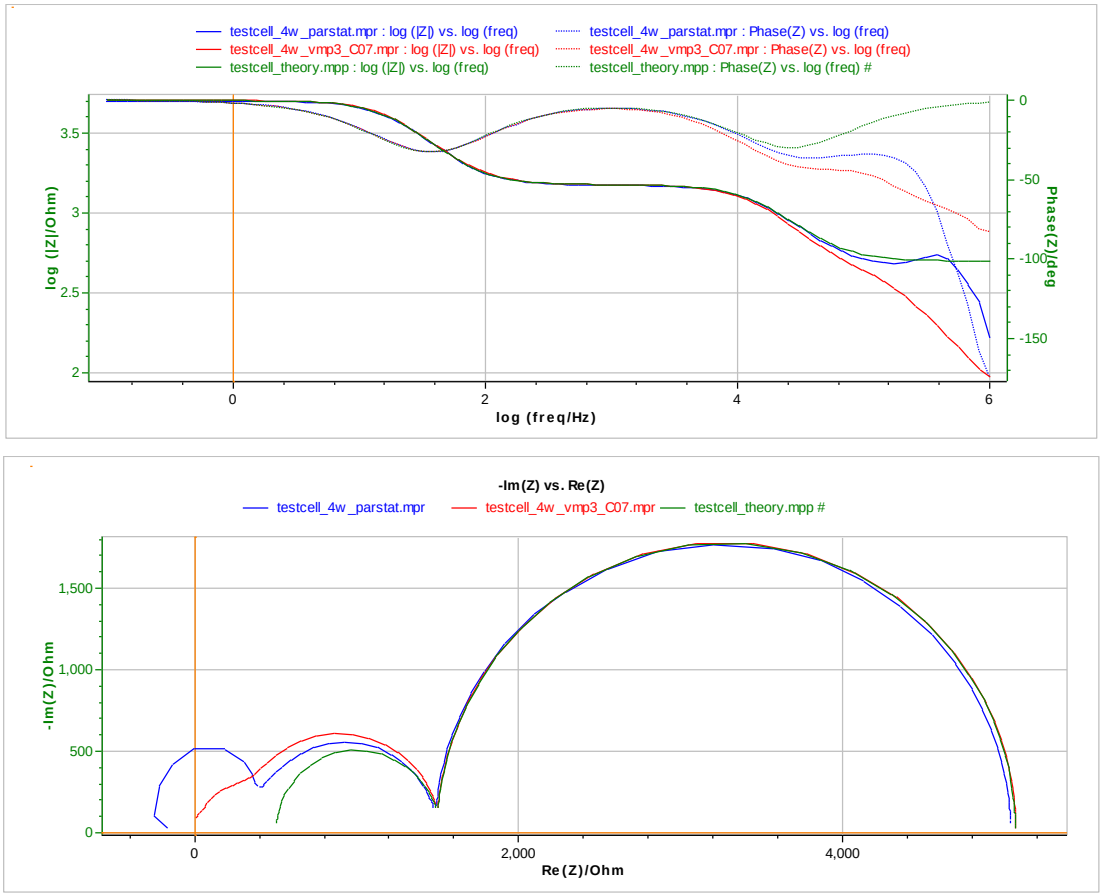

Figure 21: Potentiostat calibration curves using test circuit.

The prevalence of systematic errors in the true cement impedance spectrum limits the usefulness of both low and high frequencies. The intermediate frequency range from 100 Hz to 10 kHz seems to hold the most promise for the future study of cement characteristics. The frequency range also contains the cusp between the two dominant arcs in the Nyquist plot. This cusp is representative of the true DC impedance of the bulk cement and can be measured in both the 2-wire and 4-wire configurations.

Compressive mechanical testing

The compressive mechanical properties of base and Nanite cement samples were tested using an Instron 5569 Materials Testing System with a 50 kN load cell. The samples were kept in a sealed humid environment for 21 days after casting. Compressive strain was applied at a rate of 0.1% per second up to 5% strain, as shown in Figure 22. The compressive stress-strain profiles of the samples were very similar, however testing of additional samples after additional curing times will be required to obtain statistically relevant mechanical properties.

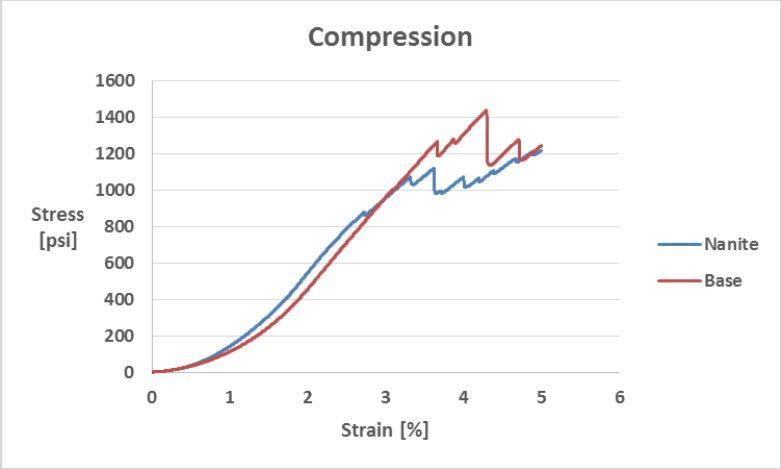

Figure 22: Base cement and MWCNT Nanite cement sample compressive stress-strain behavior.

Quarter 3: Period End Date June 30, 2014

In this quarter, Oceanit further developed experimental testing protocols and prepared material samples for cement characterization. Measurement techniques, including associated electronics hardware and software, were refined to monitor cement curing and mechanical loading

Mechanical Properties

A variety of fixture configurations were tried for mechanical testing of cement cube samples, including steel retainer caps and three compression pads of different hardness. The compression pads conform to the surface of the sample, distributing the applied load evenly, and the retainer caps provide a smooth, level surface while minimizing end artifacts without the need for capping compound. The configuration used consisted of the retainer caps in direct contact with the cement sample with polyethylene pads between the caps and the platens to provide electrical isolation.

Base cement and Nanite 2" cube samples (without electrodes) were tested after 28 days of curing with an Instron 5569 Materials Testing System (MTS) with a 50 kN load cell at 3 mm/min, which translated to approximately 125 psi/sec (Figure 23). The compressive strength (failure load) of both samples exceeded the capacity of the load cell. The elastic modulus of both samples was very similar, even though the Nanite sample clearly had more entrained air bubbles.

Uniaxial compressive stress in the material can be calculated by dividing the applied force by the sample cross-sectional area. Strain is not as straight-forward to calculate as the deformation measured is the sum of that in the cement sample and in the plastic compression pads. Loaded in series, stresses in concrete and plastic of equal cross-sectional area are equal and strains are additive. The strain in the cement can be calculated by subtracting the strain in the plastic measured with only the plastic blocks from the total strain of the system when tested together at a particular stress. Next steps in characterizing the mechanical properties of the cement will be to test the support blocks by themselves for calculating accurate stress-strain plots, elastic moduli, failure stresses, and energy to failure.

$$\sigma = F/A_0$$
$$\sigma = \sigma_c = \sigma_p$$

$$\varepsilon = \Delta L/L_0$$
$$\varepsilon = \varepsilon_c + \varepsilon_p$$

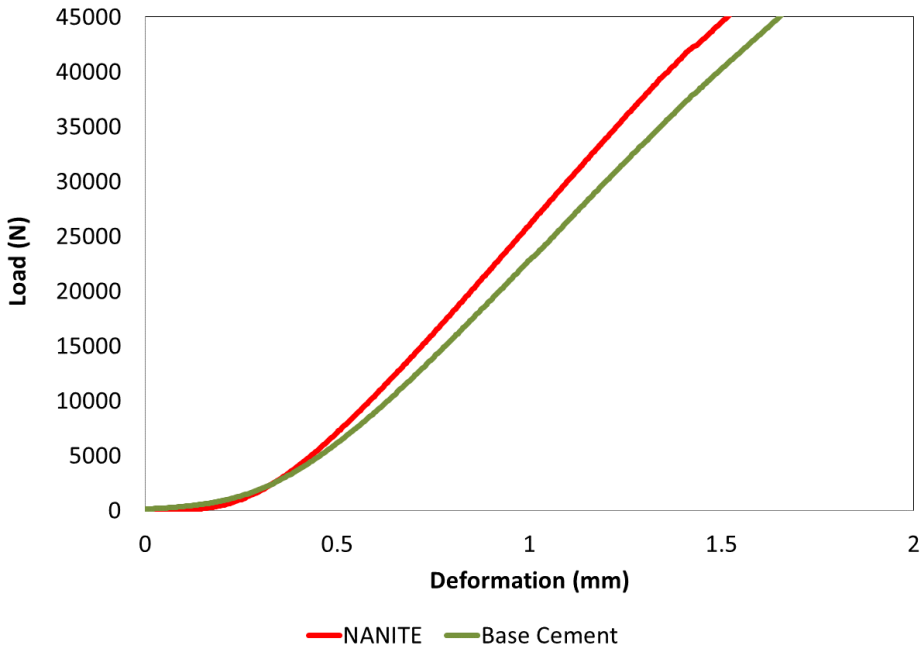

Figure 23: Load-displacement curve for Nanite (red) and base cement (green).

Permeability Test

Permeation property of concrete is one of the most critical parameters in the determination of durability of concrete in aggressive environments. Permeation, dictated by the microstructure of concrete, controls the ingress of moisture, ionic and gaseous species into concrete. Chemical degradation, e.g. sulfate attack, carbonation, and corrosion of steel casing, as a result of reaction between an external agent and the ingredients of concrete, can be greatly reduced by reducing the permeability of concrete. Chloride ion permeability of Nanite samples is studied to understand the effect of nanomaterials admixture on cement permeability and subsequent corrosion protection of steel casing.

The rapid chloride permeability test in accordance with ASTM C 1202[2] and AASHTO T277[3] will be used for the measurement of chloride ion penetration at various cement ages. The rapid chloride permeability apparatus was originally developed by Whiting[4]. The test method involves a cylindrical sample of dimensions 100 mm (4 in.) diameter and 50 mm (2 in.) thickness. The side of the cylindrical specimen is coated with epoxy, and after the epoxy is dried, it is put in a vacuum chamber for 3 hours. The specimen is vacuum saturated for 1 hour and allowed to soak for 18 hours. It is then placed in the test cell (Figure 24). The left-hand side (–) of the test cell is filled with a 3% NaCl solution. The right-hand side (+) of the test cell is filled with 0.3N NaOH solution. The system is then connected and a 60-volt potential is applied for 6 hours. Readings are taken

[2] ASTM C1202, "Standard Test Method for Electrical Indication of Concrete's Ability to Resist Chloride Ion Penetration"

[3] AASHTO T277, "Standard Method of Test for Rapid Determination of the Chloride Permeability of Concrete"

[4] Whiting D 'Permeability of Concrete,' SP-108, American Concrete Institute, 1988, pp. 195–222.

every 30 minutes. At the end of 6 hours the sample is removed from the cell and the amount of coulombs passed through the specimen is calculated.

Figure 24: Rapid chloride permeability cell (left) and system (right).

The test results are compared to the values in the chart below (AASHTO T277-83 and ASTM C1202 specifications). This test method does not replicate actual conditions that concrete would experience in the field. There is no condition where concrete is exposed to a 60-volt potential. This test method does not measure concrete permeability but measures concrete resistivity. Resistance is calculated from the current passed and applied voltage (60V). It has been shown that there is a fair correlation between concrete resistivity and concrete permeability[3] (Table 2).

Table 2: Chloride Permeability Based on Charge Passed.

Charge Passed (Coulombs)	Chloride Permeability	Typical of
>4,000	High	High W/C ratio (>0.60) conventional PCC
2,000–4,000	Moderate	Moderate W/C ratio (0.40–0.50) conventional PCC
1,000–2,000	Low	Low W/C ratio (<0.40) conventional PCC
100–1,000	Very Low	Latex-modified concrete or internally-sealed concrete
<100	Negligible	Polymer-impregnated concrete, Polymer concrete

Samples were prepared in accordance with ASTM C1202 (Figure 25). Samples are cured in a controlled atmosphere chamber with 100% humidity and room temperature; they will be tested after 28 days of curing.

Figure 25: Samples for chloride ion permeability testing.

Nanite Cement Curing Process Evaluation

A miniature 'USB dongle' electrical impedance analyzer developed for an earlier Oceanit project was employed to monitor the condition of cement test samples. Several of these low cost Nanite analyzer units can be connected to a single laptop for continuous monitoring of sample impedance freeing our high precision potenitiostat instruments for detailed analysis of individual samples.

The USB Nanite analyzer is a single board device powered from the host PC via a USB port or USB hub. An Analog Devices AD5933 single chip electrical impedance analyzer is capable of measuring impedances from 1 kΩ to 1 GΩ over the 1kHz to 100kHz frequency range. The raw data collected is in arbitrary units of admittance and is calibrated to determine the resistance values.

Oceanit's existing stock of Nanite analyzer devices were designed for operation with impedances in excess of 10 kΩ and suffer from excessive noise for lower impedance samples such as 2 inch Nanite test cubes. A prototype circuit was constructed to extend the impedance range to low frequencies with additional buffer amplifiers. The prototype has successfully been demonstrated with impedances as low as 10Ω greatly extending the utility of and precision of the device with Nanite samples. Using experience from the prototype, an upgraded dongle design is being developed. The impedance analyzer output is 400mV peak-peak with a 1V DC offset. Since the DC offset is not compensated at the receiving end in the previous design, there is a 650mV DC bias applied across the sample yielding a charging current of up to 2mA applied to the sample. The new version of the analyzer circuit will have careful compensated bias voltage or try to eliminate the need for a DC bias altogether.

Four analyzer devices were joined with spacer brackets and connected to a laptop through a USB hub. A feed-through for the electrode wires was installed on a sealable plastic box for curing. Data was acquired at 10 kHz intervals from 10 kHz to 70 kHz once per minute. Samples were produced with the four-wire array described in the Second Quarterly Report. The four electrodes used were 0.033” diameter 304 stainless steel wires and were spaced at 0.375”. The outer electrodes were used for the measurement, so the actual two-wire electrode spacing was 1.125”.

The measurements over the first day (Figure 26) and first week (Figure 27) indicated a trend during curing. There was an inflection point at six hours of curing that may be significant. There was also a sharp drop at one day, when the sample was removed from the oven. There also seems to be a daily pattern that may reflect temperature fluctuations. The impedance profile was very similar for the four samples that were monitored simultaneously (Figure 28). After the initial curing in the oven, the resistance appeared to drop slowly over time. Additional sample sets will be monitored

while curing to establish a consistent trend. The results may also be correlated with temperature change and strength development to create a model for Nanite curing. A thermocouple with data logging ability will be installed on the curing box to measure changes in temperature with time.

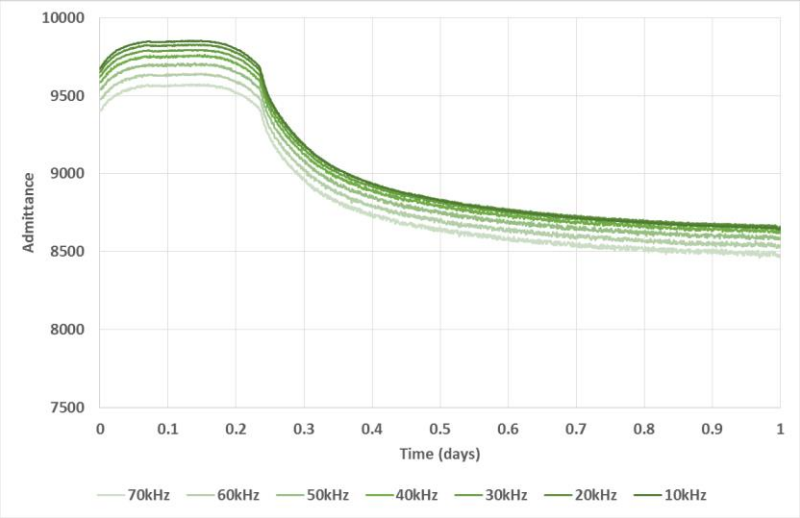

Figure 26: Nanite raw electrical impedance data collected for a range of frequencies over the first day of curing at 60 °C.

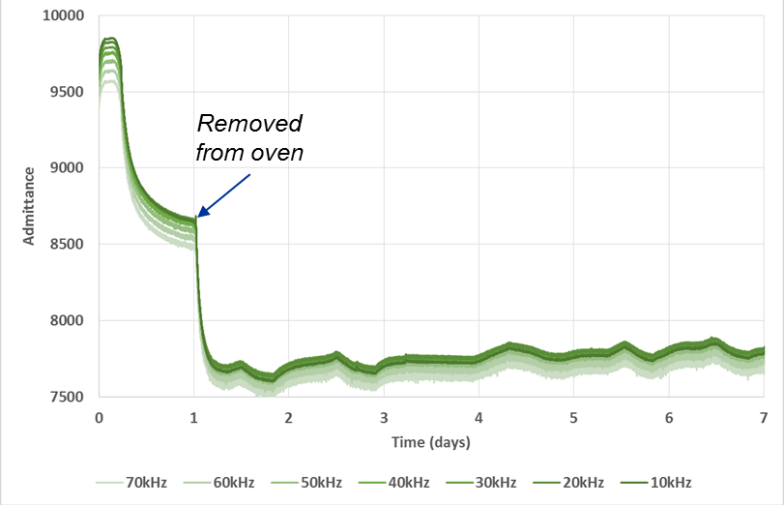

Figure 27: Nanite raw electrical impedance data collected for a range of frequencies over the first week of curing.

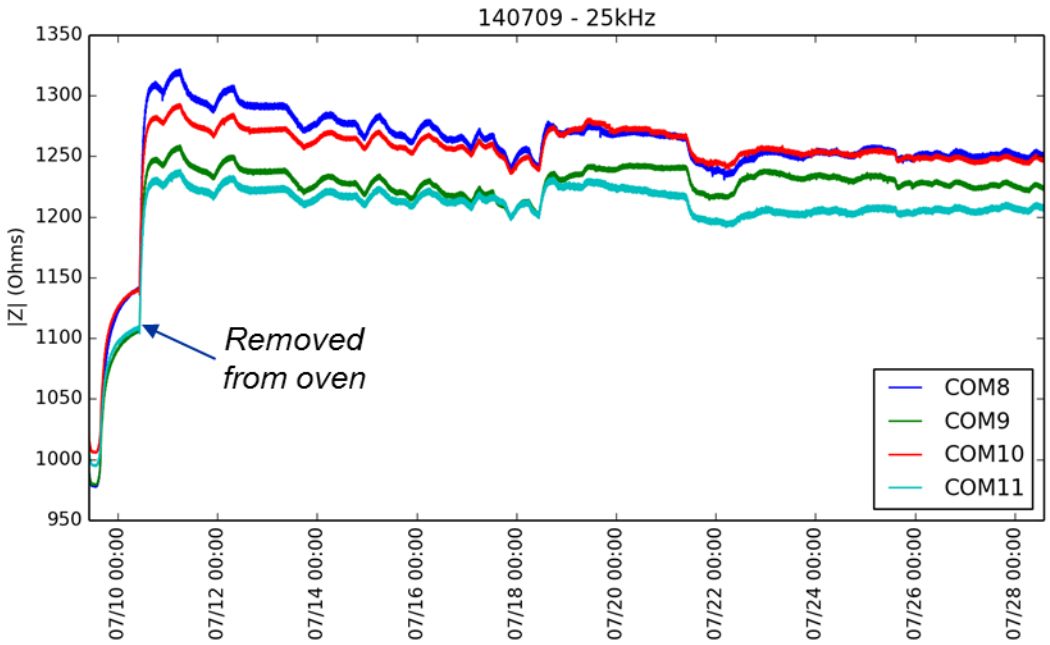

Figure 28: Nanite calibrated electrical impedance data collected at 25 kHz for four samples from the same batch during curing.

Optimization of Nanite for Electrical Resistivity Property

The electrical properties of Nanite can be used for the in-situ monitoring of other cement properties, such as curing, structural damage, and mechanical environment. A resistivity tool will be used for detecting the quality of Nanite sheath around the casing. Recent studies have investigated the basic electrical impedance tool design and data processing. Resistivity measurements thus far have primarily utilized cube samples with embedded wire electrodes. Samples of Nanite sheath between two casing pipes is also being explored as a potential electrode configuration that can be easily translated to field measurements.

The electrode configuration for impedance measurement and the method of measuring the complex impedance spectrum determine the type and quality of data obtained with electrical measurements of Nanite. An Oceanit impedance spectrum analyzer device was used to monitor complex impedance at either one frequency or across a frequency sweep during mechanical loading. A dynamic loading profile was applied to the sample using an Instron MTS as described earlier. The impedance profiles were then compared with the load profiles to determine if the mechanical environment can be accurately detected using Nanite electrical conductivity measurements.

A triangle-shaped loading profile (ramp up followed by immediate ramp down) was applied to base cement and Nanite samples while measuring impedance. The loading and unloading rate was 25 psi/sec. Base cement samples had no response to loading, just noise around a fixed admittance (Figure 29). The Nanite sample, on the other hand, gave a distinct signal that tracked well with the loading profile with little or no hysteresis or drift (Figure 30). A calibration factor for the analyzer device was determined by measuring known resistances. Applying this calibration factor results in the measured impedance versus time (Figure 31).

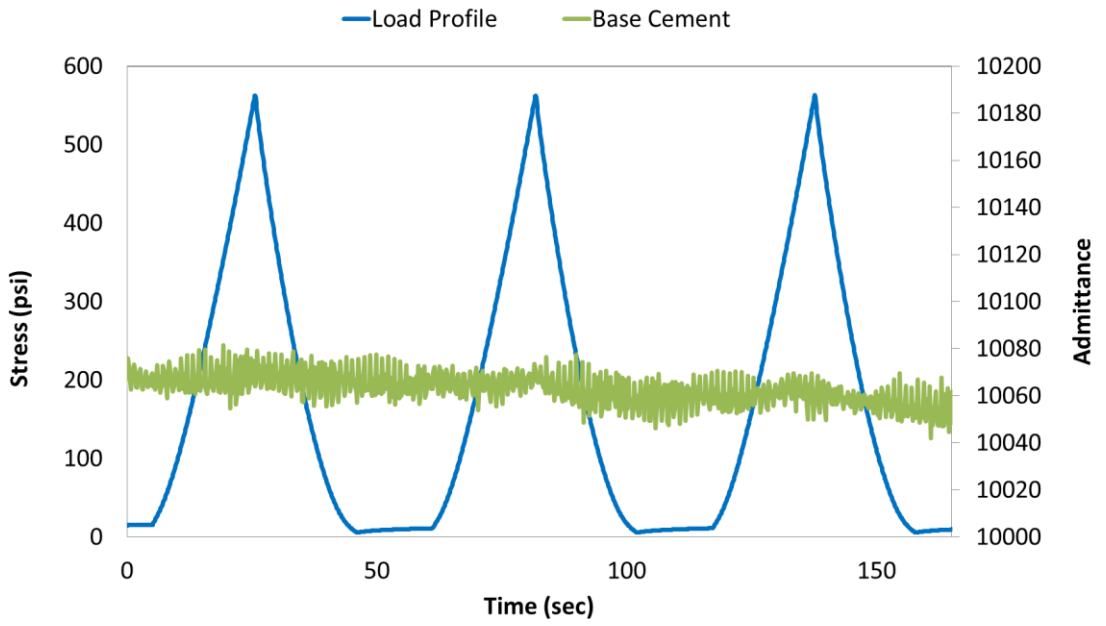

Figure 29: Triangular loading profile (blue) and admittance response for base cement (green) at 28 days.

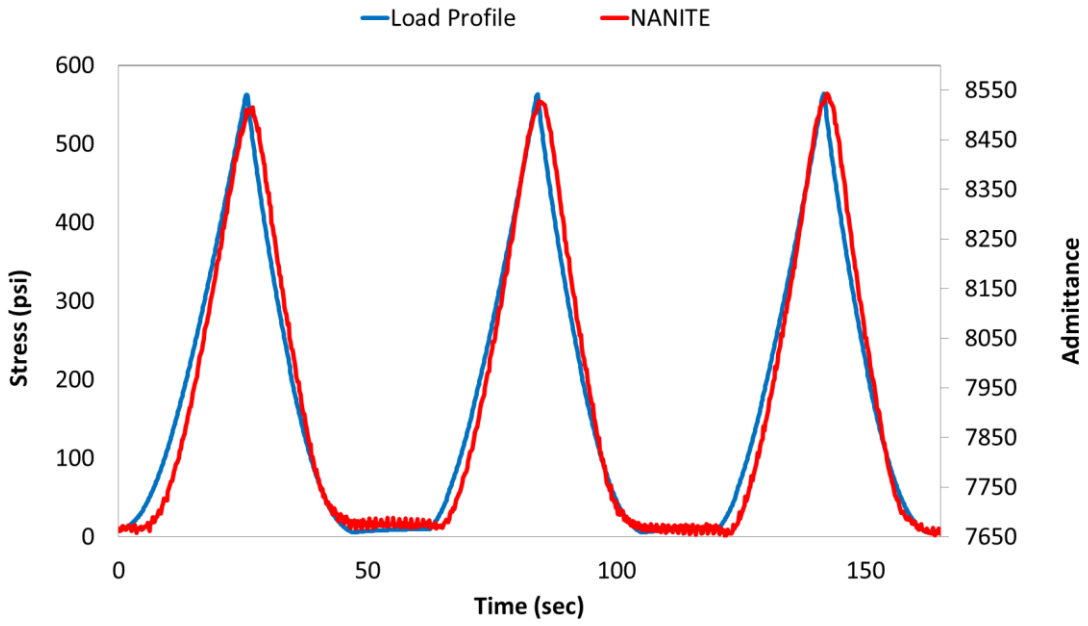

Figure 30: Triangular loading profile (blue) and admittance response for Nanite (red) at 28 days.

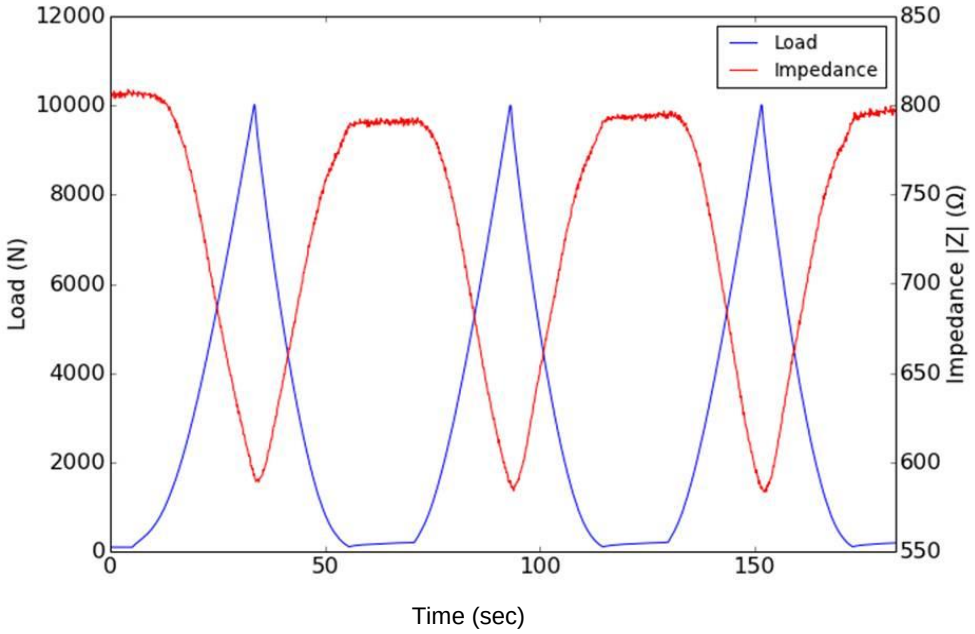

Figure 31: Loading profile (blue) and calibrated impedance measurement for Nanite (red) at 28 days.

The admittance of the sample was plotted versus corresponding stress values in order to evaluate the correlation between electrical response and mechanical load (Figure 32). A linear equation was fit to the data and the resulting $R^2 = 0.9725$. This plot also gives an impression of the linearity of the correlation as well as the level of hysteresis.

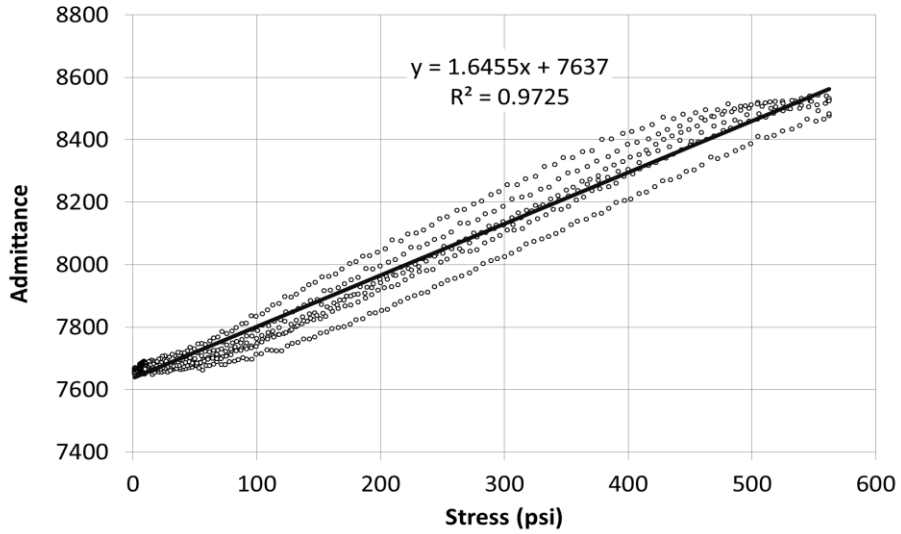

Figure 32: Admittance versus stress for one sample over three triangular loading cycles.

A step loading function was also applied to samples (10 days old) to gauge the electrical impedance response. The step size in this case was 8 kN. Again the impedance results closely matched the loading profile (Figure 33). The results indicate the importance of choosing the correct frequency

for analysis in order to obtain an accurate loading profile with minimal noise. There was no change in phase angle at any of the observed frequencies during the loading and unloading cycles.

Figure 33: Step loading profile (blue) and impedance response of Nanite (red) at 10 days.

A Nanite sample was loaded to failure after five days of curing to determine the effect of damage on electrical impedance response. There was a large admittance drop upon initial cracking, upon fracture of the sample, and upon removal of the load after fracture (Figure 34). Interestingly, there was often a drop in admittance immediately prior to a drop in load resistance. This effect offers the potential to detect micro-damage and possibly predict failure and will be investigated further.

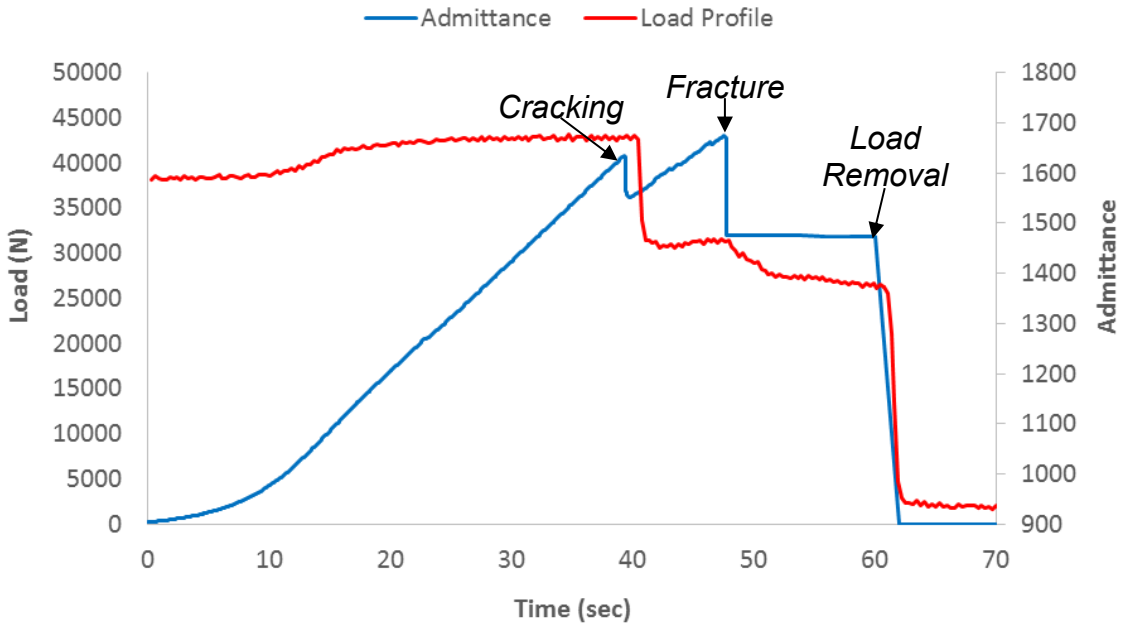

Figure 34: Load profile (blue) for loading to failure of Nanite at 5 days along with impedance response (red).

Quarter 4: Period End Date September 30, 2014

Research during this quarter focused on refining Nanite admixtures to ensure minimal impact on cement mixing and pouring as well as testing base and Nanite cements for chloride ion permeability**.**

Evaluation of the Nanite-Based Slurries' Properties

It is important to evaluate Nanite formulations for relevant properties, such as slurry density, free fluid, fluid loss, thickening time, strength development, and rheological properties under high temperature and pressure. Slurry density can be measured at Oceanit using a pressurized fluid density balance, as described previously. Tests that require additional specialized equipment have been outsourced to Oilfield Testing & Consulting, LLC (Houston, TX).

Chloride ion permeability

Permeation of concrete is one of the most critical parameters in the determination of durability of concrete in aggressive environments. Permeation, as dictated by the microstructure of concrete, controls the ingress of moisture, ionic and gaseous species into concrete. Chloride ion permeability of Nanite samples was studied to understand the effect of nanomaterials admixture on cement permeability and subsequent corrosion protection of steel casing. The rapid chloride permeability test in accordance with ASTM C 1202 and AASHTO T277 was used for the measurement of chloride ion penetration as described previously.

Two test specimens from each mix were tested at approximately 28 days after casting. The results of the testing are shown in Table 3. Testing was aborted prior to 360 minutes as prescribed in ASTM C1202 due excessively high readings caused by increasing temperature of the solution (3% NaCl). It can be seen that the Nanite cement sample shows slightly lower penetrability compared to control.

Table 3: Resistance to Chloride Ion Penetration

Specimen Identification	Specimen Reading (coulombs)	Time Completed (min)	Average (coulombs)	Chloride Ion Penetrability[1]
Control	6093	120[2]	6242.5	**High**
	6392	120		
Nanite	5792	120	5540.5	**89% of Control**
	5289	120		

1 This assessment is based on Table 1 (Chloride Ion Penetrability Based on Charge Passed) in ASTM C 1202

2 Testing were aborted prior to 360 minutes due to excessively high readings

Curing process evaluation

Oceanit produced 2" cube cement samples with electrodes configured as described in the Third Quarterly Report for electrical impedance evaluation of the curing process. All cement slurry samples were blended and cured according to API recommended practices as described previously.

Results from previous studies on curing indicated that the impedance spectra were highly sensitive to sample temperature. During this period, a setup for measuring sample environmental temperature at the same time as electrical characteristics was developed and implemented.

Simultaneous temperature and electrical impedance measurement

The long term curing log experiment was expanded to measure the ambient temperature in the curing chamber. A spike in ambient temperature of about 10 °C was observed approximately 5 hours into the curing process which returned to the oven set point of 60 °C within a few hours (Figure 35). The temperature shift within each sample was likely several times larger. This temperature transient is well correlated with the sudden increase in cement impedance at 5 hours curing. The value of this temperature transient in combination with cement impedance as a wait-on-cement indictor is being investigated further. It was also observed that there is a strong correlation between cement temperature and impedance with diurnal temperature fluctuations clearly responsible for the period drift in impedance.

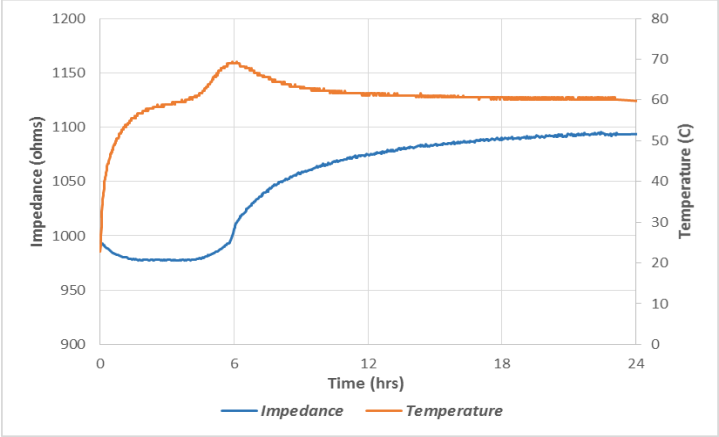

Figure 35: Electrical impedance (blue) and temperature (orange) log during the first 24 hours of Nanite cement curing.

Acoustic Properties

The acoustic properties of Nanite cement are being measured and compared to those of standard cement samples. The major goals are to increase the acoustic match between cement and slurry in the ultrasonic acoustic frequency range and to establish a relationship between acoustic and electrical characteristics from slurry to fully cured cement in the downhole environment.

During this period, the acoustic impedance characteristics of Nanite and base cement formulations were determined using an acoustic impedance tube (Tube Type 7758 from Brüel & Kjær) with four-microphone setup (Figure 36). Cylindrical cement samples with dimensions of 4” diameter and 2” thickness were produced from base slurry and Nanite slurry for testing in the impedance tube. The sample edges were taped and petroleum jelly applied in order to create a complete seal when placed within the sample test portion of the tube. The normal incidence transmission loss as a function of frequency was measured for each sample (Figure 37). Due to the size of the sample and tube, only lower frequencies were accessible. Efforts are being made to increase the

frequencies analyzed to those more relevant to acoustic bond logging analysis (100's of kHz).

Figure 36: Acoustic impedance tube (left) and schematic of sample and microphone setup (right).

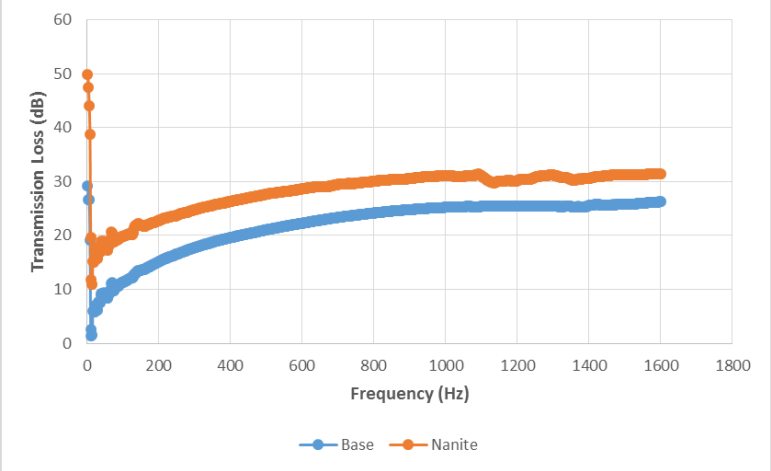

Figure 37: Transmission loss as a function of frequency

The density of the cement samples was determined to be approximately 1.9 g/cc for both formulations. However, Nanite samples showed a 5 to 10 dB higher transmission loss across the range of frequencies. This effect is interesting for improving acoustic contrast of cement as well as better matching impedance between cement and steel casing and is being further investigated.

Electrical Resistivity

Oceanit is using the electrical properties of Nanite to investigate the *in-situ* monitoring of cement properties such as curing, strength development, fluid/gas migration, leaks/structural damage and sensing down hole for both short and long term cement integrity.

Oceanit has demonstrated that the electrical conductivity of concrete is improved with the addition of conductive fillers and electrical impedance measurement can be used to monitor curing behavior and mechanical loading. The electrical properties are being improved by modifying Nanite cement with additive materials, including but not limited to conductive carbon nanomaterials. Work during this period included balancing the processing characteristics and electrical properties of Nanite

cement slurries. Various reagents and processing methods were investigated to enhance this balance, resulting in increased electrical conductivity with improved slurry mixing and pouring with Oceanit's conductive carbon nanomaterial.

The impedance analyzer module (rev 2) used for prior analysis has provided useful analysis, however posed several difficulties. The "rev 2" module was not intended for use with samples with relatively low electrical impedance such as 2" test cubes or casing pipe annuli. The rev 2 boards proved to be quite nonlinear and noisy in the sub 1 kΩ impedance regime of interest for this project. Additionally, the circuit produced an undesirable DC bias current to the sample under test. This bias induced charging effect in the samples resulting in inconsistent measurements.

The impedance analyzer "rev 3" circuit developed under this project offers several enhancements:

- Impendence measurement range extended below 1Ω
- Stable measurement at frequencies as low as 2kHz
- Linear impedance response over full measurement range
- Integrated calibration reference
- Zero DC bias current
- 10x faster serial communication interface
- 0.1Ω measurement accuracy at 470Ω

Measurement and analysis software was upgraded to support new high-speed communication interface as well as temperature logging.

An impedance analyzer test box was constructed containing a simple Randles circuit with known component values in a shielded enclosure. Common probe-tip style connectors are used on the impedance analyzer, test-box, and potentiostats for calibration and verification of performance.

The 4-wire electrode geometry was chosen for Nanite test cubes for several reasons:

1. Removal of contact resistance from DC impedance measurement
2. Minimally invasive electrode in cement samples to reduce reinforcement effects
3. Simplicity of installation during cement pour
4. Low cost

After demonstrating that DC measurements were subject to far greater drift and noise, AC impedance measurements were adopted for most experiments. When a DC bias current is not present in the sample, AC measurements with two electrodes have proven sufficient for impedance characterization. The two and four electrode geometries in a 2" cubic sample result in complex electric field distributions and current density within the sample due to the sample boundaries. A much closer approximation to uniform fields in a parallel plate capacitor can be emulated using two planar mesh electrodes in place of the wires.

A homogeneous batch of cement was prepared and cast into 2" cube samples, two of which had planar mesh electrodes and two with four parallel wire electrodes. The mesh electrodes had a spacing of 0.5" while the wires were separated by 0.375". The effective DC resistance of each sample was measured using the Biologic EC-3 potentiostat taking the minima of the imaginary impedance component as the effective DC resistance value.

Seven days after sample preparation the mean DC resistance (DCR) of the mesh electrode samples

was 59 Ω, while the wire electrodes had DCR = 312 Ω for the inner electrodes (0.375" apart) and DCR = 202 Ω for the outer electrode pair (1.125" apart). The mesh electrode results give a volume resistivity of approximately 12 Ωm. Comparison with the wire electrodes yields geometry factors of G_{outer} = 0.038 m and G_{inner} = 0.059 m where ρ = G*R relates the absolute volume resistivity of the material to the resistance measured under a certain geometry factor G (in this case compensating for the effect of using simplified wire electrodes). These geometry factors can be used to scale any results for wire electrodes used in 2" cubes to absolute resistivity.

The new "rev 3" impedance logging module was utilized to measure the impedance profile of a Nanite sample after two weeks of curing (Figure 38). Loading steps of 5 kN were applied every 10 seconds and released after 5 steps. The results indicate a much stronger measured response with less noise. The repeatability is excellent and non-linearity of the response can be adjusted with a proper calibration plot.

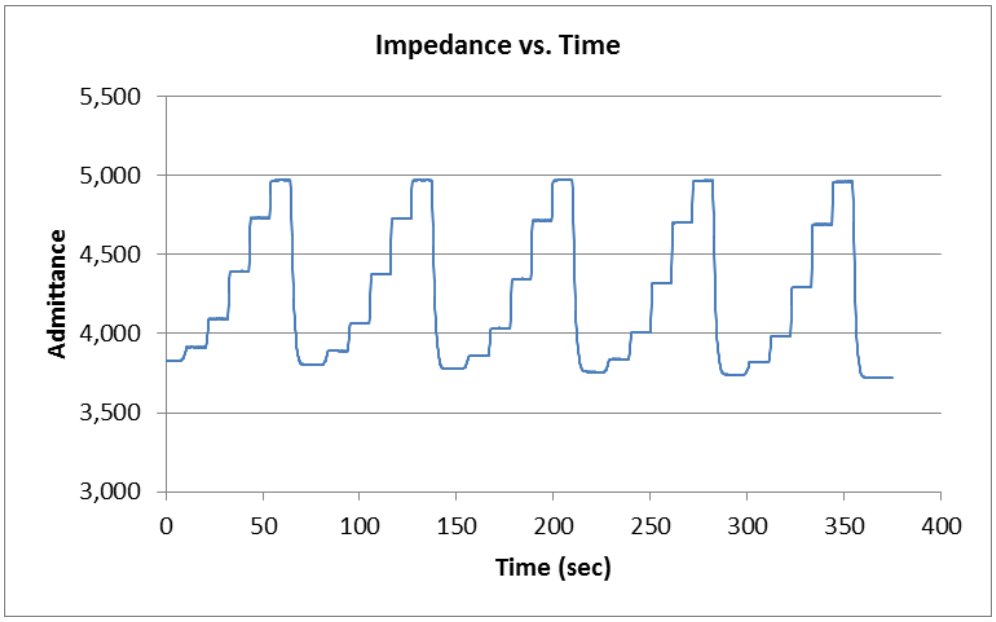

Figure 38: Impedance log using new "rev 3" impedance logging module for loading profile with 5 kN steps.

The new module was also used for measuring the response to continuous loading and unloading profiles performed by the Instron. A triangle-shaped loading/unloading profile was repeated 20 times over 13 minutes (Figure 39). The resulting impedance profile had some drift, which may have coincidentally tracked well with changes in strain. It should be noted that the strain values include displacement of the cube sample fixtures.

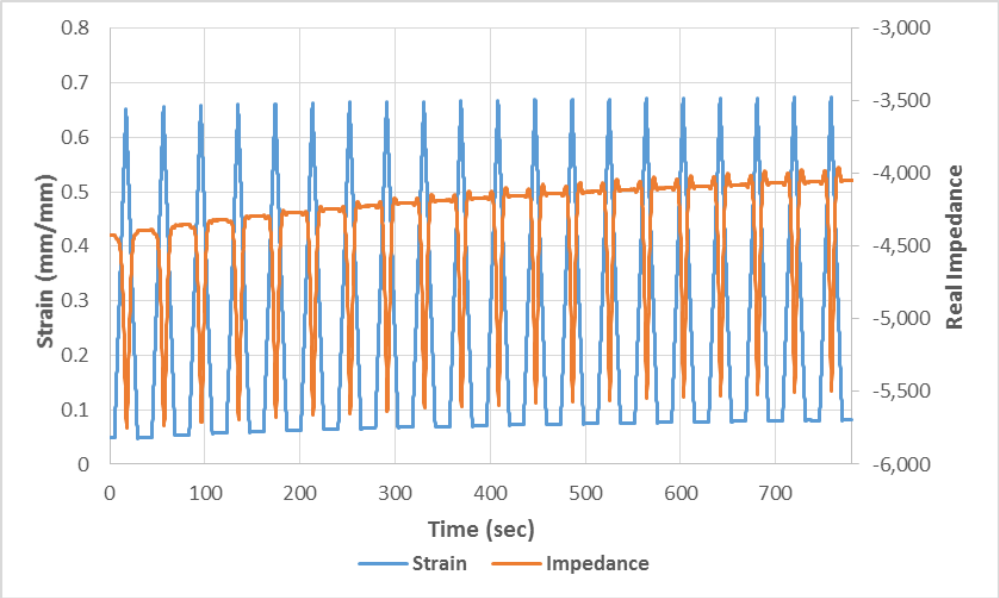

Figure 39: Strain and impedance profiles for repeated loading and unloading.

Nanite capability for detecting damage upon overloading was evaluated by testing 5 day old Nanite cement samples to failure under uniaxial compression. There was a clear change in impedance profile upon loading to failure uniaxial compression (Figure 40). This effect is being further investigated.

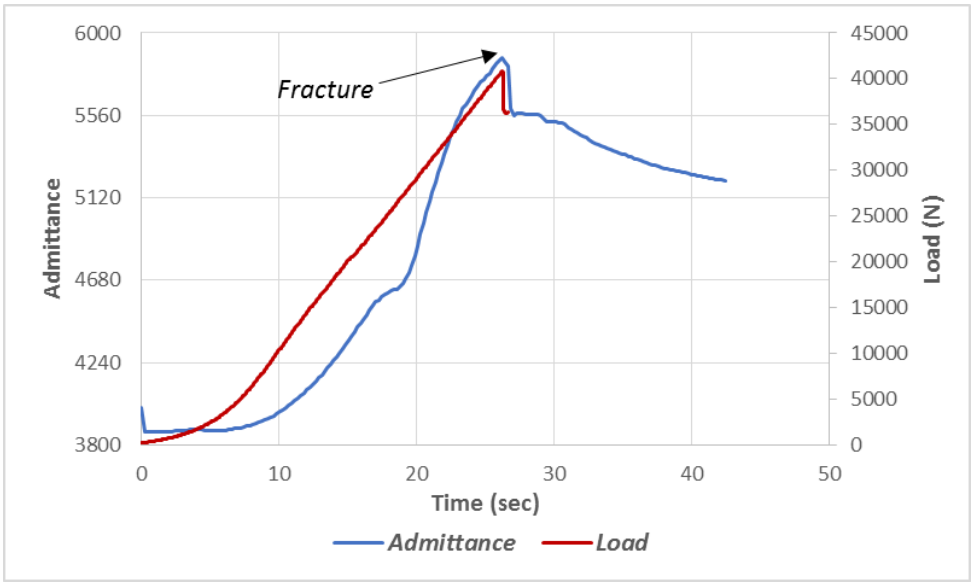

Figure 40: Impedance and loading profile vs time demonstrating sensitivity to initial failure of Nanite cement samples.

Work in the following quarters include transition to a concentric casing form factor as well as potentially coupling acoustic and electrical measurements as a new mode of cement logging.

Environmental Viability Study of Nanite Slurry

Evaluation of the environmental impact of Nanite cement was initiated by the Civil Engineering division of Oceanit. It is necessary to understand the regulatory framework and possible environmental impacts of using Nanite admixtures in well cementing operations. At this point it is premature to conduct a full life cycle analysis of Nanite because the precise composition of the admixture is the subject of this project. Despite this it is still important to understand the environmental implications of the product in order to minimize impacts.

Initially, Oceanit researched the regulations set down by various government agencies concerning environmental standards, well cementing, cement and petroleum well drilling. In particular, the regulations of the U.S. Environmental Protection Agency and Bureau of Ocean Energy Management, Regulation and Enforcement were considered. Most of the regulations concerning petroleum drilling on land are handled on the State level therefore the applicable state regulations will be reviewed. Well cementing technical specifications have also been promulgated by ISO (International Organization for Standardization) with input from the API (American Petroleum Institute) and ANSI (American National Standards Institute).

The U.S. Environmental Protection Agency (EPA) has the authority under the Toxic Substances Control Act (TSCA) to regulate nanomaterials and they intend to eventually promulgate regulations (Federal Register 2008). The problem that the nanomaterials industry, including regulators, face is that there is uncertainty on the health and environmental impacts of nanomaterials, including carbon nanotubes. In other words, no one knows to what degree this wide array of materials requires regulation. To resolve this problem, the EPA, environmental agencies from other nations, industry and the academic community are conducting research on the health and environmental impacts of carbon nanotubes.

Industries face lack of information with any new material but the uncertainties are greater with carbon nanotubes because the characteristics of this material are different because of the small particle size. In addition, the use of carbon nanotubes in well cement may affect the entire life cycle of the cementing product, from manufacturing to decommissioning. The practice of environmental and health safety with carbon nanotubes is in its infancy. Thus, there general tendency is to apply conservative environmental, health and safety practices (NIOSH 2013). Oceanit is following these practices in assessing health and safety for nanotubes.

Quarter 5: Period End Date December 30, 2014

During this quarter, curing of Nanite was studied using a combination of EIS measurement, temperature monitoring, and mechanical testing. The goal of these studies was to identify unique EIS signatures corresponding to different curing stages of Nanite, develop a model to predict Nanite setting and strength development, and customize the lab-scale EIS system for measuring early-stage curing of Nanite.

Curing Process Evaluation

The time evolution of electrical resistivity and the onset of compressive strength were evaluated for a series of Nanite samples. Cement slurry was prepared in accordance with API cement test sample specifications described previously and cast in plastic 2" cube molds in sample batches of four. Due to the high viscosity of the previously used nanomaterial admixture, the water content for this experiment was increased by 50% to ensure uniform and repeatable mixing of the cement slurry between batches. The resulting electrical and mechanical properties of this cement were more consistent than previous experiments. Stainless steel wire electrodes were aligned and inserted into the specimens with 0.5" separation. The cube specimens were connected to a battery of four impedance analyzer boards. Specimens were placed in an airtight container with a sealed penetration for the instrumentation cables, which was placed in a 70°C oven.

For each sample batch, custom EIS logging software was used to sample the AC impedance and the temperature of the samples at 30 sec intervals over the test duration as the samples cured. In addition to impedance, the ambient temperature within the curing chamber and the room temperature were simultaneously logged. At different curing interval time points for each sample (4, 6, 8, 17, and 27 hours), the specimens were removed from the curing chamber and immediately tested for compressive strength in an Instron test machine. Specimens were secured between compression blocks and loaded at a rate of 2.5 mm/min up to 2.5 mm. EIS measurements were also made with another analyzer board during the crush test to monitor changes during mechanical loading and failure as described in the Fourth Quarterly Report.

The temperature and impedance logged for each sample is shown in Figure 41. Note that the temperature curves all peak at 6.3±0.3 hrs that correlates well with a change in the impedance. The tail of this temperature spike and return to equilibrium temperature (70°C) correlates with the samples obtaining maximum early strength.

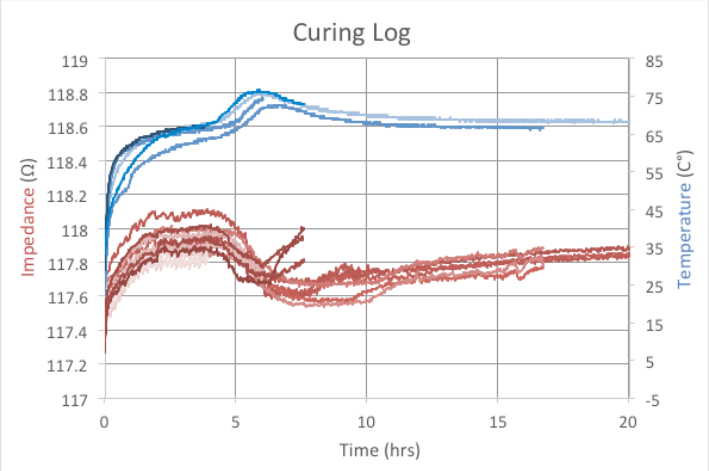

Figure 41: EIS (red) and temperature (blue) logs measured for specimens during curing.

Load profiles and EIS measurements measured during compressive strength testing of Nanite specimens from each curing interval are shown in Figure 42. Electrical impedance response during loading and failure appear for the later time point samples. The specimens from the test curing duration of 4 hrs had a mud-like integrity, minimally sufficient for compressive testing, and yielded at approximately 10N. Early-stage compressive strength was achieved mainly within the first 24 hours as shown in Figure 43.

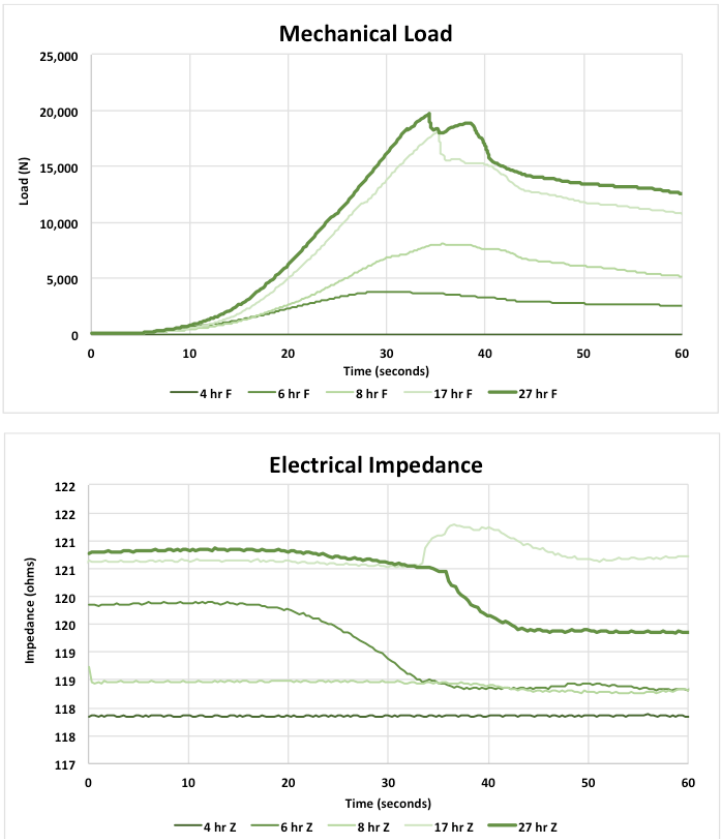

Figure 42: Mechanical loading and simultaneous EIS measurements for samples of different curing times.

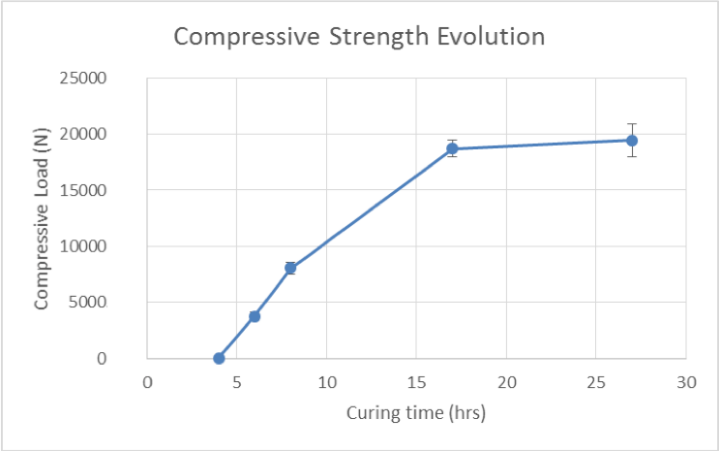

Figure 43: Maximum compressive load at failure for samples of different curing times.

Electrical conductivity enhancement of Nanite

Oceanit has demonstrated that the electrical conductivity of concrete is improved with the addition of conductive fillers and electrical impedance measurement can be used to monitor curing behavior and mechanical loading. The electrical properties are being improved by modifying Nanite cement with additive materials, including but not limited to conductive carbon nanomaterials.

During the last quarter, the effect of different Nanite admixture loading levels on resistivity-load response was determined. Samples were produced according to API recommended practices as described in the Second Quarterly Report. Different admixture suspensions were prepared in order to obtain different final Nanite cement loading levels. Electrical impedance was monitored while applying a mechanical loading profile as described in the Third Quarterly Report (5 kN steps). The results from four samples from each formulation through three loading cycles are shown in Figure 44.

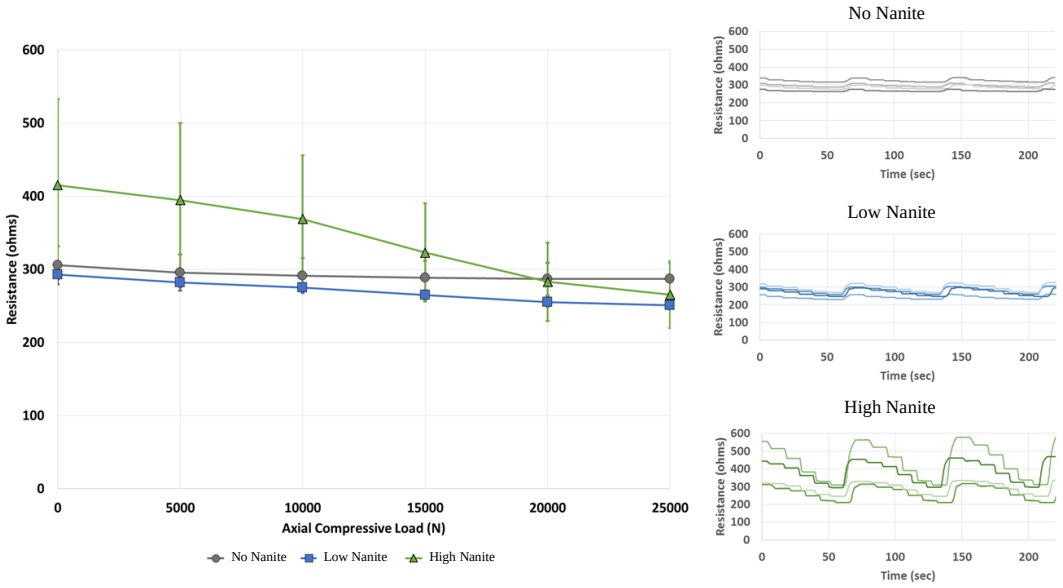

Figure 44: Resistance versus axial compression (left) for Nanite cubes increasing admixture concentration and plots of individual specimen resistivity versus time (right).

The Nanite batches with higher loading had a larger resistivity response to mechanical loading. The results indicate a dose-dependent response or a threshold for Nanite electrical responsiveness. Lower levels of Nanite admixture loading had a much smaller response but still larger than no Nanite loading, which had an overall flat response. Inter-specimen variability was larger for the high Nanite loading, suggesting that dispersion of the admixture was uneven within the batch tested. Batch-to-batch variation also needs to be addressed.

The dependence of Nanite resistance to applied compressive load was measured by subjecting a Nanite cube sample to repeated staircase loading with 8 kN steps. Figure 5 shows the correlation of the sample impedance with stress. The three series in the plot correspond to successive loading cycles. The change in slope on subsequent cycles is due to the non-recurring changes in the contact interface between the sample and the loading machine. On the first cycle in particular, the plastic loading block conforms to the contour of the cement sample while some edge cracking of the cement may occur. On subsequent cycles there is a better ‘fit’ and higher repeatability. Ideally, these measurements should be performed in the reverse direction by preloading the sample before measurements begin. The vertical offset is due to observed drift in the AC impedance of the sample under test. The origin of the impedance drift is a topic for further investigation. Further studies will validate the repeatability of this sensitivity among Nanite specimens and batches.

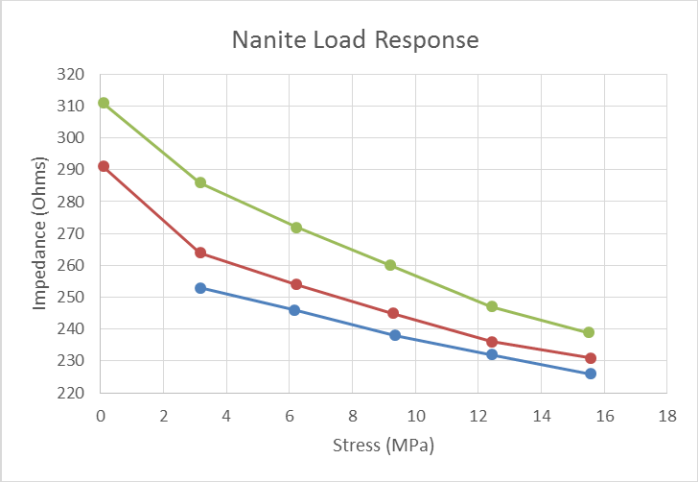

Figure 45: EIS measurements versus applied stress for three initial cycles of loading.

Electrical impedance spectrum (EIS) analyzer hardware fabrication

Four additional 'rev3' impedance analyzer units were fabricated, tested, and calibrated (Figure 46). Verification of linearity was performed using a precision 10kΩ potentiometer and multimeter. For each unit the potentiometer admittance was measured using the impedance analyzer and software in raw uncalibrated instrument units (ADC counts). The corresponding impedance was measured at each point with a calibrated Fluke multimeter with 0.1Ω precision.

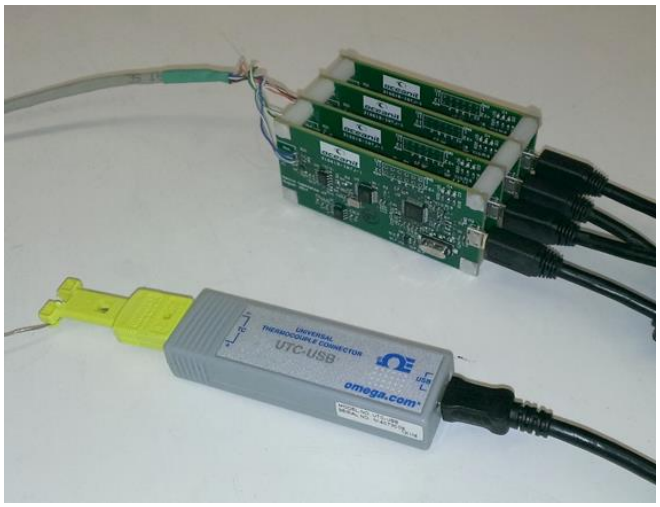

Figure 46: Nanite impedance analyzer board stack with USB temperature measurement module.

Each analyzer circuit was assembled with components chosen to achieve a measurement range of 120Ω to 5400Ω. The analyzer gain resistance can be chosen to allow measurements to impedances as low as 1Ω, however, the maximum measured impedance is limited to 45x larger than the minimum. Thus, the feedback resistor is chosen to provide an application specific measurement range. Instrument versatility can be improved in future designs by providing switchable feedback resistors. The present impedance range was chosen to suit the 2" cubic cement samples under study

for load monitoring.

Figure 47 shows the highly linear relationship between the instrument's measured admittance and actual admittance (inverse impedance). This performance is a dramatic improvement over the low-Z capability of the 'rev2' analyzer circuit. This experiment indicates that a two point linear calibration is sufficient to achieve the desired 0.1Ω resolution. The red point in the plot corresponds to the 1kΩ on-board calibration resistor and agrees with the external calibration resistor.

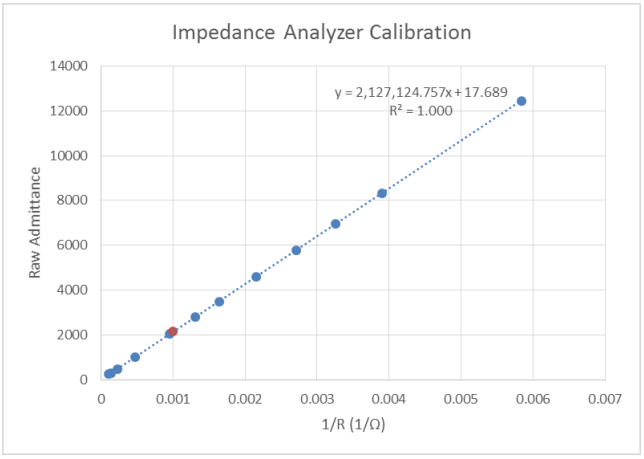

Figure 47: Calibration curve for the 'rev3' impedance analyzer.

A two point calibration was performed on all four boards using the on-board 1kΩ resistor and an external 220Ω resistor. Calibration at these two points yields a gain of an offset parameter for each board according to the relationship $Z = \frac{A_1}{C} + A_0$, where Z is the known impedance and C is the instrumentation datum. The calibration gains A_1 for the four boards were consistent to better than 0.1% with mean value 2,160,000±2,000 (Ω/count). The impedance offset A_0 = -2.5±0.2 Ω shows greater variance, however the 0.2Ω is less than the variable impedances associated with test leads and contact resistances. This single calibration factor will hereafter be applied to all acquired data for all verified hardware modules.

Application of Nanite in Downhole Relevant Form Factor

EIS monitoring during loading of concentric pipes with Nanite sheath

For application of Nanite for monitoring well bore cement integrity, it is important to transition from testing samples in cube configuration to testing in concentric casings form factors, as are commonly found down-hole. A Nanite formulation was cast between a 1" inner steel pipe and a 2" outer steel pipe with 0.065" walls. Electrodes were fastened to the inner and outer pipes using hose clamps (Figure 8, top). The concentric pipe sample was then attached to the impedance analyzer module ('rev 3') and loaded transversely in the Instron between rubber pads (Figure 48, bottom). A loading profile of 5 kN steps was applied up to 25 kN through three cycles. The electrical resistivity was monitored throughout the loading cycles (Figure 49).

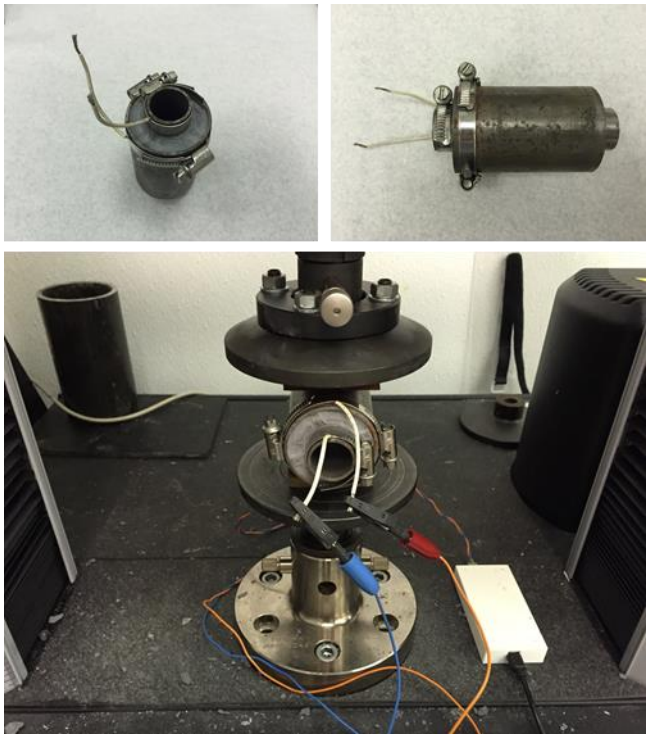

Figure 48: Concentric pipe with cement sheath form factor for testing Nanite (top). Cemented concentric pipes connected to the impedance analyzer in the Instron for resistivity-load measurements

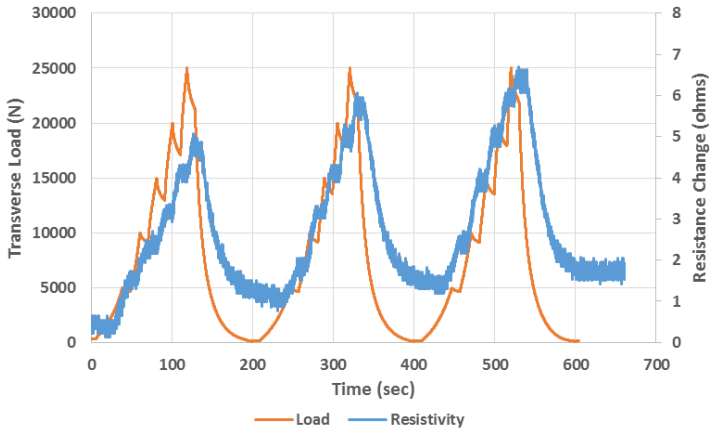

Figure 49: Transverse load and resistance change versus time for a concentric pipe with a Nanite sheath.

Resistance tracked well with transverse load with some drift over the multiple loading cycles. This is promising for measuring stress in the Nanite in a concentric casing scenario. Finite element modeling was used to estimate the radial and hoop stresses experienced in the cement sheath during transverse loading (Figure 50). It was found that significant radial stress perpendicular to the electric field lines between steel pipes was developed during such loading, which may have elicited the Nanite electrical response.

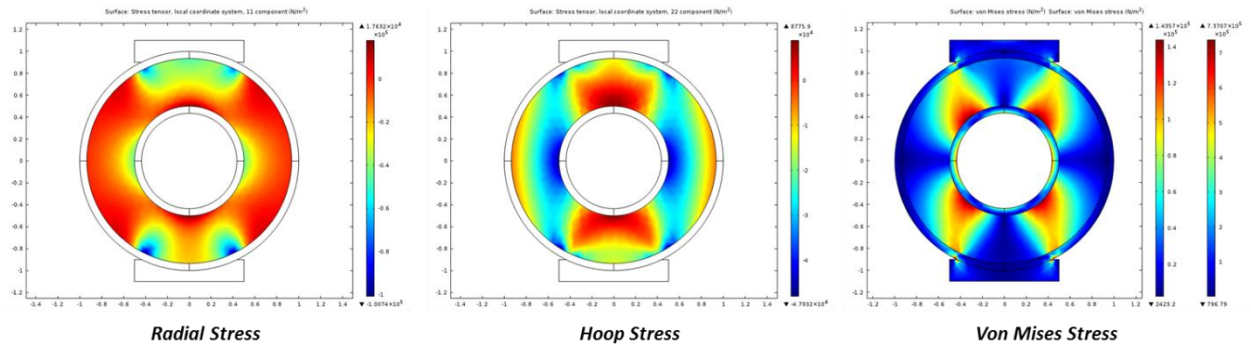

Figure 50: Concentric pipe with cement sheath modeled in COMSOL Multiphysics software with transverse load applied by compression blocks. Stress field maps are shown for radial stress (left), hoop stress (middle), and total Von Mises stress (right) under 75 kN app

Design and fabrication of pipe expansion model

To extend studies of Nanite as a material for downhole casing cement we have developed a model system to study the behavior of Nanite in a pipe annulus. The purpose of this system is simulate radial loads applied to the cement annulus between casing pipe and an outer casing or the formation. A recent study at LSU[5] demonstrated the mitigation of sustained casing pressure due to micro-annulus formation in the cement annulus between two concentric casing pipes. The LSU experiment utilized a 30,000 lb hydraulic actuator to push expansion cones with various expansion ratios through an inner 2" casing pipe surrounded by a 0.6" cement annulus and a 3.5" outer pipe. The team has demonstrated the ability to 'heal' a cement annulus through the application of a pipe expansion.

The Oceanit system extends the LSU concept to incorporate Nanite's electrical sensing capabilities using the inner and outer pipe as electrodes for use with the impedance analyzer rev3. We will validate the electrical response of Nanite to radial loading in a concentric pipe form factor as well as assess the healing characteristics of the Nanite formulation compared with base cement. Oceanit's demonstration incorporates the Nanite electrical sensing capability to assess the state of the cement before, during, and after the expansion and determine whether the expansion of the inner pipe against faulty cement produces an electrical impedance signature that will enable real-time assessment of a remediation job using this technique.

This demonstration shown in Figure 51 uses a concentric pipe arrangement with the annulus filled with Nanite. The design can optionally support plastic sealed end caps with inlet and outlet ports for measurement of the cement's gas permeability throughout the expansion experiment.

[5] Kupresan, Heathman, and Radonjic. "Experimental Assessment of Casing Expansion as a Solution to Microannular Gas Migration." IADC/SPE 168056, 2014.

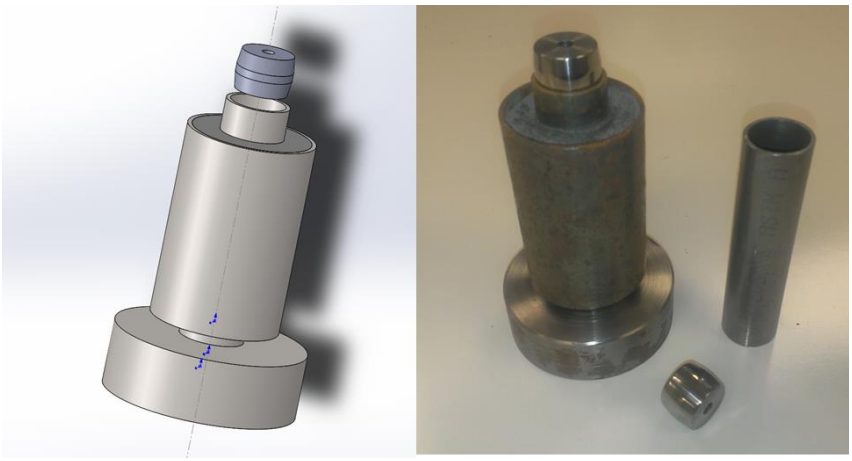

Figure 51: Pipe expansion apparatus model (left) and fabricated system (right).

Radial stress is applied by the insertion of a conical expansion plug (Figure 51) through the inner pipe. An 8° wedge half-angle provides a good compromise between maximal mechanical advantage for induced radial load and friction between steel surfaces. Our 50kN Instron testing machine combined with the 7x mechanical advantage of the cone will apply a maximum radial stress of 700MPa over the contact area sufficient to exceed the yield strength and permanently deform the pipe and cement. Initial testing will be performed with a 2% pipe expansion ratio, which we expect to induce sufficient stress to reach the yield point of both the inner pipe and the cement annulus.

Quarter 6: Period End Date March 31, 2015

During this period, curing of Nanite was studied using a combination of modified EIS measurement and temperature monitoring. The goal of these studies was to identify unique EIS signatures corresponding to different curing stages of Nanite, develop a model to predict Nanite setting, and customize the lab-scale EIS system for measuring early-stage curing of Nanite.

Curing Process Evaluation

The effects of curing on electrical impedance properties were determined for a set of samples. A modified electrical impedance analyzer was constructed in order to obtain a higher signal-to-noise ratio for very low impedance samples, such as those in the early stages of curing. This was performed by reducing the impedance of the feedback resistor in the device circuit. A stack of four analyzer boards along with a logging thermocouple were used to track the impedance of four samples during curing. Nanite slurry admixture was prepared in accordance with API cement test specifications at an appropriate water-to-cement ratio. The slurry was cast into 2" cube molds with embedded diameter stainless steel electrodes along the center plane at 0.5" separation. Five minutes after casting, the electrodes were attached to the analyzer boards and the samples were placed in an airtight container with a sealed penetration for instrumentation cables and placed in an oven at 60°C. The samples were removed after approximately 65 hours and monitoring continued at room temperature. The electrical impedance analyzers were used to sample AC impedance at 30 second intervals. The results are shown in Figure 52.

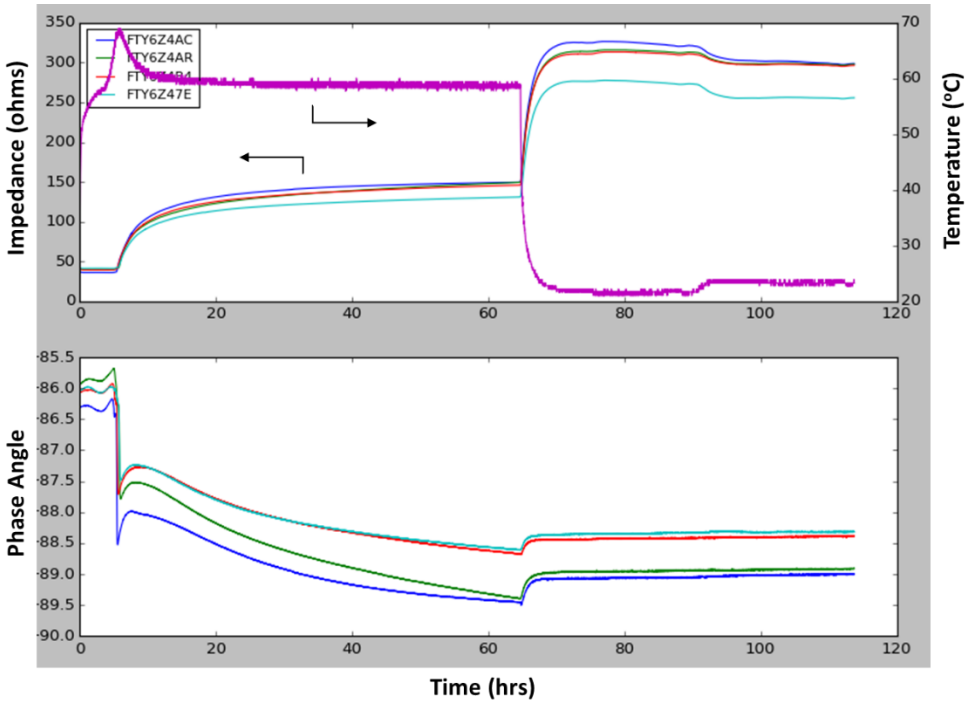

Figure 52: Impedance and temperature (top) along with phase angle (bottom) as a function of curing time for Nanite samples.

A clear spike in temperature was noted at 6 hours of curing, indicating a high rate of cement hydration at that point. This corresponded with a rapid rise in impedance above the detection floor limit and a simultaneous drop in phase angle. This was the same curing time that rapid strength development was observed (see previous quarterly report). The temperature subsequently settled down to the ambient oven temperature while the impedance continued to gradually increase and level off.

Cement curing involves initial rapid chemical dissolution of the calcined mineral components followed by hydration processes in which ions transport to and from the surfaces of anhydrous cement particles through growing layers of hydration products. Free water permeates the hydration products, enabling further reaction. The exothermic hydration processes result in an adiabatic rise in temperature of the cement, indicating the degree of hydration. As the hydrated layers grow, the particles become interlocked and the material transitions from a slurry to an open-celled porous structure to a closed-cell porous structure.

The electrical impedance properties of cement depend on the water content, ion concentration, and pore interconnectivity. Changes in impedance during curing likely involve evolution of the microstructure in a multiphase porous media and changes in apparent ion diffusivity and overall charge mobility. The process also involves the corresponding heat generation and strength development that accompany cement hydration kinetics. The history of the electrical impedance properties can therefore be used to predict the hydration state and mechanical strength of curing Nanite.

Optimization for Electrical Resistivity

Oceanit have also used the electrical properties of Nanite to investigate the *in-situ* cement properties such as curing, strength development, fluid/gas migration, leaks/structural damage and sensing down hole for both short and long term cement integrity. A measurement method was developed to detect the quality of the Nanite cement sheath around a casing. The electrical properties have been improved through modification of Nanite cement with additive materials, including but not limited to conductive carbon nanomaterials. The choice of electrode material used for electrical impedance measurements was found to have a significant effect on its load measurement properties.

Oceanit investigated the optimal selection of electrode materials for electrical impedance measurements in Nanite. Prior to this study tests were exclusively performed with alloy 304 stainless steel, generally in the form of 0.049” diameter wire. In this study the performance of stainless steel electrodes was compared with carbon steel, copper, and gold wire. A new 3D printed electrode alignment jig was fabricated that allows four electrodes to be cast in a 2” cube in several possible configurations (Figure 53). This allows two pairs of electrodes of different composition to be cast into the same cube. For our tests, a pair of stainless steel electrodes were included in every sample as a control for comparison with the test metal.

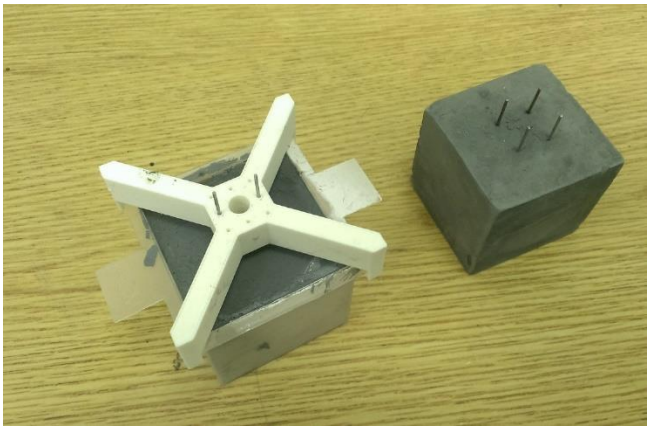

Figure 53: Casting jig for flexible electrode configurations

Alternating current (AC) electrical impedance measurement were chosen for Nanite to overcome the large drifting offsets observed for DC impedance measurements of cementitious samples due to electrochemical effects. Drift in the AC impedance is also observed; however, this effect is distinct from the DC drift. The observed AC impedance drift is not correlated with the DC level and the observed impedance drift present in most experiments are directly correlated with the humidity of the sample being studied. Figure 54 shows an example of steady baseline impedance drift for a cyclically loaded sample. Upon immersion of a cement cube sample in water, shown in Figure 55, the impedance drops linearly until removed from the water, where the impedance rises again as the sample dries. Finally, the sample was re-immersed in water and the resulting fall in impedance is observed. The effect of free water in the cement can also explain hysteresis observed when a compressive load is applied resulting in pore fluid migration.

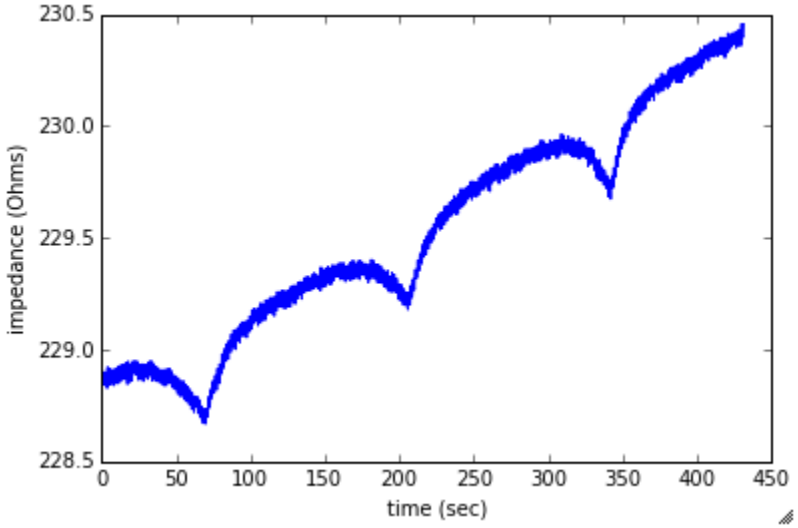

Figure 54: AC impedance drift

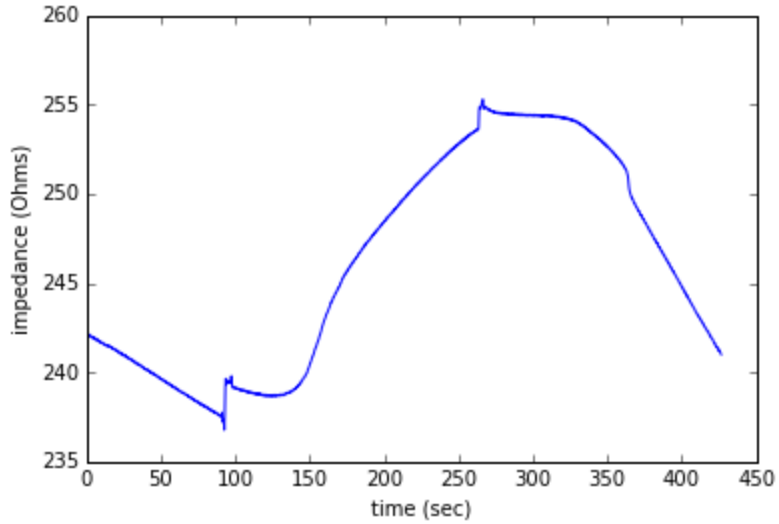

Figure 55: Dependence of impedance on sample humidity. Sample was immersed in water, removed at 100 sec, and re-immersed at 260 sec.

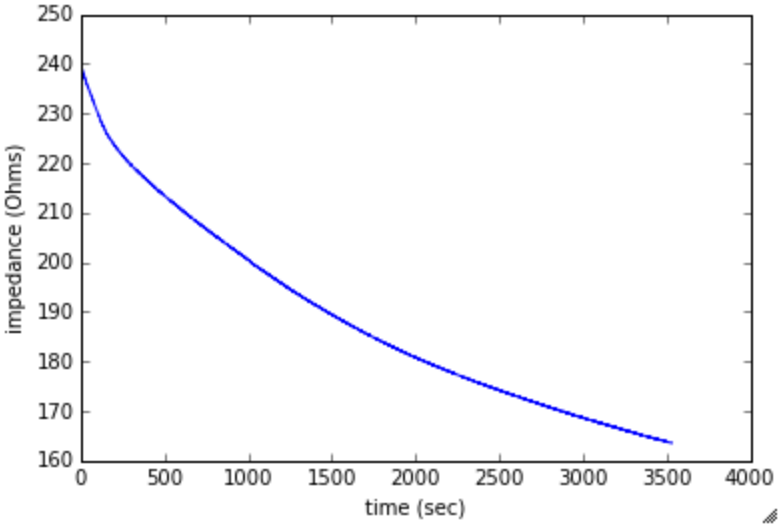

Figure 56: Impedance drift for continuous immersion in water

Electrical Impedance measurements

The goal of this subtask was to utilize the resistivity logging technique to determine the quality and placement of annulus cement. Specialized resistivity hardware and software were developed and optimized towards this goal. Five of the 'rev3' impedance analyzer boards were re-ranged to accurately measure impedances as low as 50Ω. This lower impedance range in necessary to accommodate applications involving electrode geometries different from the 2" cubic samples used thus far. In the previous quarter we demonstrated the linearity of the analyzer calibration curve and the validity of a two point calibration to achieve 0.1% accuracy. All eight of the impedance analyzer boards presently in service were re-calibrated using the same technique.

Oceanit's proprietary electrical impedance analyzer software tool saw several improvements this quarter. The attached analyzer boards are now identified automatically by serial number and

calibration data is automatically loaded and applied to recorded data. The graphical user interface was ported from the wxPython GUI toolkit to PySide as a solution to several longstanding usability bugs. Several other outstanding software bugs were fixed to improve reliability and usability of the tool.

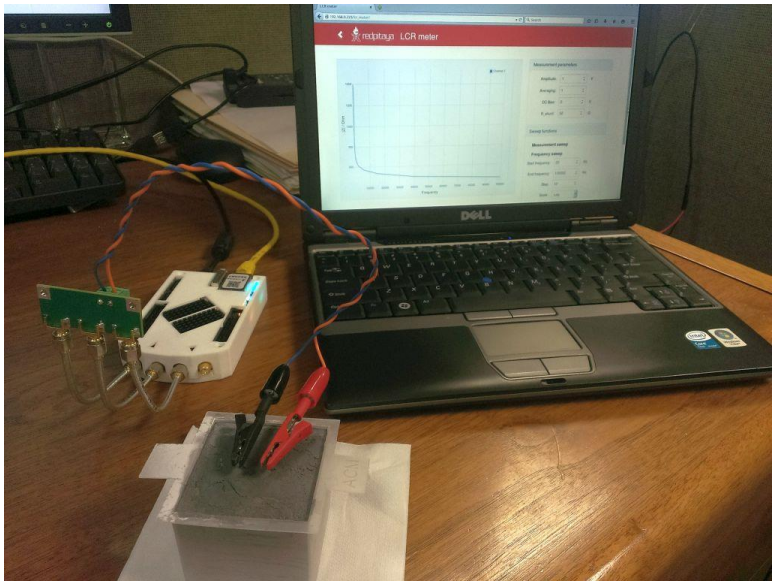

Figure 57: Red Pitaya-based impedance analyzer preliminary testing

In addition to the 'rev3' impedance analyzer tool, Oceanit has investigated the use of a high-performance tool utilizing the Red Pitaya platform[6]. The Red Pitaya is a commercially available open-source laboratory tool consisting of a Xilinx Zynq system-on-chip SoC and dual channel 150MS/sec 14bit analog to digital converters. The Pitaya serves as an arbitrary waveform generator, oscilloscope, and data acquisition and control computer on a single small board with control over Ethernet.

Oceanit has developed a peripheral enabling the Pitaya to make superior impedance measurements to the 'rev3' analyzer with additional capacity for measuring the impedance associated with transient loading events. These capabilities extend Nanite's ability to measure long term variations in cement condition to include transient events such as cracking that may yield insightful signatures.

Design and fabrication of pipe expansion model

To extend studies of Nanite as a material for downhole casing cement we have developed a model system to study the behavior of Nanite in a pipe annulus. The purpose of this system is to simulate radial loads applied to the cement annulus between casing pipe and an outer casing or the

[6] http://redpitaya.com/

formation. We will validate the electrical response of Nanite to radial loading in a concentric pipe form factor as well as assess the healing characteristics of the Nanite formulation compared with base cement. In addition to the pipe expansion components previously detailed, a steel push rod attachment for the Instron material testing machine was fabricated.

Preliminary tests have been performed using the apparatus shown in Figure 58 demonstrating the ability to expand the 1" inner casing pipe by 2% while monitoring the electrical impedance. This work enables testing of Nanite properties under radial loading configurations relevant to downhole applications and will be continued and expanded.

Figure 58: Pipe expander testing with Instron machine

Optimization of Nanite for Acoustic Properties

The goal for this work was to observe the effect of various commonly used additives on altering acoustic properties of cement. The focus of this effort has been in evaluation and study of the current admixture, making a determination as to whether the addition of nanomaterial has any effect on well logging operations.

Slurry density was best found to be characterized through weight and viscosity measurements, as well as during curing experiments. Slurry density was found to change minimally when comparing Nanite to base cement; rather viscosity was found to an important consideration when ensuring no disruption to normal cementing processes. Compressive strength of cement formed from Nanite slurries were found to be equivalent to conventional slurries in all the load analysis and strength-at-failure experimental trials conducted thus far. No additional modifications or additives are necessary at this time to achieve improved compressive strength.

Cement casing in the downhole environment is typically measured via cement bond logging, whereby the coupling of cement to casing and formation can be determined. Ultrasound pulses are sent to impact casing/cement/formation stacks in the downhole condition. Reflection of these ultrasonic pulses occurs at areas of acoustic impedance mismatch, such as a thin layer of water or air trapped between cement and the surrounding formation. As such, high amplitude reflected signals are indicative of poor cement bonding.

Nanite samples containing nanomaterials were cast into discs 25.4 mm thick, and 29.2 mm in diameter, as seen in Figure 59. These discs were placed within a Brüel & Kjær™ commercial acoustic impedance tube, and transmission loss was measured and compared to transmission loss for standard cement without additives. A 4-microphone setup based on ASTM E1050-10 was used with a nominal 1" diameter tube width, allowing for incident transverse waves with frequencies up to 6400 Hz to be accurately produced.

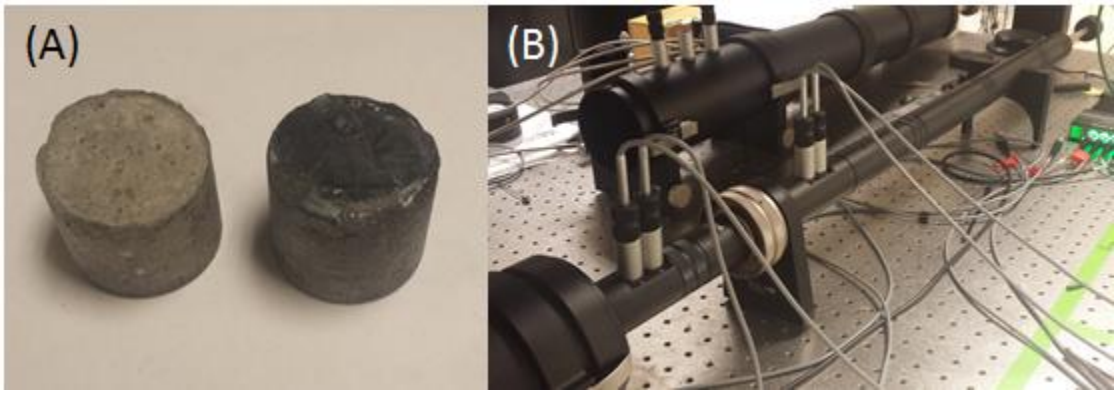

Figure 59: Acoustic testing of Nanite. (a) Samples of base (left) and Nanite (right) to be tested. (b) 4-mic acoustic impedance tube setup. Samples are loaded between the microphones (silver ring), and transmission loss is recorded.

Samples were weighed and compared at various stages of curing (5 days, 28 days). No variation in transmission loss was noted between base cement and Nanite samples of similar weights and ages. Minimal variation in transmission loss was also detected as a function of curing time, and sample weight was minimally changed over the course of curing (less than 10% variation). No significant harmonic peaks were detected in this range. Sample transmission loss curves can be found in Figure 60.

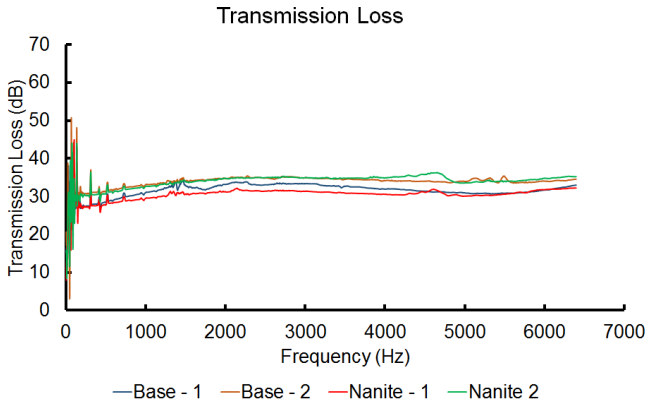

Figure 60: Transmission loss for Base and Nanite samples, showing minimal variation in transmission loss across samples.

While it was thought that the addition of carbon nanomaterial might fundamentally alter the

formation and acoustic absorbing properties of the base cement, this does not appear to occur with the currently optimized admixture. However, it also is an indication that Nanite does not demonstrate any acoustic properties less favorable than existing base cement, or materially affect the compatibility with or accuracy of cement bond logging tools.

Quarter 7: Period End Date June 30, 2015

Nanite Electrode Optimization

Oceanit continues to investigate the electrode materials and form factors necessary to optimize electrical resistivity measurements for cement integrity monitoring. Experiments suggest that the choice of electrode metal has a significant impact on the load responsivity in 2" Nanite sample cubes. Nanite samples were fabricated with wire electrodes made from several materials:

- Stainless steel
- Mild steel
- Copper
- Gold coated silver
- Nickel plated steel

Stainless steel continues to be the electrode material of choice although differences in surface texture may be as important as the metal composition.

To further elucidate the effect of the electrode to cement bond on resistivity measurements we fabricated several 1" thick x 2" square Nanite slabs with parallel plate electrodes on the 2" faces. Steel electrodes were bonded to both Nanite and base cement samples. Unfortunately, the planar electrode bond was not strong enough and one or both electrodes detached from the samples during demolding. None of the bonds survived after compressive testing and the resulting impedances were inconclusive. Clearly the mechanical integrity of the electrode bond in any configuration is important to the sensing capability.

Nanomaterial Dispersion Method Optimization

Oceanit has investigated the use of a 500W immersion sonication probe as an alternative to shear mixing with a homogenizer. This method appeared to produce superior nanomaterial dispersion. The sonic dispersion method is a widely-used method of nanomaterial dispersion in the polymer nanocomposite literature. However, the high cavitation stresses induced by sonication are known to break down and shorten carbon nanotubes as well as exfoliate agglomerations. While the sonication method has been used exclusively at Oceanit for the past six months we now revisit the homogenizer considering literature suggesting that shear mixing may be more effective at dispersing CNTs in aqueous solution without shortening the tubes. We have prepared numerous admixtures using both methods and compared the resulting admixture viscosity, opacity, and examined SEM images of dried samples.

While sonication is an effective means of dispersing single nanotubes (SWCNTs) and multiwall (MWCNTs), it has been shown[7] that the excessive stress on MWCNTs results in significant shortening of the tubes. High shear rate mixing on the other hand is ineffective at dispersing SWCNTs and less effective for MWCNTs yet does not damage the tubes. The shear stress delivered to the admixture by a homogenizer generator at a fixed speed is proportional to the viscosity of the fluid. Thus, we expect that homogenization of a more viscous admixture will yield superior a superior dispersion. Oceanit compared the nanostructure and effectiveness of two admixtures prepared with 4hrs homogenization with the same speed. Both samples were held in an ice water bath for the duration of homogenization to stabilize temperature increased due to

[7] Huang and Terentjev, "Dispersion of Carbon Nanotubes: Mixing Sonication, Stabilization, and Composite Properties", Polymers 2012, 4, p275-295

mixing.

Carbon Nanotube Functionalization

Work began on experiments to explore the use of different nanoparticle sources for Nanite admixture. To date the most successful samples have used COOH functionalized MWCNTs, however, it is important to explore other options that may reduce cost or impart improved performance. Figure 61 shows the load response profiles for cement specimens produced using our standard COOH functionalized CNT based admixture compared with unfunctionalized tubes of the same grade and manufacturer without COOH functionalization. The functionalized samples show far more sensitivity to load and the unfunctionalized samples performed worse than base cement. The viscosity of the admixtures shown in Figure 62 indicates that unfunctionalized CNTs are not dispersing well in water resulting in lower viscosity.

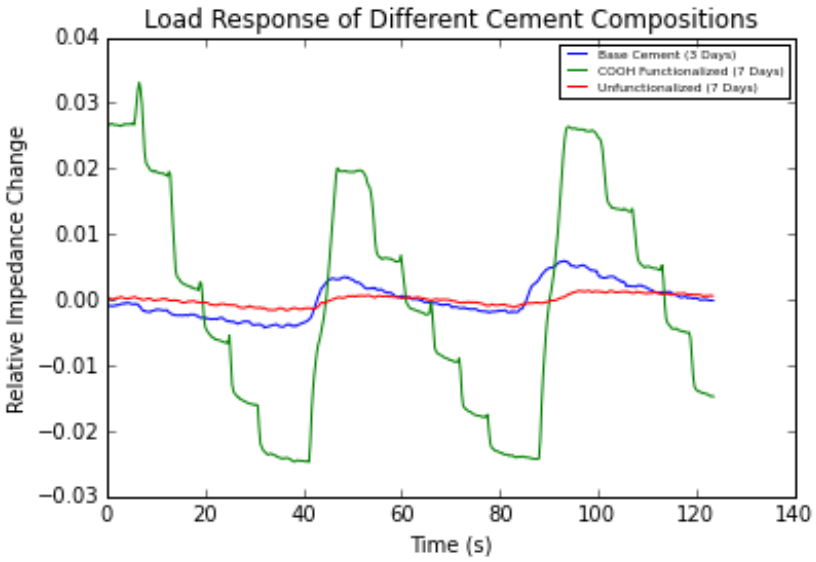

Figure 61: Impedance response to load for admixture with and without CNT functionalization compared with base cement.

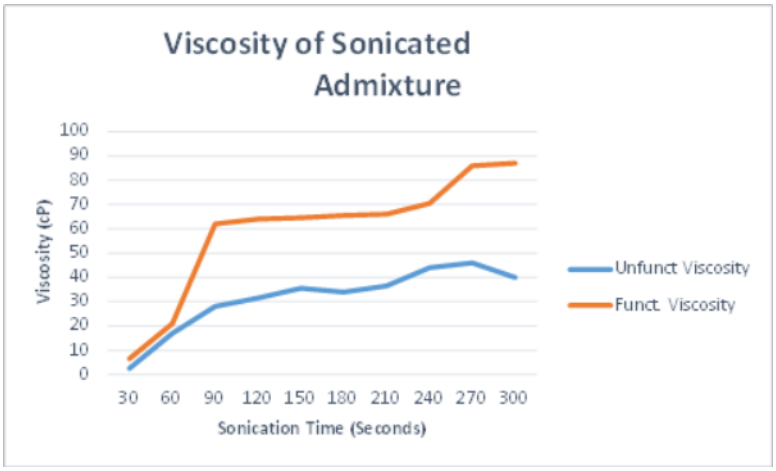

Figure 62: Effect of COOH functionalization on admixture viscosity

Nanite Set Cement Resistivity and Nanostructure

Several batches of Nanite sample cubes have been observed repeatedly since casting to track the time evolution of the load response and impedance as the samples age. Figure 63 shows little variation in the baseline impedance from 3 to 30 days curing and the variation in the sensitivity is less than 20% after 7 days.

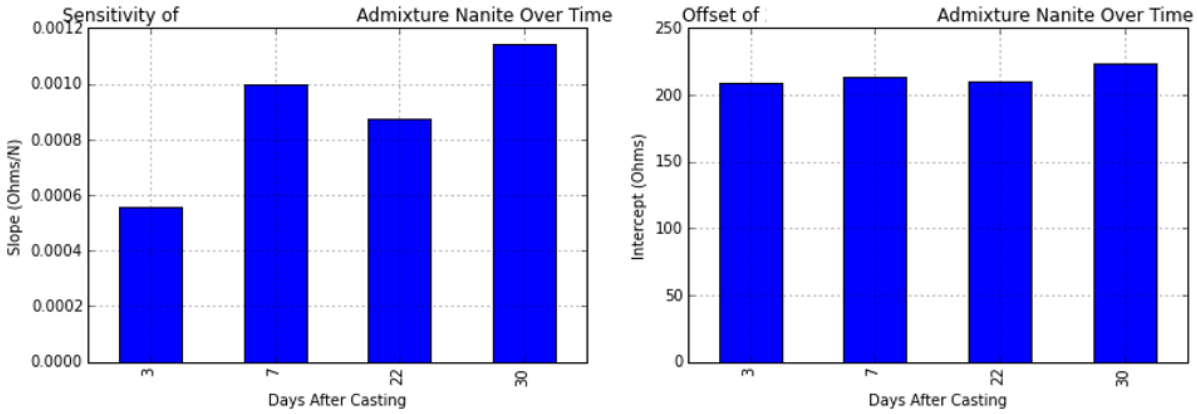

Figure 63: Evolution of impedance response

The nanostructure of set cement was studied by scanning electron microscope for Nanite specimens prepared with various formulations. Chips were taken from the cube interior and dried in a 55°C oven for 4 hours. Individual carbon nanotubes were not discernable from calcium silicate hydrate (C-S-H) crystal formations in the cement but were visible primarily as clusters in rifts in the cement or as inclusions in calcium hydroxide (CH) crystals (Figure 64).

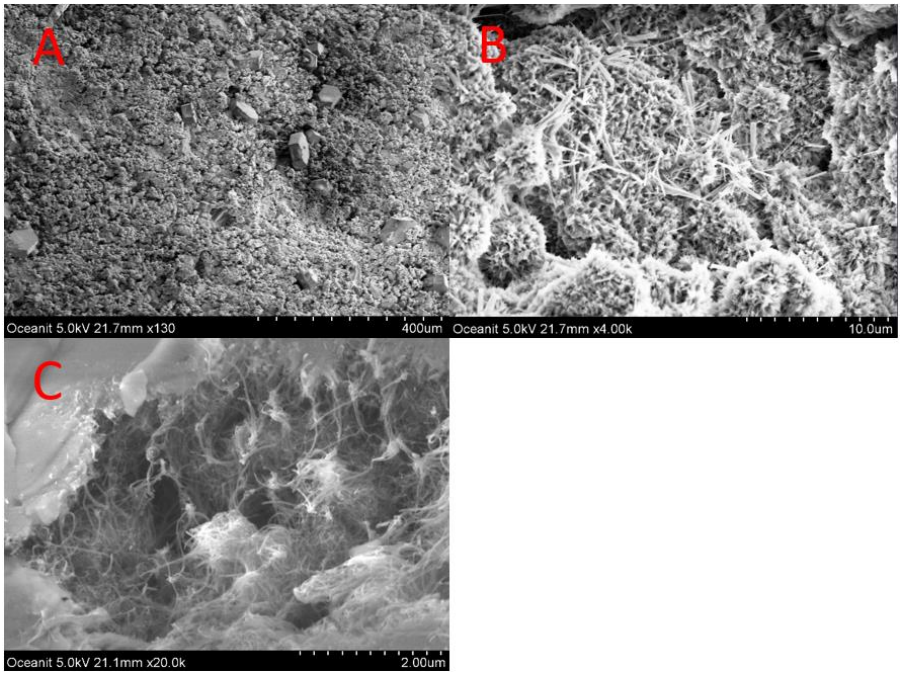

Figure 64: (A) Typical cement facet, (B) C-S-H crystal formation, (C) CNT cluster as inclusion in a CH crystal

The SEM in Figure 65 show carbon nanotubes interwoven through the structure of cement acting

as reinforcement and electrical pathways. The surface of a void in the cement is lined with visible carbon nanotubes interspersed with C-S-H.

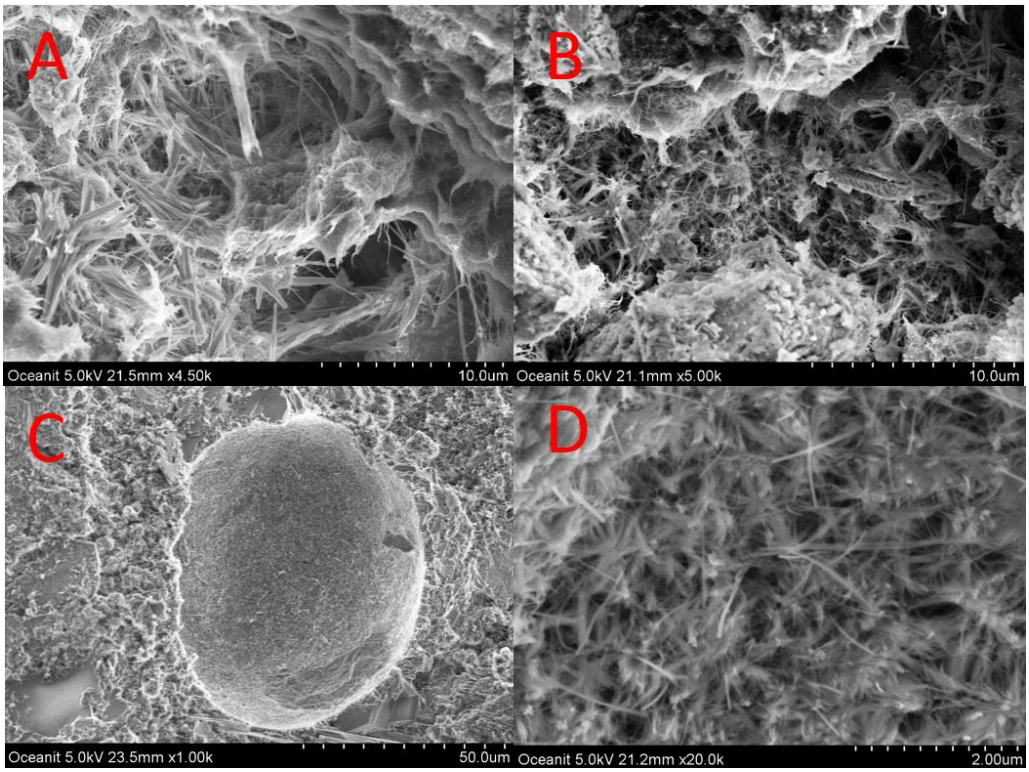

Figure 65: (A,B) Carbon nanotubes interwoven into C-S-H structures, (C) Void in cement with CNTs visible on surface, (D) close up of void showing C-S-H and CNT structures.

Quarter 8: Period End Date September 30, 2015

Investigation of Nanite for Gamma ray/Neutron detection

Oceanit initiated investigation into using radiographic methods for concrete characterization. Our proposal was to use embedded neutron capture targets, such as boron, in concrete. The boron would then capture neutrons and emit gamma rays, which would be detected by a gamma ray logger. The proposed method would require the neutrons to pass through the pipe and then into the cement as shown in Figure 66. Neutrons would be absorbed, transmitted, and reflected through each material to varying degrees. The neutrons that are absorbed would generate gamma rays that are emitted in a characteristic pattern and spectrum. The gamma ray flux would be indicative of the material density.

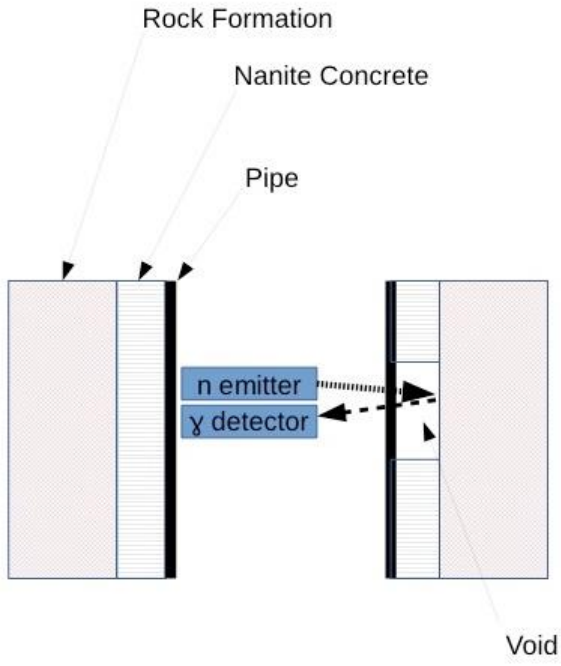

Figure 66: The geometry for the neutron assisted gamma ray detection technique

Since the exterior of the borehole is not readily accessible to instrumentation, both the source and the detector need to be inside the pipe. Thus, the neutron source and the gamma ray detector will be inside the pipe.

We have:

- Investigated prospective materials to enhance cement neutron sensitivity
- Began conceptual design for neutron/gamma sensitivity test experiments
- Studied applicability of neutron sensitive cement for downhole applications

As a standard neutron capture material, boron remains our material of choice, but we will be continuing to investigate other options in the next few weeks.

The experiments that we need to do fall into the two categories of neutron capture and the transmission of gamma rays through different materials.

One of the most immediate concerns was how well the signal gamma rays could travel through the

pipe. This was addressed by McCalister[8], who showed that the attenuation through steel will not prevent the detection of the gamma rays (Figure 67).

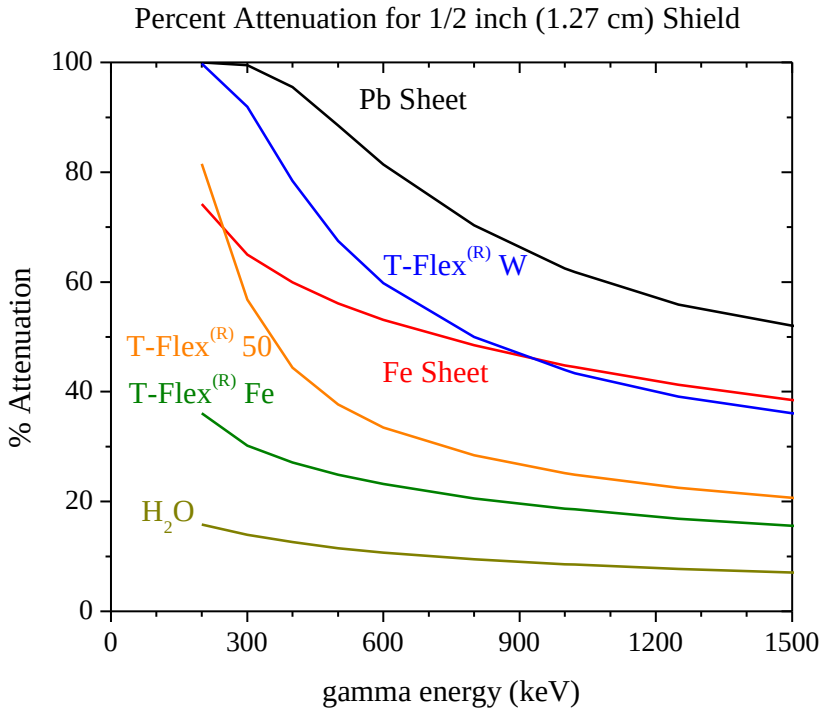

Figure 67: Attenuation of gamma rays in various materials

The next steps are:

1. To find a laboratory that can do the radiographic testing
2. To continue to research appropriate neutron capture materials.
3. To formulate the testing protocol for downhole application.

Nanite Specimen Fabrication Procedures

Improved Cube Molds

Previously, all Nanite cube samples were prepared in disposable mold liners provided by American Cube Mold Inc. These liners had proven a convenient and modular means of sample fabrication. These molds however tend to produce surfaces that are not perfectly flat due to contraction of the cement and the formation of vacuum pockets within the mold. When these samples are compressed in the Instron machine, even when conformal pads are used, the stress distribution does not appear to be uniform. We believe that this surface irregularity is partly responsible for inconsistent early test results. Additionally, testing with 2-wire electrodes embedded into the cubes showed optimal response with the electrodes laying in the plane perpendicular to the force

[8] McCalister, "Gamma Ray Attenuation Properties of Common Shielding Materials," PG Research Foundation, Inc. 1955 University Lane Lisle, IL 60532, USA http://www.eichrom.com/PDF/gamma-ray-attenuation-white-paper-by-d.m.-rev-4.pdf

while samples with mesh electrodes performed best with the electric field parallel to the force applied. Some later samples prepared in the old mold liners had their faces sanded to a uniform flat surface before testing and showed contrary results for the wire electrodes. We expect that stress concentration around the outside edge for the cube (due to a concave surface) resulted in a change in the stress orientation at the cube center.

New cube molds consisting of thick polyethylene plates procured from the same vendor have produced far higher quality test cubes with flat and parallel faces. Cubes produced with the new molds do not require a conformal load pad and testing is performed with cubes clamped in the Instron between two stiff acrylic plates for electrical isolation from the test equipment. Results with the new molds have exceeded expectations and more will be procured to expand sample production capability.

The adoption of mesh electrodes, while more labor intensive to fabricate, has reduced the risk of electrode de-bonding from the cement while also providing a larger electrical test volume effectively reducing the dependence of set cement homogeneity.

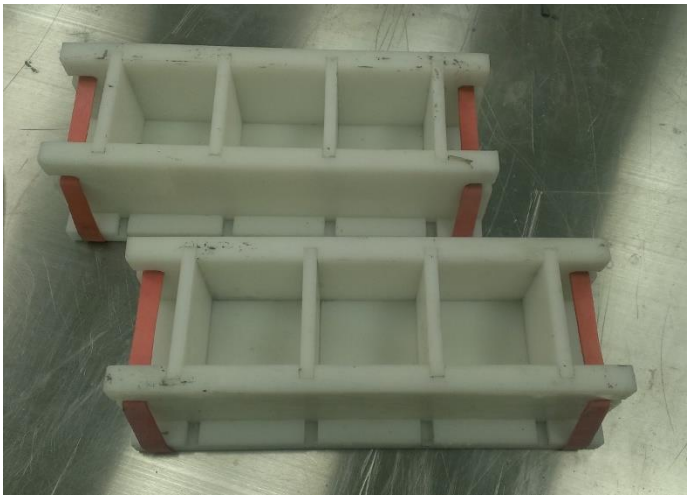

Figure 68: Polyethylene cube modes from American Cube Mold Inc.

Water Bath Curing

The API 10B recommended practice for cement cube curing is to immerse sealed molds in a water bath below 66 °C. Nanite cubes for resistivity testing contain protruding electrodes which preclude the use of fully sealed molds. Early specimens were cured in air tight boxes with a 100% RH environment. The boxes were placed in a 60 °C oven for 24 hrs and subsequently stored sealed with high humidity until demolding and testing. Tracking the ambient temperature in the box while oven curing exceeded 80 °C at around 6 hrs as the cement slurry enters the hardening stage indicating that the sample temperatures may approach 100 °C. This high temperature may affect the ultimate material properties so clearly a water bath provides a thermal reservoir important to the process as a heat sink.

The revised curing procedure is to place the unsealed molds in a sealed, humid container for 24 hours at room temperature to avoid excessive heating from the cement hardening reactions. After 24 hrs the cubes are de-molded and placed in a saturated lime bath at room temperature for 28 days in accordance with ASTM-C109 for cement cube testing. Cement cubes fabricated this way have demonstrated more uniform electro-mechanical properties than any previously attempted

technique.

Admixture Scale-up

Oceanit has finalized the Nanite admixture formulation and is currently developing a process to scale production up from 500 mL batch sizes to many liters. Small batches of admixture must be homogenized for several hours using an ice water batch to maintain constant process temperature. For larger batch sizes a circulating cooling water system is being designed. Several 1 L batches have been prepared so far using a setup capable of processing 4 L.

Admixture production scale-up is important to meet the demands of planned testing at external laboratories.

Nanite Electrical Resistivity Modelling

Nanite Load Response Geometric Effects

To characterizing the sensitivity of Nanite bulk resistivity it is important to carefully exclude other factors influencing the measurement. The interfacial region between embedded or surface electrodes varies considerably depending on the condition of the contact and the load applied. In most practical cases the surface effects are neglected, however, to precisely measure bulk properties of the cement we must perform 4-point Wenner array style electrical measurements to remove the effects of electrode contact resistance. In the case of 2" cement cubes with embedded electrodes we attach surface electrodes to the outer faces of the cube in parallel to the interior electrode planes. The surface electrodes consist of copper sheet completely covering the cube surface with a thin layer of EKG coupling gel between the copper and cement to improve electrical contact. The top and bottom surface electrodes are used to source a roughly uniform AC current density through the bulk of the cube. The parallel mesh or wire electrodes are used to sense the electric field within the sample. The voltage across the inner electrodes is made with a high impedance instrument making the system essentially immune to contact resistance. Since our standard resistivity tool does not yet have 4-point measurement capability, the PARSTAT 2273 potentiostat is used. The PARSTAT, while capable of performing precise 4-point measurement sweeps, does not natively have the capability to make time domain measurements of AC impedance. By using a cyclic load profile to compress the sample in the Instron test machine we can match peak locations in the data and interpolate the PARSTAT data onto the Instron time axis using custom post processing software. This procedure is cumbersome but has produced reasonably good results allowing the impedance sensitivity of the bulk cement to be measured.

Besides the effect of contact resistance, it is also important to consider the change in resistance do to the geometrical changes in the sample shape under compression. To understand the scope of this effect we perform a perturbation analysis on the overall resistance of the sample. We treat the Nanite sample as an Ohmic resistor with homogeneous and isotropic bulk resistivity, ρ. The resistance for of a prismatic volume of length l and cross section A is given by:

$$R = \frac{\rho l}{A}$$

When a uniform stress σ_z is applied axially to the sample with linear elasticity a strain $\varepsilon_z = \frac{\sigma_z}{E}$ for Young's Modulus E. Since the sides of the sample are unconstrained we must also include the Poisson ratio, ν.

$$\varepsilon_z = \frac{1}{E}\left[\sigma_z - \nu\left(\sigma_y + \sigma_z\right)\right]$$

$$\varepsilon_y = \frac{1}{E}\left[\sigma_y - \nu(\sigma_x + \sigma_z)\right]$$

$$\varepsilon_z = \frac{1}{E}\left[\sigma_z - \nu\left(\sigma_x + \sigma_y\right)\right]$$

The sensitivity of R to small perturbations in stress is given by:

$$\frac{1}{R}\left(\frac{\partial R}{\partial \sigma_z}\right) = \frac{1}{\rho}\left(\frac{\partial \rho}{\partial \sigma_z}\right) + \frac{1}{3K}$$

Where $K = \frac{E}{3(1-2\nu)}$ is the bulk modulus of the material.

Figure 69: Nanite 2" cube specimen with grid electrodes under test

Nanite Compressive Modulus Estimation

Accurate strain gauge measurements within the cement sample are necessary to accurately measure the elastic moduli of Nanite. The Instron mechanical testing machine does measure crosshead displacement however resolution is limited and the elastic properties of the load cell and sample mating apparatus must be included in series with the cement sample.

The extension to force relationship was measured for the machine with and without a cement sample installed. With no cement cube the extension was -0.01648 ± 0.00005 mm/kN. With cement the response is -0.01343 ± 0.00004 mm/kN and subtracting yields the cement elasticity with the series effect the machine removed as 0.00305 ± 0.00006 mm/kN. Conversion to units of stress and strain using sample geometry gives a Young's Modulus of 6.4 ± 0.1 GPa. While this result is a factor of two lower than the expected modulus of cement it provides, a reasonable lower limit considering the systematic challenges in measurement for a 2" cube form factor without an embedded strain gauge.

Nanite Load Response Modelling

The development of a physics model for Nanite piezo-resistivity requires a detailed understanding of the actual stresses present within the sample in a particular kind of load. Compressive loading of a 2" Nanite cube ideally results in a uniform axial stress field within the sample. In practice, however the boundary effects result in significant divergence. The contact surfaces with contact friction with the load pads cannot deform in the same manner as the central plane of the sample resulting in additional stress concentration at the cube corners. The induced stresses were modeled in COMSOL and as we see in Figure 70 the stress is uniform along the cube central plane where the electrodes are generally inserted. It is clearly important to keep electrically sensitive area away from the load faces while studying the bulk properties of cement.

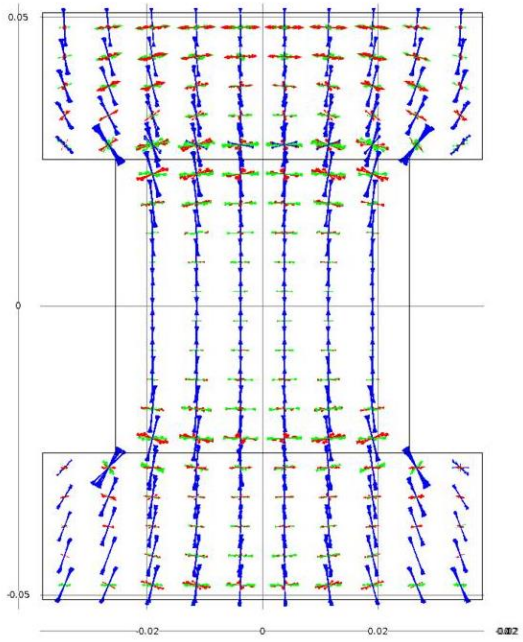

Figure 70: Principal stresses under compression show relatively uniform axial stress within the cube center in the sensitive region between the electrodes.

Nanite Data Acquisition and Analysis Techniques

Data Processing and Analytics

The large volume of diverse experimental data generated over the course of the project thus far has posed a serious challenge. As the formulations, procedures, electronics, and software have evolved over the course of the project, eventually reaching a relatively mature state, we are confronted with a heterogeneous library of useful data. For example, it was recently useful to retest cement samples fabricated on 2014-11-17 and track the change in the aging material. Advancements in our data analysis software now allow us to process and integrate the data collected using now obsolete procedures and instruments.

Using the Pandas[9] data analysis library for the Python programming language we can now load all past test results into a database-like data structure and apply many data reduction and analysis

[9] http://pandas.pydata.org/

techniques. We also make heavy use of the IPython Notebook and Jupyter[10] to perform data analysis workflows in a digital notebook with all states of the process and computation recorded with inline documentation. The evolution of specimen behavior is tracked over time and plotted in various useful formats.

Figure 71 shows a snapshot of all the experiments performed on samples fabricated in the last four months and with further queries this dataset can be sliced into useful subsets for study. Each test consists of metadata describing the test conditions and sample properties along with load response data such as shown in Figure 72. The slope of the impedance vs load data gives the piezo-resistive modulus of the sample. Figure 73 shows an example repeatability test for successive measurements on a single sample. Variations in the impedance response over the sample curing process are presented in Figure 74.

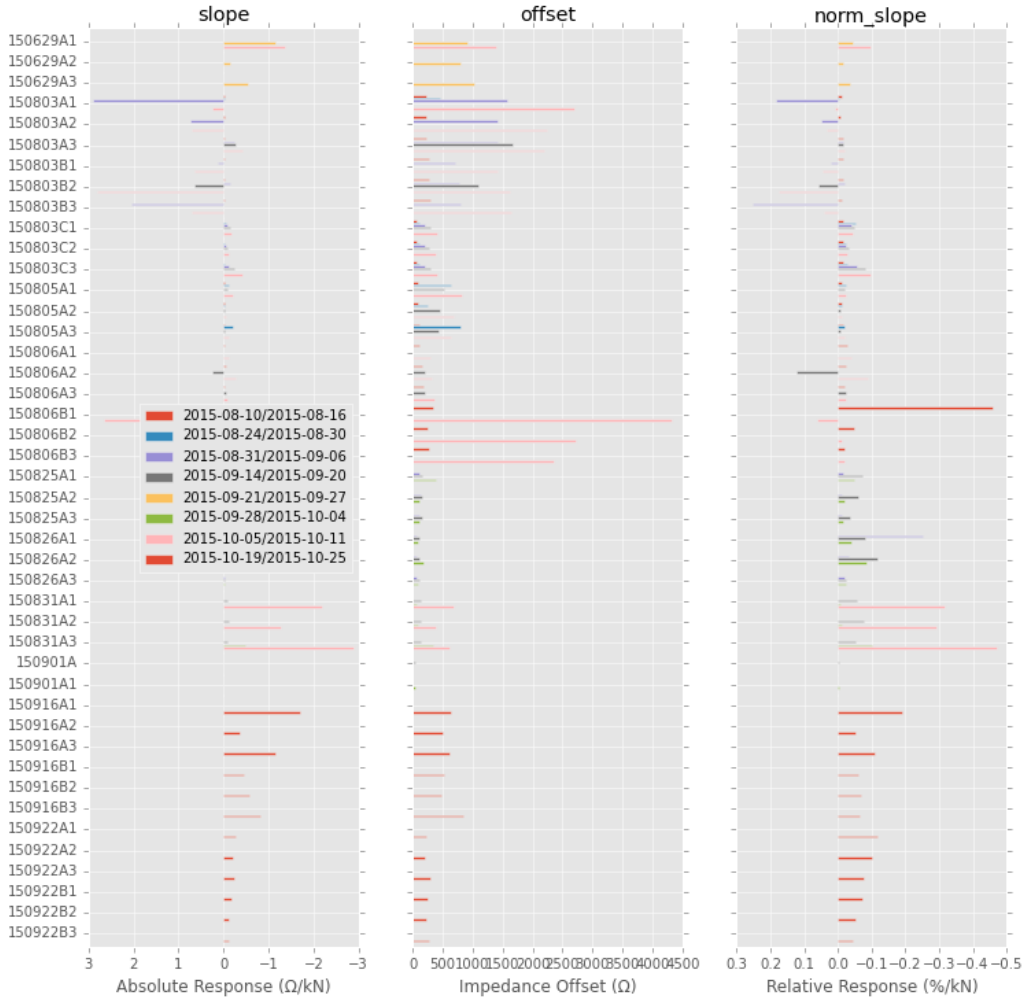

Figure 71: Aggregated results for selected samples produced over the last four months. The dataset can easily be sliced into subsets to look at trends overtime in particular sample types.

[10] http://jupyter.org/

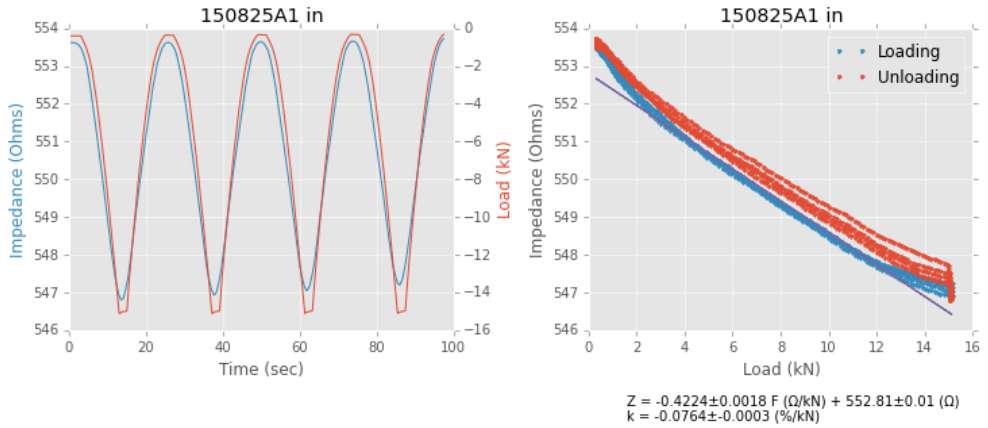

Figure 72: Typical load response data set showing the electrical response to load on the left and impedance as a function of load on the right. The slope of the right graph provides the piezo-resistive modulus of the material.

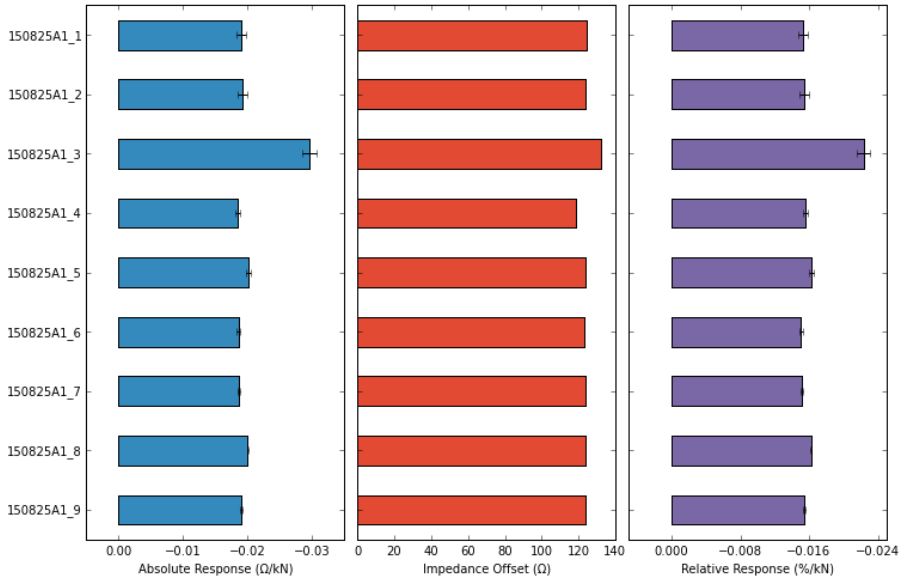

Figure 73: Load response measurements on a single sample yield a repeatability error of 4%

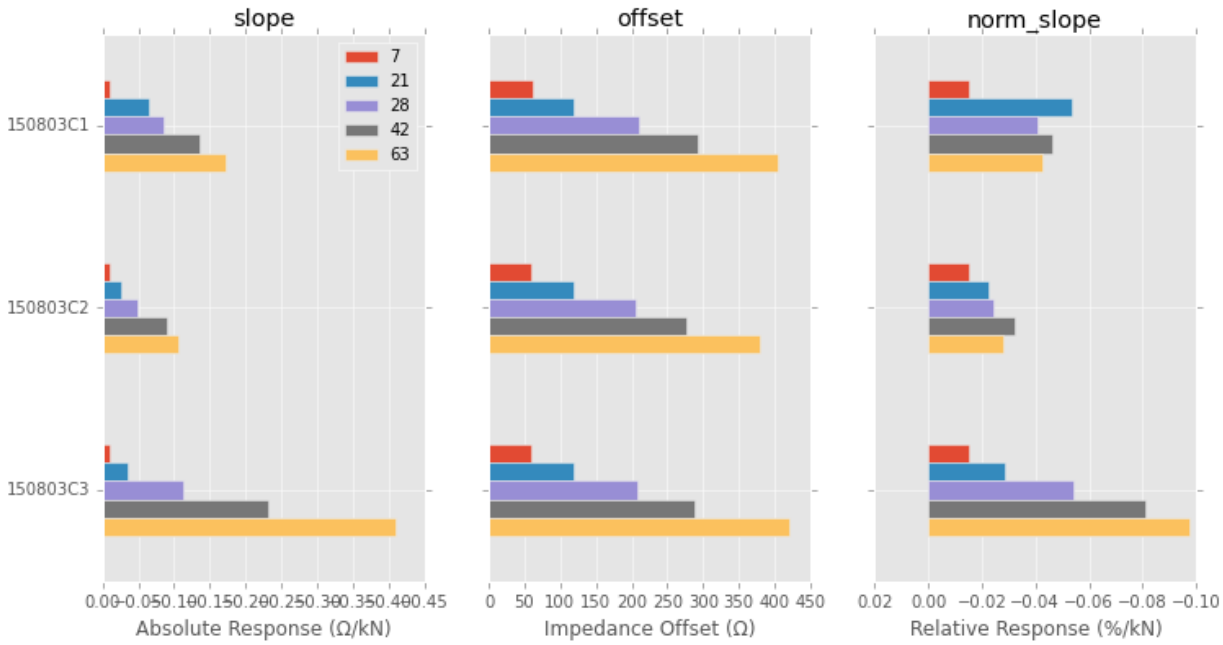

Figure 74: Tracking the Nanite piezo-resistive load response as a function of sample age

High-resolution, High-speed resistivity Tool

Practical measurements of the Nanite material's response to mechanical loading is limited by the resolution of the electrical resistivity tool. The impedance analyzer rev 3 resolution is limited to approximately 0.01% by the 12-bit digitizer and also suffers from an intrinsic duty cycle of less than 7%. Oceanit is presently developing an improved impedance analyzer based on the open hardware Red Pitaya instrumentation platform. The 125 MS/sec 14-bit digitizers are expected to increase the analyzer resolution by a factor of four while allowing for higher duty cycles and higher sample rate acquisition. The presence of dual ADC channels will allow four wire impedance measurements with the addition new front-end electronics under development.

An early prototype of the Pitaya based data acquisition software shows a promising increase in resolution, however, at the moment the duty cycle limitations of the rev 3 board still persist. We hope to overcome the duty cycle limitations imposed by the data buffer sizes in our ongoing software development effort.

Four-wire Electrical Impedance Measurements

Oceanit has developed and optimized configuration for measurement of cement bulk resistivity dependence to load. In a two-wire electrical measurement a current must flow through the interface between electrodes and the material which has a non-zero contact resistance. This resistance produces an additional voltage drop across the contact interface adding in series to the voltage drop of interest across the cube. Thus all two-wire measurements necessarily include and additive contribution from the contact resistance which may itself depend on pressure, temperature, humidity, bond quality, etc. independent of those properties of the cement under study. In many applications, particularly in a field deployed system, the contact resistance can be characterized as part of the system and its effects neglected. However, in a laboratory environment it is essential to the understanding of the material properties that they be measured in isolation.

The addition of two more electrodes can practically eliminate contact resistance from the

measurement. One pair of electrodes (outer) is used to source an AC current across the sample while a secondary pair of electrodes measure that voltage across a particular volume of cement. Since source current is independently measured, the contact resistance between the source electrodes and the cement is of no consequence and does not impede current flow. The sense electrodes only measure the voltage across the specimen and carry no current so no voltage drop develops across an arbitrary contact resistance provided that the contact resistance is much smaller than the voltmeter input impedance.

In the case of Nanite, a typical contact resistance for young samples is 47±4 Ω which is 10 % of the sample impedance while also possessing a sizable load response in addition to that of the cement. This demonstrates that the for a 1MΩ sense voltage input impedance the contact resistance in a 4-wire measurement can be neglected.

Copper sheets cut to 2”x2” with soldered connections to the test leads are used as the source electrodes. To ensure high contact uniformity between the cement and unbonded copper we apply a thin layer of Spectra 360 EKG contact gel between the cement face and copper. The resulting contact resistance is highly dependent on applied pressure but does not influence the measurement as discussed above. Figure 76 illustrates the 4-wire setup for mesh grid electrodes while Figure 75 shows the actual test setup with two inner wire electrodes and copper sheet outer electrodes. It was found that with a uniform current density applied throughout the sample that the choice of parallel wire or mesh grid electrodes did not greatly affect the measurement.

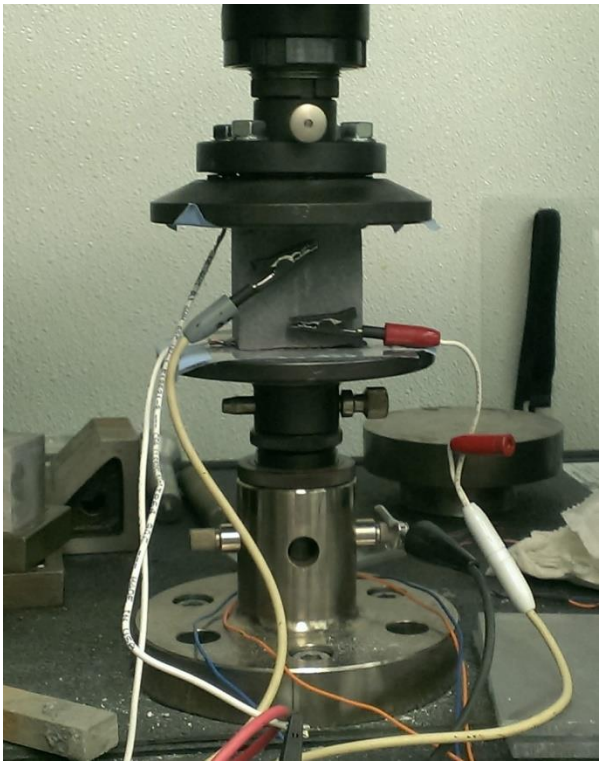

Figure 75: 4-wire Electrical Impedance Testing using copper surface electrodes and gel couplant.

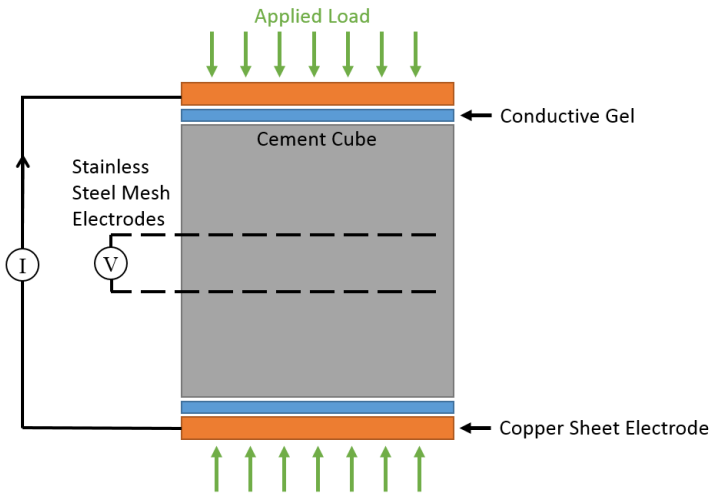

Figure 76: Four wire electrical impedance measurements allow determination of the material's bulk resistance without the effects of electrode contact resistance

Quarter 9: Period End Date December 31, 2015

Nanite Electrical Resistivity Modelling

Nanite Electrical Resistivity Temperature Sensitivity

The dependence of Nanite impedance on temperature was tracked for samples with a variety of formulations. The samples were placed in a temperature regulated oven and allowed to heat until a reference sample's core temperature reached equilibrium with the oven thermostat. The reference cube had a hole drilled to its center where a thermocouple was cemented in place.

In the first experiment, three samples each of four different formulations including one batch of Nanite mortar with sand aggregate were tested. Figure 77 shows the relative impedance shift of the samples tested at four points between 30°C and 90°C. While the three mortar samples at the top show a lower dependence on temperature, the remaining three Nanite formulations show no statistically significant difference in response.

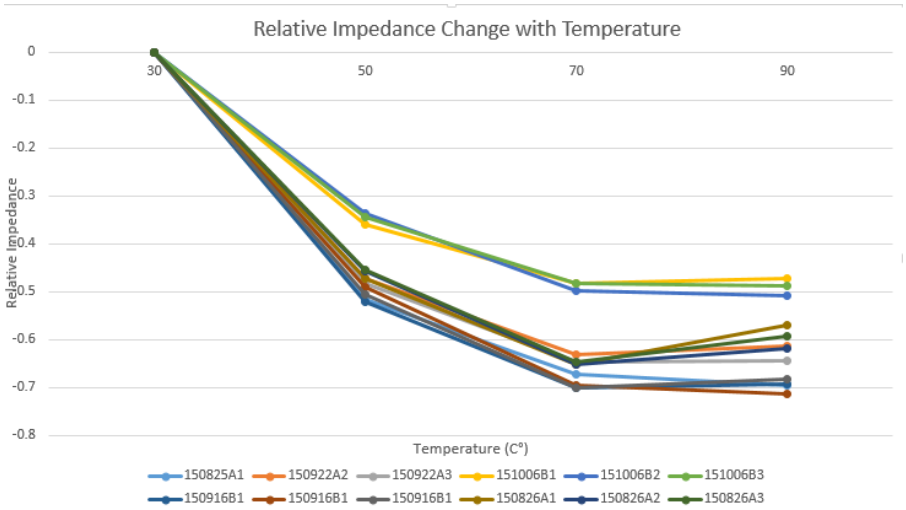

Figure 77: The variation with temperature of 12 Nanite cubes was tracked in a temperature controlled oven. The upper three traces are for cement with aggregate while the other nine samples showed no statistically significant difference in response.

The temperature dependence was measured again from 30°C to 60°C with 5° steps for one sample chosen from each formulation previously tested. Additionally, we chilled each sample to 4°C to provide a lower temperature data point. Figure 78 shows that although the 4° measurement was unsuccessful, there is a linear dependence of impedance with temperature of about 1.3%/C° in the range 30-60°C. The 4°C test was performed out of sequence and under different humidity conditions as those performed in the oven.

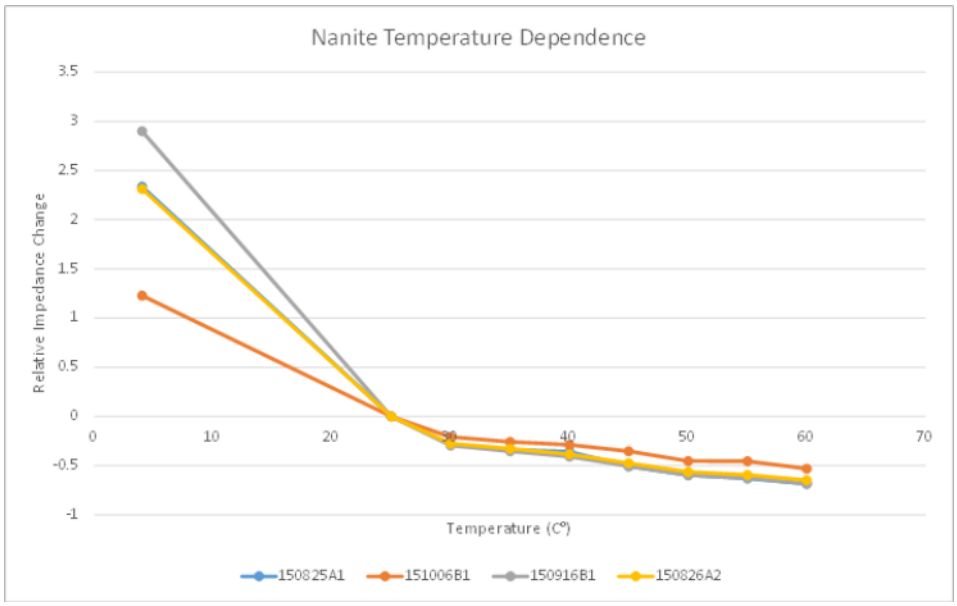

Figure 78: The temperature dependence was tracked with smaller step sizes for a subset of the Nanite cubes used in the first experiment.

This experiment provides a useful scale for the temperature dependence effect of Nanite. Since no difference is seen in the temperature coefficient for Nanite vs base cement, it is possible to use base cement or different concentrations of Nanite to control for temperature sensitivity.

Alternative Nanite Form Factor Testing

Oceanit is investigating the preparation of Nanite samples in form factors other than 2" cubes for use with alternative testing and deployment modes. Nanite samples were cast in a 4"x4"x2" form factor with 0.5" electrode mesh spacing, roughly equivalent to four connected 2" cubes. Mechanical and electrical testing on these specimens will verify the impedance response scaling relationships that are needed to deploy Nanite in arbitrary form factors such as a pipe casing annulus or plug.

Defoaming Agent Testing

Oceanit has modified the Nanite admixture formulation to include a defoaming agent. Inclusion of this chemical has completely removed the foaming behavior that was observed during admixture homogenization and cement mixing. Without the buildup of a foam layer we observed no separation of the admixture during mixing and no deposition of nanomaterials on the walls of the mixing container, which have proven problematic in early sample preparation.

Cement made from the new admixture including the defoamer was significantly less viscous while blending according to API standards, and at low admixture concentrations behaved indistinguishably from base cement. Previously problematic Nanite cement was prepared and cast without incident. An alternate Nanite sample was mixed and cast for the first time with the new admixture. Preliminary testing of these samples indicates no adverse impact on cement performance. Since the first samples have not yet reached 28 days curing, only limited testing has been performed.

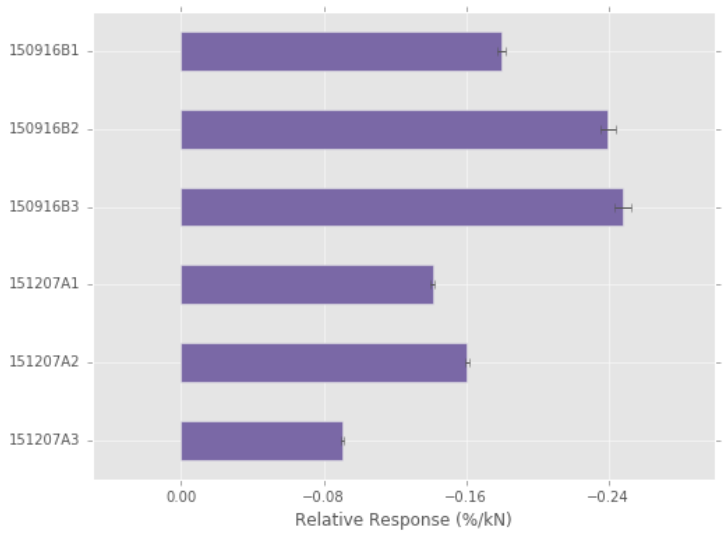

Figure 79: Nanite without defoamer (150916B) compared to Nanite with defoamer (151207A).

Figure 79 shows a comparison of the load response for Nanite samples prepared with and without defoaming agent. The defoamed cement shows a lower although still respectable response of 0.13%/kN, however it is important to note that the defoamed results are preliminary and steps were not taken to control humidity temperature or sample age in this comparison.

Nanite Data Acquisition and Analysis Techniques

High-resolution, High-speed resistivity Tool

Oceanit has been investigating the use of the Red Pitaya open hardware platform as a basis for a high-speed, high-resolution electrical impedance tool. While this Pitaya is a powerful computing and data acquisition platform, we have encountered significant technical issues in its use for this application. While in principle the Pitaya can meet our speed requirements with its 125 MS/sec ADCs, the existing firmware and software provided by the hardware vendor are only suitable for acquisition of a 1 millisecond sampling window, the same as our custom rev 3 impedance analyzer.

While we believe that a 10 μsec sampling window with impedance acquisition rates is technically possible with this hardware, we have decided that the level of effort involved is better directed elsewhere at the present. As an alternative, we are in the process of producing revision 4 of the Oceanit impedance analyzer hardware. While still subject to the same sample window limitations of the rev 3, the new hardware is able to sample the impedance with an improvement over the previous design with improved noise performance. The new design also incorporates new software programmable gain and calibration modes and other general optimizations based on our extensive experience with the previous design.

The new design also features an I2C translation chip that allows for multiple boards to reside on a single I2C bus. The Impedance Converter from Analog Devices, which forms the heart of the system, has a fixed address. Thus the addition of the I2C translation chip allows one or more I2C devices to be translated to a different address.

The form factor of the board was designed so it could mount and be stacked directly on top of a Raspberry Pi. This allows for direct control and remote monitoring of the system via the Ethernet

connection on the Pi. Special attention was paid to minimize noise in the design and layout. Full ground and power planes were used along with separate supplies for both digital and analog circuitry. Sensitive analog components were grouped closely together and kept away from digital components and control lines.

Electrode Separation Dependence

The application of Nanite cement sensors in form factors other than the 2" cubes used for laboratory testing requires the development of a more complete model of electrical resistivity of the material. To verify the previously assumed bulk resistivity scaling behavior we measured the variations in measured impedance for various electrode grid spacing in 2" Nanite cubes. Three cubes previously fabricated with 4 mesh electrodes each were retested in a 4-wire test configuration using the previously described method of surface electrodes with conductive gel as the excitation electrodes and various permutations of the four inner grid electrodes to sense electric field in the sample. The electrodes of each cube were labeled a, b, c, and d and each electrode pair was individually tested for impedance response under load in the Instron machine. The impedance-load responses of each of the samples with different electrode configurations are shown in Figure 80.

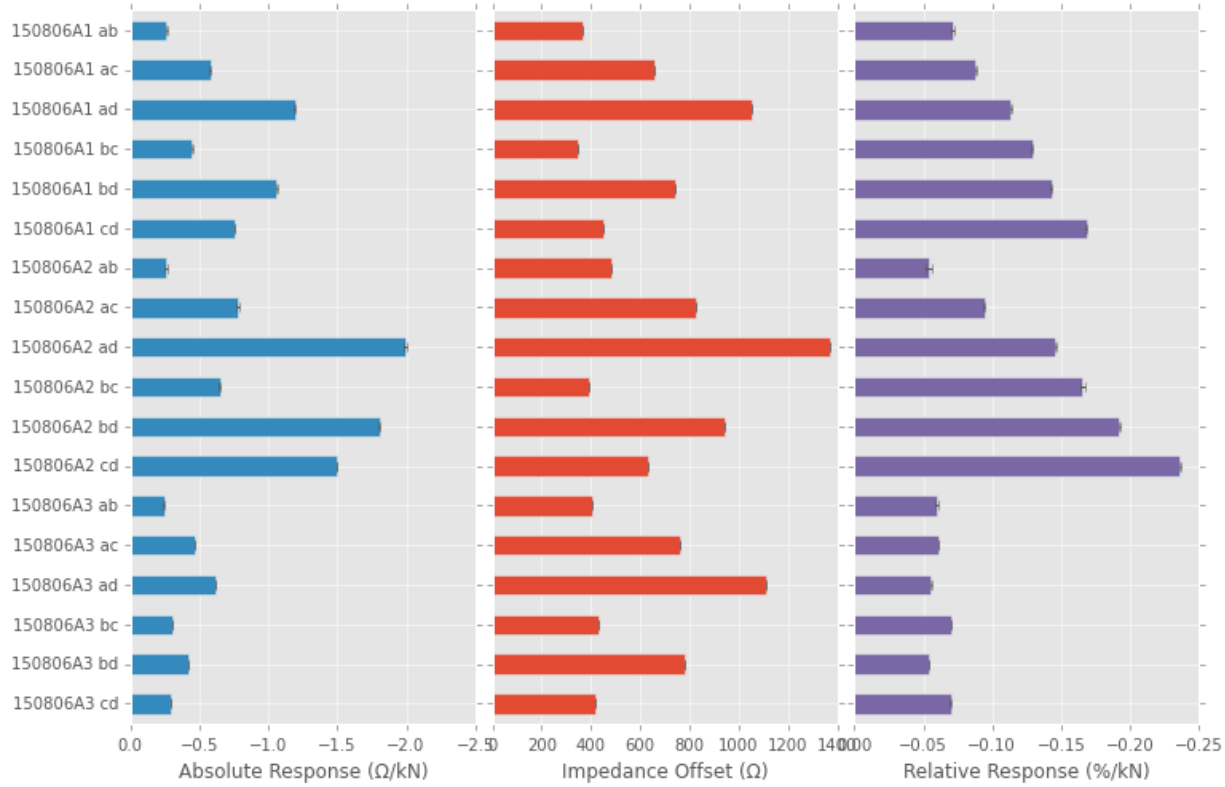

Figure 80: Load response (left), impedance offset (middle), and relative response (right) for three samples with six different electrode configurations from four electrodes (labeled a, b, c, and d).

By comparing the results from the different samples with the electrode pair configuration, it was found that the offset impedance and relative response both depended on the electrode pair selection. The effect of spacing and electrode selection were further analyzed by averaging the offset and relative response for electrode pairs with the same spacing or that shared individual electrodes. The impedance offset was found to correlate directly with the electrode spacing, which

can be explained by simply having a proportionately longer resistance path through the material. However, the relative response of impedance to load did not show a dependence on electrode spacing, which is promising for scaling the impedance measurement method to determine applied load. There was also an effect on the relative response to load of the individual electrodes used in pairs. The individual electrodes had no apparent effect on the offset aside from the average electrode spacing (a=d>b=c). However, the relative impedance response to load increased with electrode distance from one face of the test cube. These findings are summarized by the graphs in Figure 81.

Figure 81: Impedance offset (left) and relative impedance response to load (right) for electrode pairs (top), electrode spacing (center), and individual electrodes (bottom).

Subscale Proof Testing

Oceanit is presently researching potential pathways for field deployment of Nanite in oil and gas wells. One promising pathway recommended by an advisor with one of our JIP partners is to develop Nanite for compatibility with existing cased-hole formation resistivity (CHFR) tools. The presence of a casing pipe precludes the use of traditional formation resistivity tools due to the presence of a continuous low impedance path and led to the development of modern CHFR tools. Figure 82 depicts the electrical current paths in cased-hole logging. When current is injected into the casing pipe by the top electrode it returns to the surface directly via the casing pipe and indirectly via leakage from the pipe into the formation. Due to the finite, albeit low, resistivity of the casing pipe in conjunction with the resistivity of the formation there is a continuous voltage gradient present along the pipe. The CHFR technique relies on both exquisite measurement of nano-volt/foot scale potentials and μΩ scale casing resistance calibrations in a noisy downhole environment.

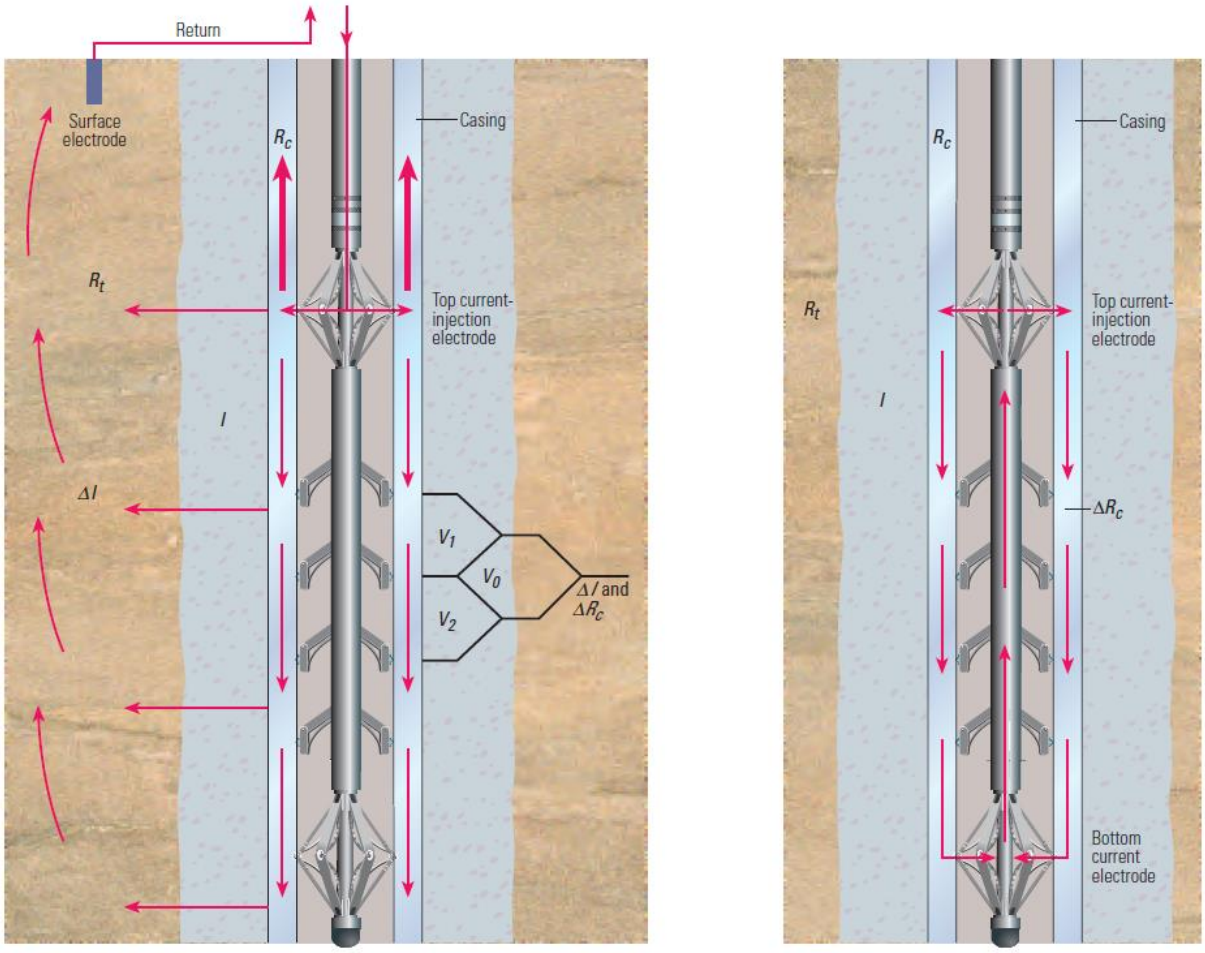

Figure 82: Behind-casing resistivity logging tool operating principles.[11]

The modified electrical resistivity characteristics of Nanite may be used in conjunction with such resistivity logging tools to indicate the presence and condition of downhole cement not currently

[11] K. Aulia, et al., "Resistivity behind Casing", Oilfield Review, Spring 2001

distinguishable from the formation with traditional well cement.

Oceanit is currently developing concepts for a laboratory-scale proof of principle demonstration of Nanite cement electrical interrogation behind a steel casing pipe. We are investigating the use of sensitive laboratory instruments to make the necessary precision resistivity measurements in an in-house borehole analogue apparatus. The borehole analogue will allow us to test the electrical an acoustic performance of Nanite and related products in the annulus between a casing pipe and simulated formation. Figure 83 shows two concepts for a simulation of defect detection behind steel casing pipe in the laboratory. The first configuration allows the placement of defects in Nanite located behind a steel plate without the sensor size restrictions of a pipe. The second configuration would allow a cement annulus to be tested within a simulated formation.

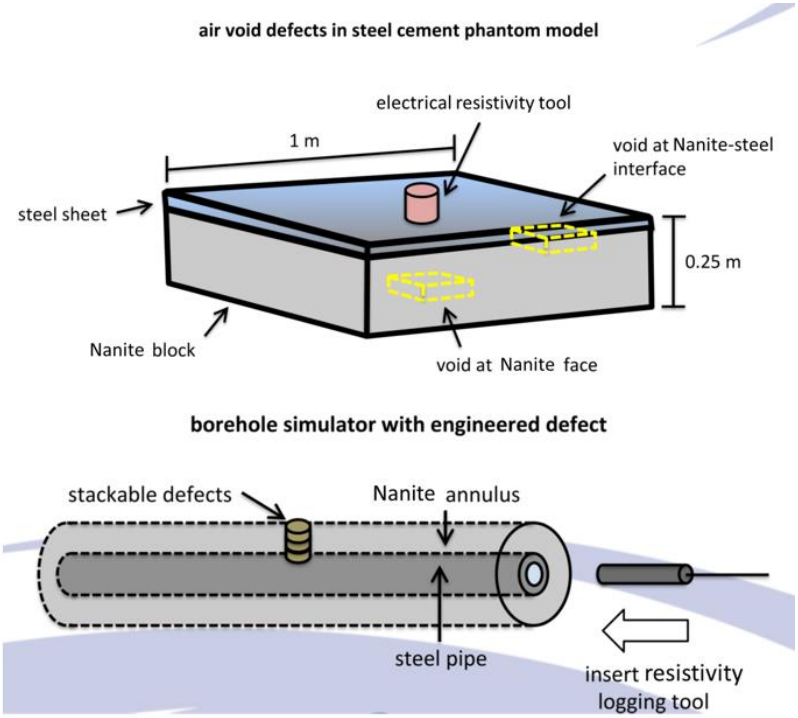

Figure 83: Cement behind case simulator concepts

Quarter 10: Period End Date March 31, 2016

Nanite Electrical Resistivity Modelling

Nanite Admixture Separation

In this period Oceanit investigated the contribution of nanomaterials of different densities to the electrical impedance response to load. While the Nanite admixture is a relatively stable dispersion, some separation is observed when the mixture is stored. The admixture is always blended well before use in preparation of cement specimens. A 1L batch of standard Nanite admixture was allowed to settle for one week before being carefully decanted into two 0.5L samples consisting of the top and bottom fractions of the settled admixture. The bottom fraction contains the higher density CNT agglomerates while the top fraction presumably contains more of the well dispersed CNTs.

Admixture from the top and bottom fractions was reconstituted with dispersant solution to prepare admixtures of nominal CNT content (although in reality the concentration is lower due to the retained water). The reconstituted admixtures were used to prepare two batches of 2" cement cubes for load response testing.

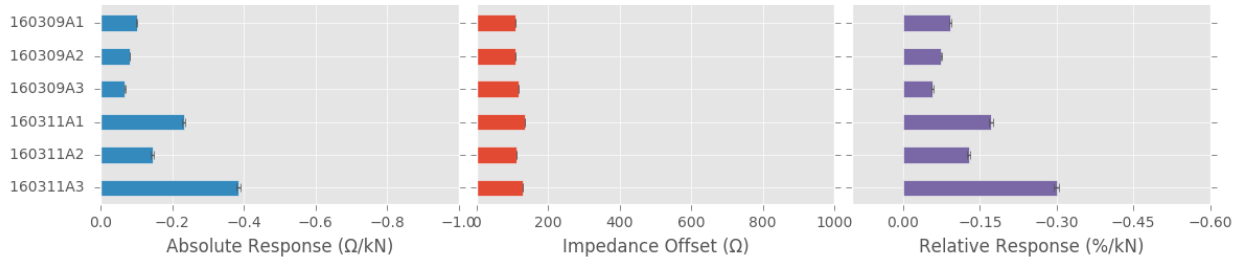

Figure 84: Load response testing results for a batch of 2" cement cubes with CNT admixture content.

After 28 days of curing the cubes were tested for their impedance response to load, Figure 84. We see that the bottom fraction has approximately twice the impedance response of the top fraction. Recall that these samples for each fraction were prepared with the same concentration of carbon nanotubes. Thus, the difference in electrical responsivity is attributable to the morphology of the CNTs. We believe that the bottom fraction (better performing) consisted of larger and higher density agglomerations of nanotubes while the top contains smaller and individually dispersed tubes. This is contrary to the expectation that a well dispersed network of CNTs is responsible for load response. These results are preliminary and warrant a more detailed investigation into the role of nanotube agglomeration in composite behavior.

Alternative Cement Additive Characterization

In our continuing efforts to optimize the sensitivity of Nanite cement to load, Oceanit investigated several alternative nanomaterial fillers and dispersing agents that have been described in the recent self-sensing cement literature.

With our standard multiwall carbon nanotube Nanite formulation as a control we prepared cement cubes with single wall carbon nanotubes and chopped carbon fiber (CF). We also dispersed MWCNTs in alternative dispersants, and mixed with both homogenization and sonication methods.

Alternative Nanite Form Factor Testing

Nanite samples were cast in a 4”x4”x2” form factor with 0.5” electrode mesh spacing, roughly equivalent to four connected 2” cubes. The samples were cured for 28 days before testing the electrical impedance response to compressive loading. The response of the two samples were 0.033%/kN and 0.018%/kN, and the mean of 0.025% is consistent with ¼ of the response of a standard 2” cube for a sample with 4x the electrode area. Taken together with the previously reported results for dependence on electrode spacing we believe that electrical impedance response to load scales linearly with the dimensions of the electrode geometry and is characterized by a constant bulk resistivity response curve regardless of geometry. This result means that Nanite is scalable to any desired form factor provided that an impedance tool can be made to cover the relevant impedance range. Our difficulties in measuring the response of different form factors presumably lies in the inability of present instrumentation to probe impedances under 10Ω with adequate SNR. These limitations will be addressed in future experiments and hardware designs.

Nanite Data Acquisition and Analysis Techniques

High-resolution, High-speed resistivity Tool

Oceanit has received and tested fully assembled Rev4 impedance analyzer circuit boards. The new boards have similar capabilities to the previous generation but serve as add on boards to the Raspberry Pi single board computer, Figure 85. The direct hardware connection without the need for a USB interface allows high sample rates. The new boards also have greater flexibility in the selection of range and calibration modes.

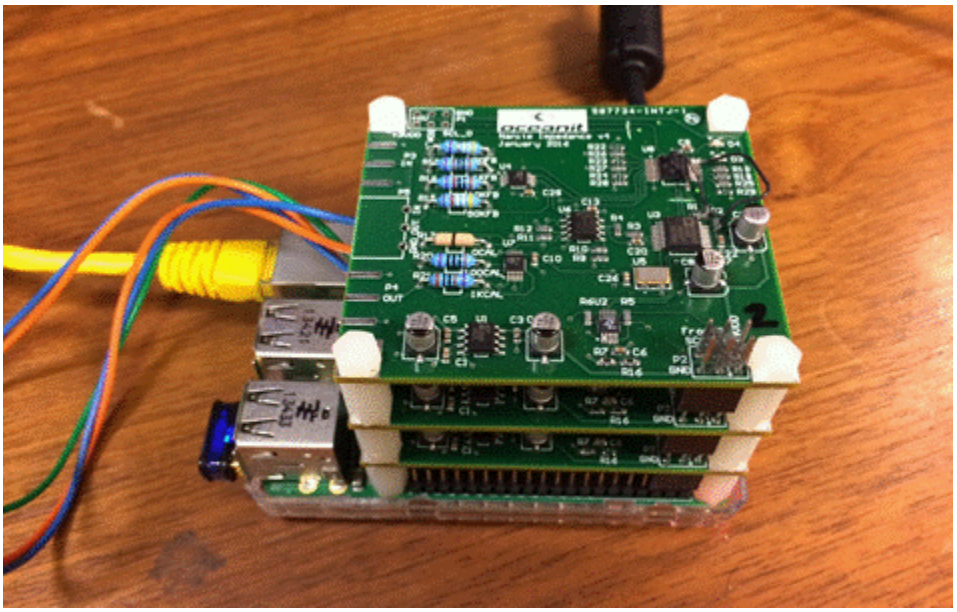

Figure 85: Rev4 of impedance analyzer circuit boards assembled with Raspberry Pi

The impedance analyzer software was modified to operate with the new boards with additional functionality. Since the new boards have an array of calibration resistors, the board can be automatically calibrated in every gain and range mode available. Auto-calibration at the start of data logging is now the default mode of operation. Raw ADC data is also stored in data files since the calibration values applied are not static between sessions. Auto-calibration allows the user to select the most appropriate gain and range configuration for the sample under test without bothering to perform calibration of every configuration manually.

High speed sampling was demonstrated with the ability to synchronously record data from two analyzer boards installed on the same Raspberry Pi.

Since the Raspberry Pi is generally operated without a display, interactions with the hardware are done over a network connection. The ability to run data and web servers on the Raspberry Pi will allow the development of a web based client software in place of a dedicated software client to be installed on a computer. For field operations the device could be controlled via a phone or tablet PC.

Subscale Proof Testing

Oceanit is presently researching potential pathways for field deployment of Nanite in oil and gas wells. In addition to studying the applicability of cased-hole formation resistivity tools to downhole measurement of Nanite resistivity we are also pursuing alternative pathways for electromagnetic interrogation of Nanite. One promising technology is the orthogonal fluxgate detector.

The orthogonal flux gate uses a conductive magnetic micro-wire core, and a small pickup winding coiled around the core. The core is driven by a biased AC excitation current which causes the magnetic material to develop an oscillating azimuthally directed magnetization. The pickup winding detects the component of the magnetic flux along the axis of the micro-wire core.

A non-zero external field aligned with the core axis causes the magnetization vector to periodically rotate in an out of alignment with the pickup winding. Normally the magnetization due to the external field along the axis would stay constant, but under saturation conditions the azimuthal driven field results in a rotation of the magnetization towards the azimuthal plane. This causes the flux to shift and induces a signal in the pickup winding.

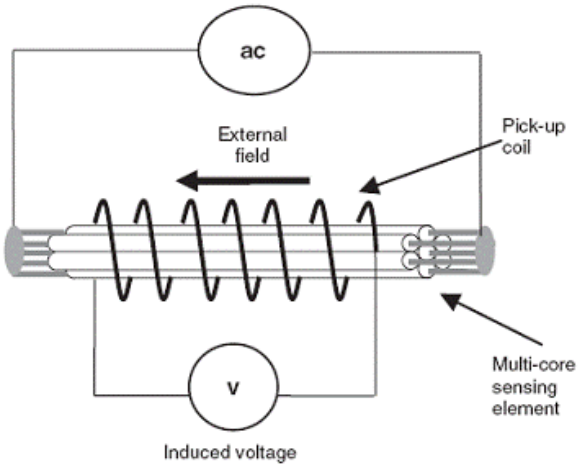

Figure 86: Orthogonal flux gate concept with multi-core sensing element.

Operating in this fashion with a pure AC excitation signal results in a pickup signal with even harmonics of the excitation frequency (i.e., the excitation signal reaches saturation twice per cycle). The second harmonic is often used to provide information about the field. The magnitude of the harmonic is proportional to the externally applied field along the sensor axis, and the phase determines the orientation or sign of the field.

This harmonic detection method is functional but the orthogonal fluxgate is susceptible to partial

saturation of the core (which introduces hysteresis into the output signal), and skin effects (which dampens the magnetization at higher frequencies). The solution to the first of these parasitic effects is to use multi-wire cores, Figure 86. Cores in close proximity to each other cooperate in saturating their respective cores while increasing the effective cross-section of the sensor. The resulting enhancement in sensitivity is greater than that due to areal increase, and exhibits a non-linear character as the number of cores increases.

The skin effect effectively limits the operating frequency to the point at which the increased sensitivity and reduced noise is countered by the increased noise caused by the skin effect limiting the full saturation of the core. The only reasonable solution is to restrict the operating frequency.

The orthogonal flux gate operating in harmonic mode has higher noise than other magnetometer technologies even though the spatial resolution is far greater. It is possible to significantly reduce the noise by operating the fluxgate in fundamental mode.

This mode adds a DC bias to the excitation current. The unipolar saturation means the pickup signal is at the excitation frequency. The noise reduction is empirically found to be an order of magnitude less in fundamental mode compared to harmonic mode. This is purely due to operational issues and is unrelated to the underlying structural details for the sensor.

The orthogonal fluxgate sensor arrays have great potential for mapping the spatial distribution of Nanite casing around the production pipe. The Nanite admixture using CNTs grown using Fe catalysts exhibit much higher permeability than standard cement. The well adhered pipe/Nanite complex should be more effective at shielding the ambient geomagnetic field than regions which are rife with voids. The local magnetic field where there is good coverage of Nanite around the pipe should be lower than regions where the coverage is not as compete.

Additionally, there may be situations where the surrounding geological formation may have deposits with significant magnetic characteristics which can be detected using the same fluxgate sensor array.

Quarter 11: Period End Date June 30, 2016

Admixture for Oilwell Cement Testing

Nanite admixture testing was conducted in the cementing laboratory at Oilfield Testing & Consulting (OTC) at Oceanit's request. Nanite admixture was compared to control slurry for rheology, thickening time, free fluid, fluid loss, and UCA compressive strength. These test were conducted according to API Recommended Practices 10B-2 and 10B-4. The slurry was formulated to give a density of 16 ppg in both the cases of Nanite admixture and control. A retarder was included in the formulations for Nanite and control cement in order to extend the set time to accommodate required conditioning for free fluid and fluid loss tests.

Table 4: Nanite formulation used for outside testing (Formulation #1)

Material	Concentration	Lab Test Amount/ 600 mL	Lot #
Lehigh Class H Cement	100% BWOC	800.63 g	160401
Retarder	0.88% BWOC	7.04 g	2/2/2015
Fresh Water	42.3% BWOC	338.94 g	OTC Distilled

Table 5: Control cement formulation used for outside testing (Formulation #2)

Material	Concentration	Lab Test Amount/ 600 mL	Lot #
Lehigh Class H Cement	100% BWOC	790.64 g	160401
Retarder	0.88% BWOC	6.96 g	2/2/2015
Admixture #46	44.0% BWOC	349.02 g	#16-0525-02

Table 6: Slurry conditioning schedule

#	Target Pressure (psi)	Target Temp (°F)	Time To Temp (min)	Time At Temp (min)	Time To Pressure (min)	Time At Pressure (min)
A	Atmospheric	190	16	30	N/A	N/A
B	1,000	258	30	30	60	30
C	6,237	258	50	Until Set	50	Until Set

An atmospheric viscometer (rheometer) was used to make measurements at the indicated rpm. A heating assembly was used to maintain the temperature ±5°F during testing and to pre- heat the rotor, bob, & cup.

The viscometer was initially rotating at 3 rpm as the cup was raised. Each reading was stabilized for 10 seconds before recording the dial reading. The temperature was taken before the first reading and after the final reading (before and after performing gel strength tests). Readings were taken first in ascending order followed by descending order and the ratio of the readings is calculated.

The ratio (up:down) gives an indication of settling (ratios >1) or gelation (ratios <1).

Gel Strength at 3 rpm is measured immediately after taking the rheology readings. First, the slurry in the cup is mixed at 300 rpm for 1 min to disperse any gels. The setting is then changed to 3 rpm, and the viscometer turned off for 10 seconds. Immediately upon turning the viscometer back on, the maximum dial reading deflection is recorded as the "10s GS." Shutting the viscometer back off for 10 minutes, the process is repeated or the "10m GS" and a 3rd, final temperature is recorded. Gel Strength = 1.065 x DR for R1B1F1.

Table 7: Rheological results for Nanite (#1 and #1A) and control (#2 and #2A) formulations

(Dial Readings with rotor/bob/spring combination of R1/B1/F1)

Fluid#	**#1** (80°F)			**#1A** (190°F)			**#2** (80°F)			**#2A** (190°F)		
rpm	*up*	*down*	*ratio*	*up*	*down*	*ratio*	*up*	*down*	*ratio*	*up*	*down*	*ratio*
300	133	133	1.00	54	54	1.00	40	40	1.00	10	10	1.00
200	95	98	0.97	31	38	0.82	28	27	1.04	7	6	1.17
100	60	60	1.00	20	24	0.83	14	14	1.00	4	4	1.00
60	43	43	1.00	15	18	0.83	10	9	1.11	3	3	1.00
30	29	27	1.07	11	12	0.92	6	6	1.00	3	2	1.50
6	13	12	1.08	5	6	0.83	3	3	1.00	2	1	2.00
3	8	9	0.89	4	5	0.80	3	2	1.50	2	1	2.00
3	10s GS, DR:		N/A	10s GS, DR:		4	10s GS, DR:		N/A	10s GS, DR:		1
3	10m GS, DR:		N/A	10m GS, DR:		13	10m GS, DR:		N/A	10m GS, DR:		10

The Free Fluid was a measurement of the clear or colored fluid that comes to the top of a column of fluid after a static period (generally two hours), which may occur at ambient or heated conditions. The fluid was removed by a syringe and measured to a precision of 0.2 mL. This Free Fluid is expressed as a percentage of the original volume. The specified cylinders are used for testing, i.e. clear, 250 mL graduated (±2 mL) cylinders with a ratio of slurry height to width (H:W) of approximately 6:1 – 8:1.

Table 8: Free fluid results for Nanite (#1A) and control (#2A)

#	Static Period: Heat/Amb.	Static Period (hr)	Cylinder Ratio (H:W)	Cylinder Angle (Inclination)	Total Volume (mL)	Free Fluid Volume (mL)	**% FF**	Settling?
1A	Ambient	2	6:1	45°	250	30.0	**12.0**	Yes
2A	Ambient	2	6:1	45°	250	60.0	**24.0**	Yes

To prepare for the tests, 500 (± 50) psi is applied during the conditioning period or sufficient pressure to prevent boiling. A thermocouple is placed in the wall of the apparatus. If the temperature is over 190°F, a condenser and/or a backpressure regulator are used. A backpressure of at least 100 psi is applied for the actual test, to prevent filtrate evaporation. For slurries that contain salt, such as NaCl or KCl, a backpressure regulator, instead of a condenser, is used for every Fluid Loss test. The test is performed at 1000 (±50) psi differential pressure (cylinder pressure – back pressure).

The fluid flows through a screen of mesh size 325 (backed by a 60-mesh screen) and is collected

within 6 minutes of conditioning if ≤190°F and within 30 seconds of inversion. A 100 mL cylinder is used for collection at the designated times of ½, 1, 5, 10, 15, 20, & 30 minutes (the fluid can alternately be weighed, but OTC collects fluid by volume). API FL is twice the volume collected in 30 minutes. If the test blows dry in <30 min, the Calculated API FL = volume at time t x 10.954 / t ^{½}.

Table 9: Fluid loss results for Nanite (#1B) and control (#2B)

#	FL Cell Type	Test Temp (°F)	Test Time (min)	Final Volume (mL)	API FL (mL)	Filter Cake Height (in)
1B	Stirred FL	258°F	0.25	96.0	**2103**	3.00
2B	Stirred FL	258°F	0.23	99.0	**2261**	2.50

Thickening times were measured for Nanite and control slurry formulations. The slurry cup was inspected, ensuring that it was clean and dry. Slurry cup assembly was checked to ensure the paddle moved freely. After preparation, the slurry was stirred vigorously just before filling the cup. The hydrocarbon oil used was from the manufacturer or Shell (Ondina), each meeting the criteria of: 6-79cST @ 100°F, 0.83-0.93 S.G., 0.45-0.6 BTU/lb/°F, 0.065-0.08 BTU/(hr ft2 °F/ft). The filling of the cup was by the instrument instructions. Grease was applied only to the threaded areas. Entrained air was removed by tapping on the side of the cup while the slurry was poured into the cup until the point where it flowed out of the hole upon capping. The cup was checked, again, to ensure the paddle turned freely. The test was initiated within 5 minutes of mixing.

Table 10: Thickening time results for Nanite (#1C) and control (#2C)

#	Test Temp (°F)	Test Press (psi)	Initial Bc	30 Bc at hh:mm	50 Bc at hh:mm	70 Bc at hh:mm	100 Bc at hh:mm
1C	258	6,237	14	05:20	05:24	05:25	N/A
2C	258	6,237	8	05:25	05:29	05:30	05:33

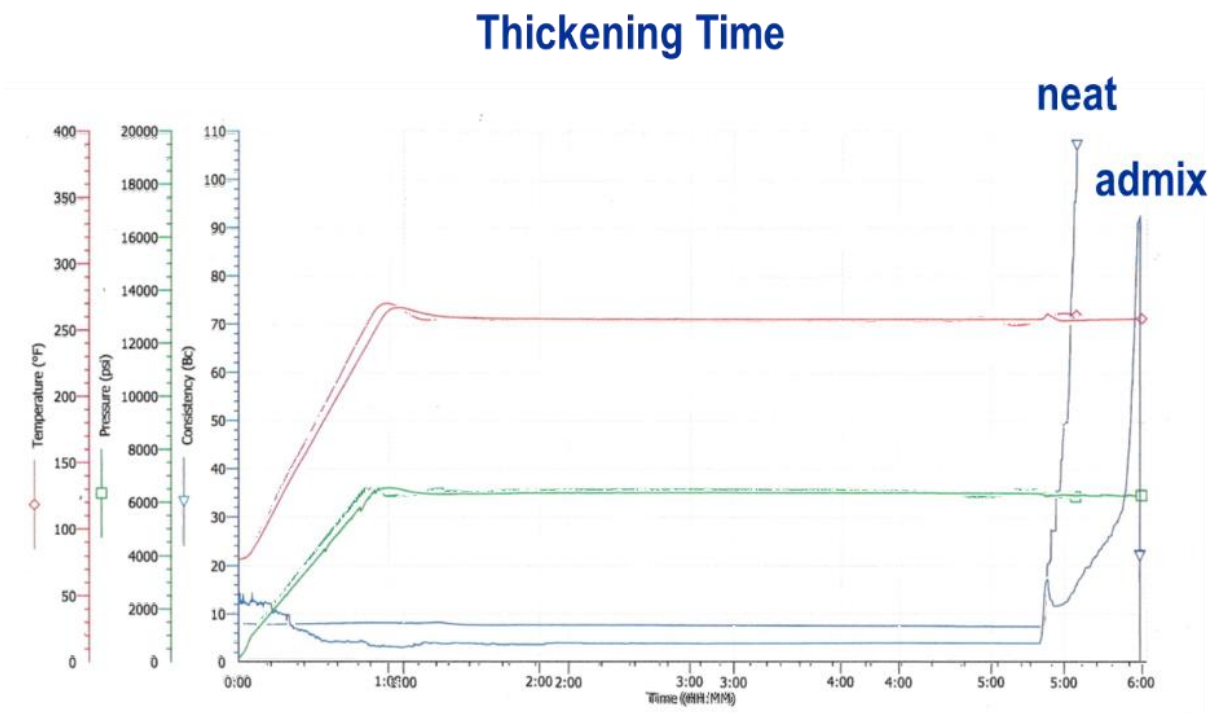

Figure 87: Thickening time measurements

Nanite Electrical Resistivity Modelling

Gauge Factor and Modulus Characterization

The gauge factor (GF) of a sensing material is defined as the ratio of the relative change in electrical resistance to the mechanical strain in the specimen and is an important specification of the sensitivity of a sensor. The gauge factor and compressive modulus of Nanite samples is measured by affixing a thin film resistive bridge strain gauge to 2" Nanite cubes with epoxy.

For a Nanite cube with attached strain gauge the measured Young's modulus is 13.3 GPa which is in the typical 10-50 GPa range for neat Portland cement. The piezoresistive response of the sample was also typical of Nanite at 0.1%/kN. This translates to piezoresistive modulus Q = 386 MPa corresponding to the stress required to produce a 100% relative impedance response.

The gauge factor can be computed as the ratio of the Young's modulus to the piezoresistive modulus:

$$GF = \frac{E}{Q} = 33.6$$

Alternatively the gauge factor can be computed as the slope of the strain vs impedance plot in Figure 88. Thin film resistive strain gauges, such as the one used for this experiment, have a maximum gauge factor of 2. This experiment demonstrates that this Nanite specimen has a piezoresistive sensitivity 17 times greater than a conventional strain gauge and is ideal for load sensing applications.

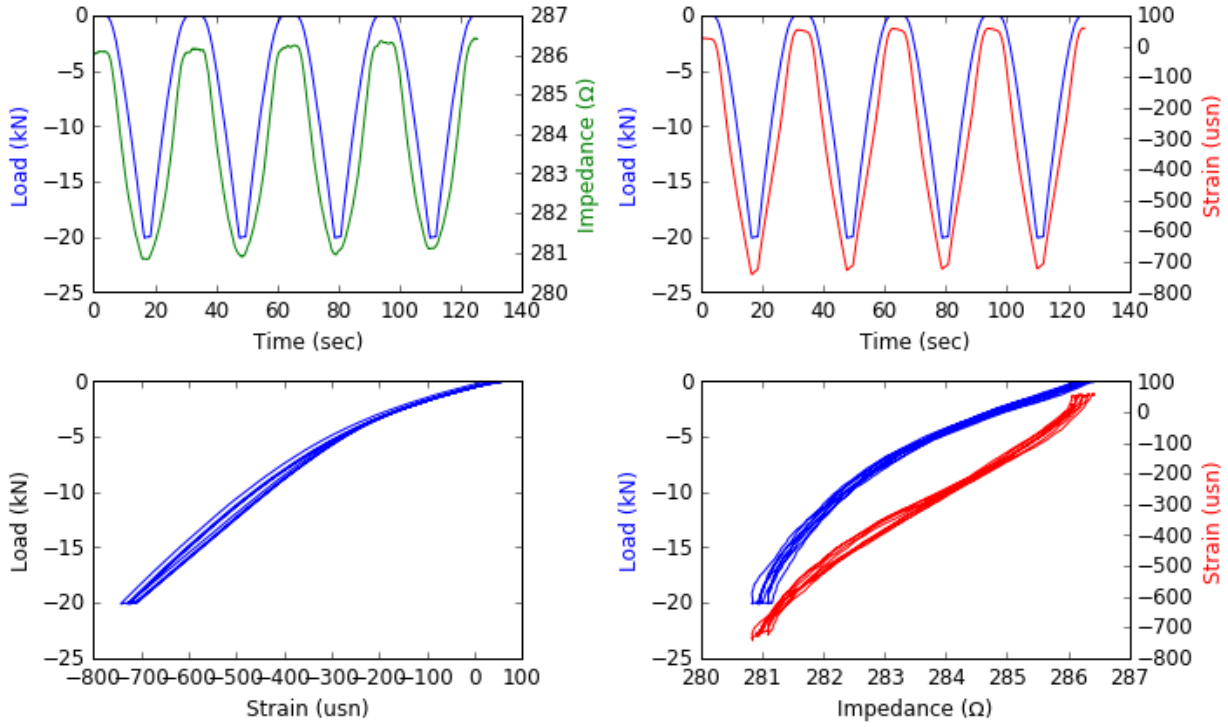

Figure 88: Electrical response and compressive modulus measurements on a Nanite sample.

In many complex loading configurations, the stress in the material will not be purely compressive nor will the electric fields be perfectly aligned with the stress tensor and a linear combination of longitudinal and transverse piezoresistive coefficients must be considered. Additional studies will be performed to address the transverse strain in the cement to determine the Poisson ratio of the material and the piezoresistive coefficients for transverse loading. Transverse loading with the existing electrode geometry can cause excessive shear at the electrode planes and will be considered.

Nanite Data Acquisition and Analysis Techniques

High-resolution, High-speed resistivity Tool

A performance electrical resistivity tool based on the Red Pitaya open instrumentation board has proven effective for 2-wire electrical impedance spectroscopy and was discussed in a previous report. Two wire AC impedance spectroscopy suffers from strong low frequency artifacts associated with electrode polarization. In this quarter we developed prototype frontend electronics consisting of a precision instrumentation amplifier to extend its capabilities to 4-wire Wenner probe type testing. 4-wire measurements enable study of the low frequency characteristics of the cement samples including DC response without the overwhelming contribution of the electrode polarization and contact resistance. With modification to the Nanite electrode geometry to reduce inductive artifacts we expect to also gain the ability to probe the RF behavior up to 50 MHz with this instrument with the benefits of a compact and portable system.

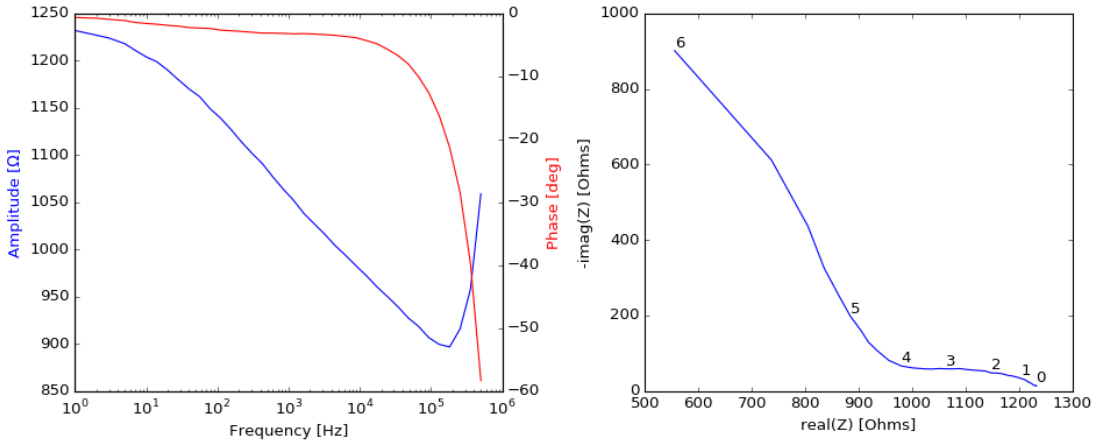

Figure 89: Nanite 4-wire impedance spectrum shows convergent impedance at low frequencies. (left) Bode plot, (right) Nyquist plot with frequency indicated by log(frequency) decade markers.

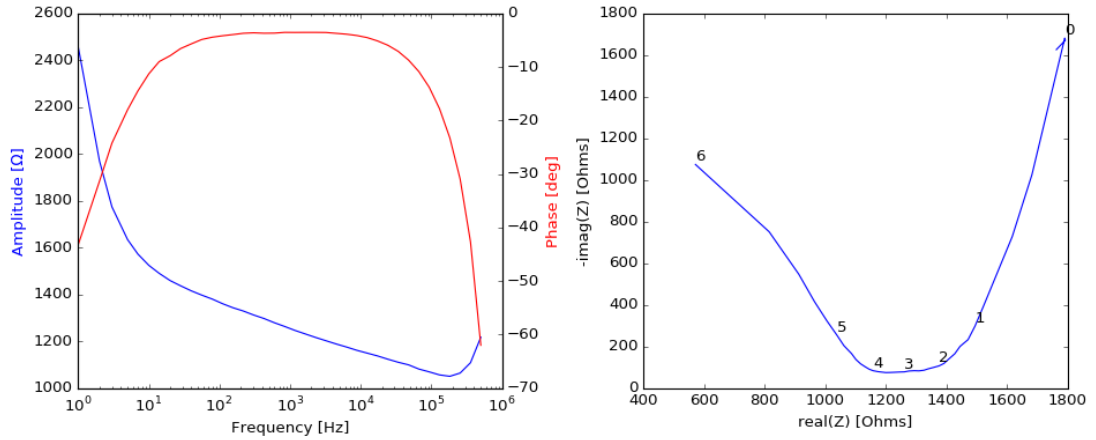

Figure 90:Nanite 2-wire impedance spectrum shows divergent impedance at low frequencies due to electrode polarization effects. (left) Bode plot, (right) Nyquist plot with frequency indicated by log(frequency) decade markers.

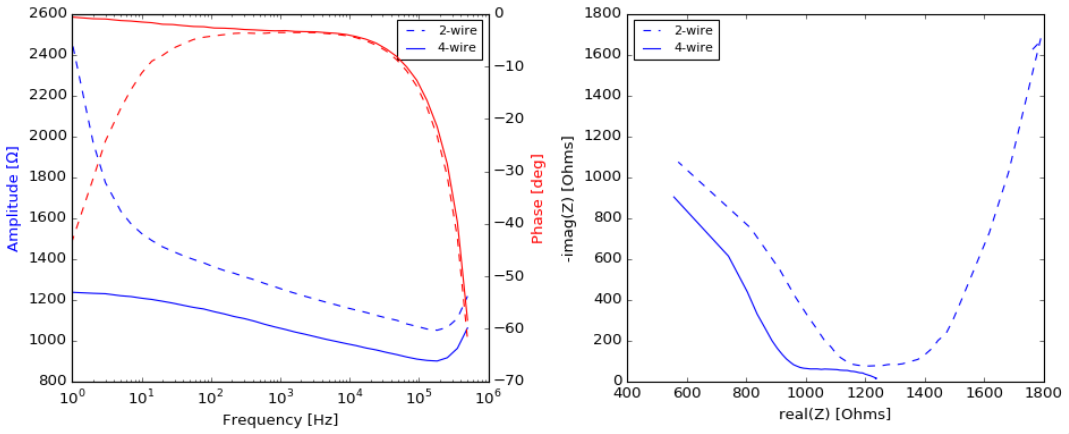

Figure 91:Comparison of 2-wire and 4-wire Red Pitaya impedance spectrum for a Nanite specimen. Above 1 kHz the difference in impedance is a 200Ω real shift associated with the electrode contact resistance.

Subscale Proof Testing

Nanite Acoustic Sensing Properties

The acoustic properties of Nanite have been previously studied via transmission loss experiments using an air impedance tube. These experiments yielded null results for acoustic contrast enhancement due to the presence of nanoparticles in the cement. In the past year, however, Oceanit has expanded its acoustic test capabilities in the sonic and ultra-sonic regimes though other oil and gas related research projects. In this quarter we leveraged these new acoustic measurement capabilities to revisit the properties of Nanite and validate the previous results.

An ultrasonic measurement system was employed to characterize Nanite acoustic characteristics with respect to base cement at higher frequencies. A signal generator connected to an ultrasonic transducer through an amplifier was used as the sound source. An additional ultrasonic transducer connected through a signal amplifier and digital acquisition card to a laptop was used as the receiver. A custom LabView interface was used to visualize and collect the signals. Indirect measurements were taken with the two transducers on the same side of the sample block which was elevated in that air. Samples of 2”x2”x6” of Nanite and base cement in both neat and foamed formulations were characterized using the acoustic testing setup. The transmission loss as a function of frequency was calculated for each of the sample types and compared. Nanite samples in both neat and foamed formulations showed no differences from their base cement counterparts in terms of acoustic properties.

Concentric Casing Pipe Multifunctional Hydraulic Test Fixture

Oceanit is developing a lab-scale test fixture to facilitate studying the applicability of Nanite cement downhole. The multifunctional hydraulic test fixture will allow the controlled pressurization of the inside of a pipe surrounded by a cement annulus. The fixture consists of a pair of flanges used to seal the ends of a test pipe section. The fixture can accommodate any pipe length and is sealed by tightening six bolts spanning the flange pair and surrounding the test piece. The flanges will be fabricated with multiple O-ring glands to accommodate multiple size pipes, initially from 1” to 3” in diameter.

The test pipe will be cast inside of a larger concentric pipe with a cement annulus of Nanite or control cement fill. The cement annulus can be prepared with defects and various electrode configurations. The system can also be modified in the future to measure gas permeability of the cement annulus. During testing the inner sealed pipe is pressurized with water or oil using a high-pressure metered displacement pump up to 1500 psi with ~7 psi control resolution allowing detailed study of the electrical impedance response under uniform radial loading.

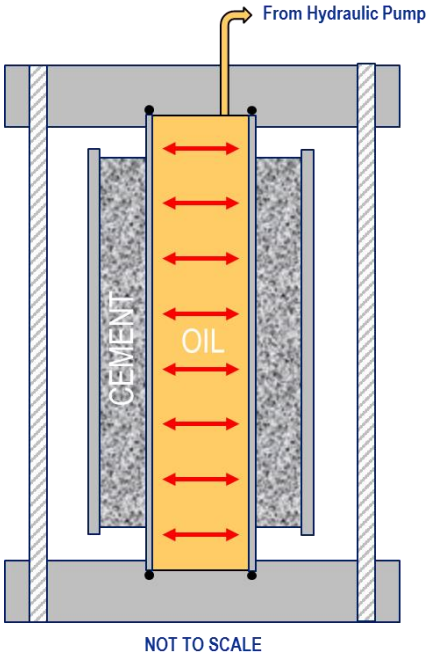

Figure 92:Hydraulic test fixture cross section schematic.

The hydraulic test fixture was modeled in COMSOL Multiphysics finite element modeling software and pressurization of the pipe was simulated to determine potential failure mechanisms and geometric requirements. The results match well with analytical pressure vessel calculations.

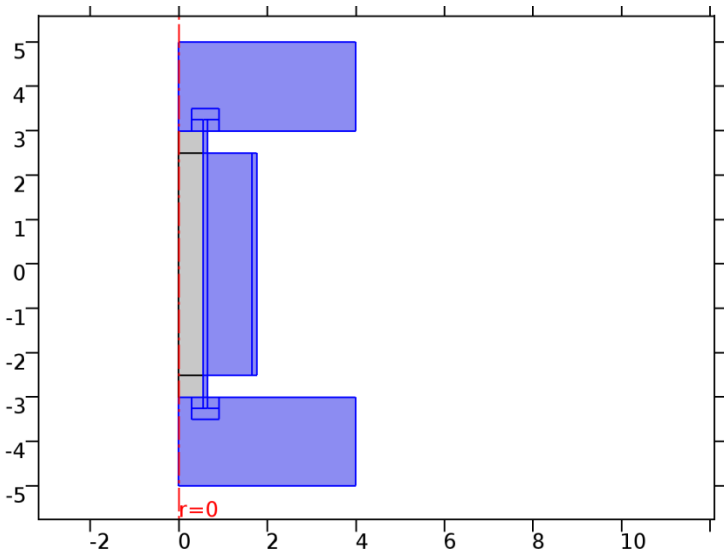

Figure 93:Axisymmetric model of hydraulic pipe fixture (dimensions are in inches). Pressurization was modeled as interior boundary loads and the top and bottom plates were constrained as rollers.

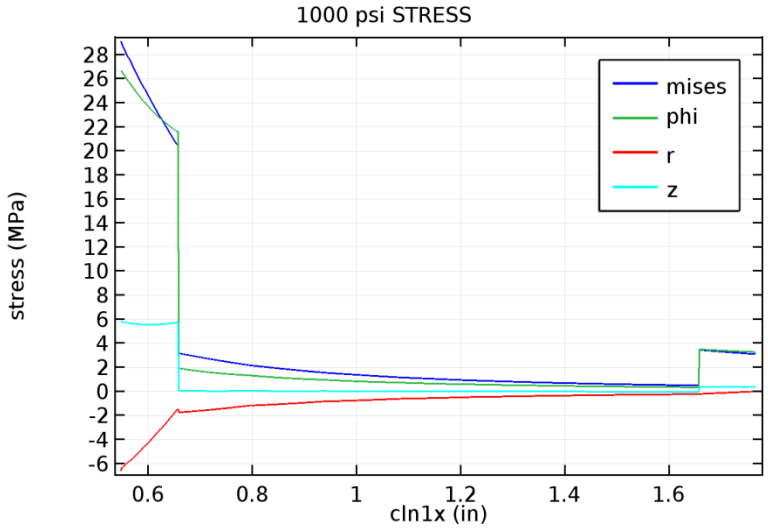

Figure 94:Stress as a function of distance across the midpoint of the pipe (transverse section). Von Mises and stress in the orthogonal radial directions are shown for 1000 psi pressurization.

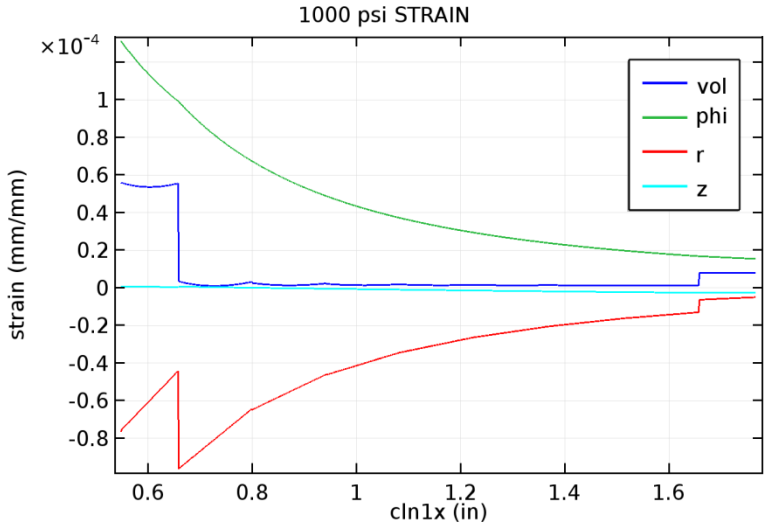

Figure 95: Strain as a function of distance across the midpoint of the pipe (transverse section). Volumetric and strain in the orthogonal radial directions are shown for 1000 psi pressurization.

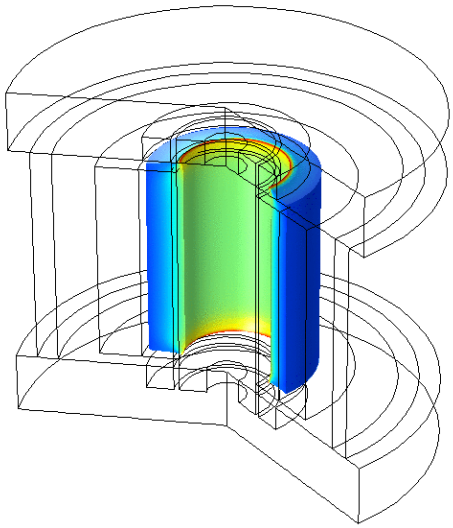

Figure 96: Visualization of Von Mises stress distribution in cement annulus of the hydraulic test fixture. The design is aimed at reducing stress concentrations at the edges. This information can aid in electrode position selection.

Abandoned-Well Cement Plug Monitoring

Nanite has potential for the long term monitoring of cement plugs installed during well abandonment. Electrical impedance measurements of Nanite can be used to detect fractures and potential leakage pathways in a cement plug. Oceanit is investigating applications of time-domain reflectometry (TDR) to measure the pressure gradients, localize faults and cement debonding from the steel casing pipe.

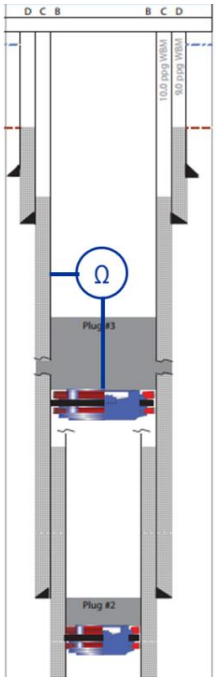

Figure 97: Measurement of cement resistivity using a coaxial electrode cast into a cement plug.

Quarter 12: Period End Date September 30, 2016

Electrical Resistivity Tool

Oceanit has developed an improved revision of a high-resolution, high-speed resistivity tool based on the Red Pitaya data acquisition instrument. The previous version of the impedance measurement frontend for the Red Pitaya only measured current and voltage in a two electrode configuration. To expand the capabilities to 4-point impedance measurements an add-on board was fabricated containing an instrumentation amplifier. The instrumentation amplifier makes a differential measurement of the voltage drop across the device under test and requires only a single Pitaya input channel. The other input channel is used to measure the current by reading the voltage across a shunt resistor to ground. An initial handmade prototype was fabricated and performed well but was fragile and susceptible to noise so a custom PCB was fabricated as an add-on board for the Pitaya. The final system is capable of making 4-wire AC impedance measurements with resolution of 0.01% with excitation frequencies ranging from 100 Hz to 1 MHz. Excitation voltage can be varied from 0 to 0.6V peak-to-peak and impedance range can be selected by replacing a single surface mount feedback resistor.

Data Analysis Tools

As the collection of Nanite specimens and data grows, so does the complexity of comparing analyses from different dates and experiments. The non-linear response curve of Nanite specimens to load has been measured for many samples over three years while experimental techniques and Nanite formulations have steadily improved. It is of interest to see how performance has changed over time but often the comparison of data is not straightforward. Typically, the Nanite response curve is approximately linear over some region of applied load and a linear approximation to the response has been made over the range 5kN to 20kN applied force. The exact range used has varied over time and also depends on the maximum force to be applied to the specimen during testing. Young specimens are typically tested with only 10kN load while mature specimens are tested to 20kN or higher. The earliest tests were often conducted as high as 40kN. Comparison of the linear approximations of the load response for different samples, or a single sample tested at different dates are often invalid as they overlook changes to the response curve shape. While automated processing is necessary for this volume of data it is necessary to compare the actual response curve shapes.

Subscale Proof Testing

Oceanit is presently researching potential pathways for field deployment of Nanite in oil and gas wells. Several pathways for the interrogation of Nanite to obtain presence and condition information are being investigated. In this quarter we have focused on the development of a test fixture and methodology for the hydraulic pressurization of an analogue casing pipe surrounded by an instrumented Nanite cement annulus.

Concentric Casing Pipe Multifunctional Hydraulic Test Fixture

Oceanit is developing a lab-scale test fixture to facilitate studying the applicability of Nanite cement downhole. The original multifunctional hydraulic test fixture has now been modified to operate with water rather than oil and use off-the-shelf pipe fittings.

The test fixture consists of the following components:

- Eldex 3SM: High pressure liquid metering pump (pre-existing Oceanit equipment) with 0.01 to 20 mL/min pumping rate up to 1500 psi. Remote controllable by RS232 connection.
- Dial pressure gauge: 0-2000 psig
- Omega PX319-3KGV pressure gauge: 0-3000 psig with 100mV output and ¼" NPT fitting.
- Manually actuated plug and needle valves to vent high pressure and regulate flow
- LabJack T7-Pro: Data acquisition from pressure gauge, strain gauge, and thermocouples.
- Solenoid valve: to vent high pressure under remote control.
- Red Pitaya-based electrical impedance measurement tool with new 4-wire frontend.
- Computer with Python-based control software

Preliminary testing was performed on specimens consisting of 9.5" inches of 1" diameter schedule 80 steel pipe within a 6" length of 3" diameter steel tubing. The annulus between the two pipes is cleaned and filled with cement. Specimens were cast with both Nanite and base cement. For this experiment the inner and outer pipes themselves were used as electrodes to make a global impedance measurement of the cement.

The 1" inner pipes were connected to the hydraulic system using 1" diameter Swagelok fittings. With the fittings tightened only enough to prevent water leakage, the fittings are easily reusable, so that the specimens can be interchanged. One end of the pipe is connected to the hydraulic pump and valve manifold while the other end is connected to a needle valve used to bleed out air when filling the system with water. The full system is shown in Figure 98.

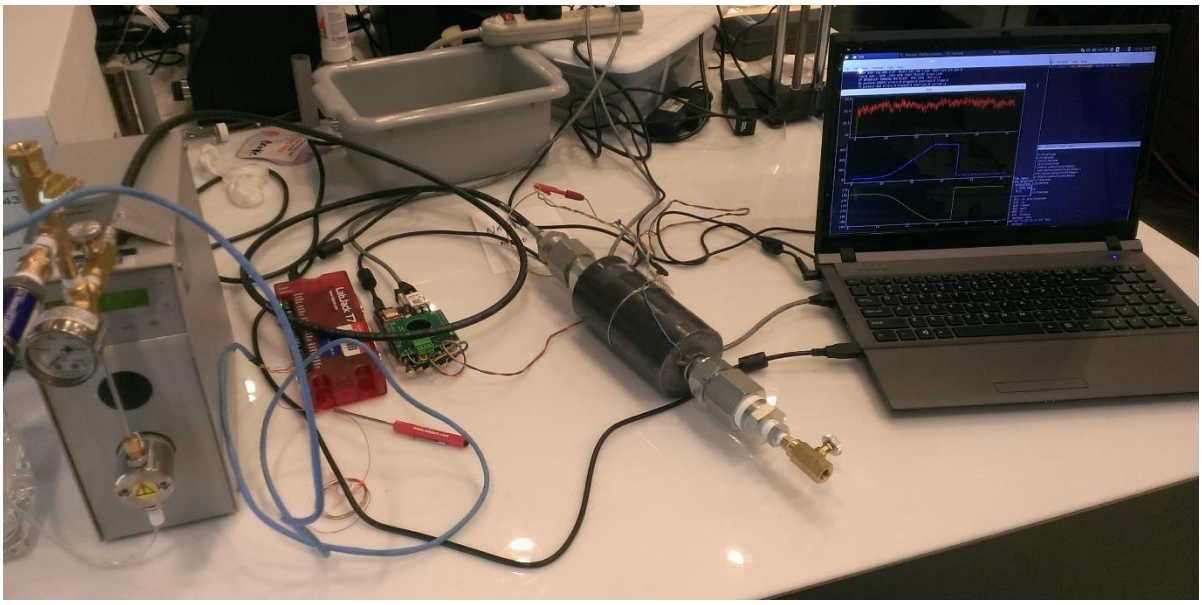

Figure 98: Apparatus for 1" pipe pressurization test. The hydraulic pump, specimen, and data acquisition system are shown.

The resistance of the cement annulus can be calculated starting with the current density in the cement of resistivity ρ and pipe length L.

$$J(r) = \frac{I}{2\pi r L}$$

Ohm's law gives the electric field in the annulus:

$$E(r) = J\rho = \frac{I\rho}{2\pi rL}$$

And the voltage drop across the cement is calculated by integrating across the annulus where a and b are the inner and outer pipe radii respectively.

$$V = \int_a^b E(r)dr = \int_a^b \frac{I\rho}{2\pi rL}dr = \frac{I\rho}{2\pi L}\ln\left(\frac{b}{a}\right)$$

Thus the resistance is given by:

$$R = \frac{V}{I} = \frac{\rho}{2\pi L}\ln\left(\frac{b}{a}\right)$$

The measured resistance of a test specimen is 53Ω for a 6” long annulus with a=0.5”, b=1.44” giving a cement resistivity of 48Ωm. Since the resistance is measured with a 2-wire technique there is additional contact resistance included. Using typical past resistivity values of 13Ωm for Nanite yields a cement annulus resistance of 14.4Ω and thus a contact resistance of approximately 38Ω over the full surfaces of the 1” and 3” pipes.

The specimen is filled with water by running the pump at high speed with the end bleed valve open and the pipe held upright to allow air bubbles to escape. When water begins to flow from the needle valve it is closed and the valve manifold vent valve is opened to release air trapped in the manifold. With all valves closed and as much air as possible purged from the system the pump is run at speeds between 2 and 4 mL/min to pressurize the pipe.

The data acquisition software records the pressure, electrical impedance, and temperature. During preliminary tests the system was assumed to be in thermal equilibrium and a thermocouple was not installed. Preliminary test specimens were also not fitted with strain gauges.

Figure 99 shows the response of Nanite resistivity to cyclic pressurization of the vessel to approximately 1000 psi. Sensitivities are obtained from the mean slope of the response curves in yielding 1.45%/MPa. Future tests will be conducted with multiple distributed electrodes and larger specimens.

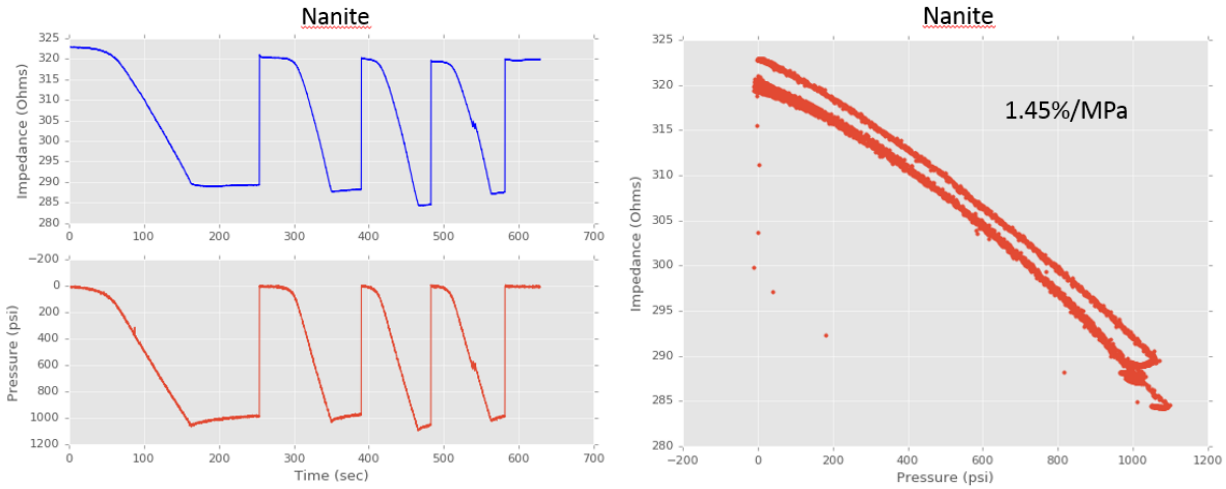

Figure 99: 1" pipe 1000 psi cyclic loading and load response curves

These initial results are promising and we have proceeded to prepare additional 1” pipe specimens fully instrumented with a strain gauge and a variety of electrode geometries under consideration for large scale testing and field deployment.

The 1” concentric pipe mold assembly was instrumented with additional tape band electrodes and annular ring electrodes as illustrated in Figure 100. Copper tape band electrodes were applied to the outside of the inner and inside of the outer pipe over a layer of Kapton insulating tape. An additional copper tape electrode was applied to the outer pipe in a similar fashion at 2” spacing between and 1” spacing from the top of the outer pipe. 18 awg stainless steel wire was fashioned into rings and placed into 3D printed holders that were slid onto the inner pipe before tape application. Two ring electrodes were placed on the assembly at 2” spacing between and from the ends of the outer pipe. Figure 101 shows the final electrode assembly. The tape and floating ring electrodes were soldered to ribbon cable that was run up the inner pipe. A strain gauge was also applied to the middle of the outside of the inner pipe and wired with the ribbon cable. 3D printed spacers were used to keep the pipes concentric and centered during cement casting. The final assembly ready for cement casting is shown in Figure 102.

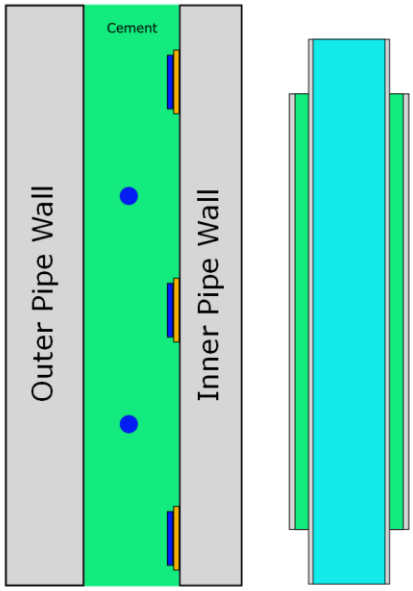

Figure 100: Cement annulus electrode concept. The inner pipe wall is banded with copper tape electrodes on a layer of Kapton tape for insulation. Concentric annular loop electrodes are suspended in the cement.

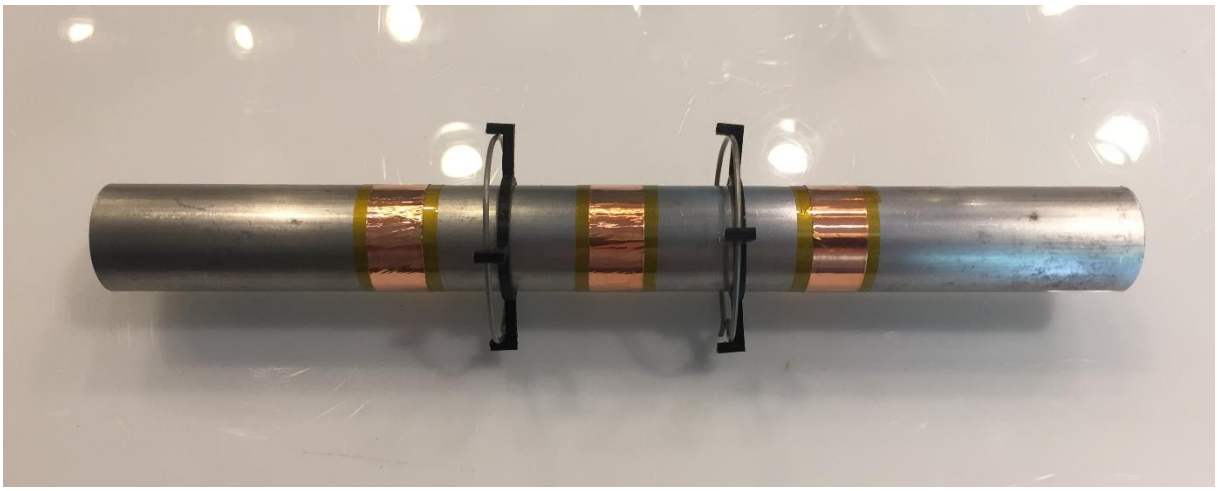

Figure 101: 1" pipe section experimental electrode configuration

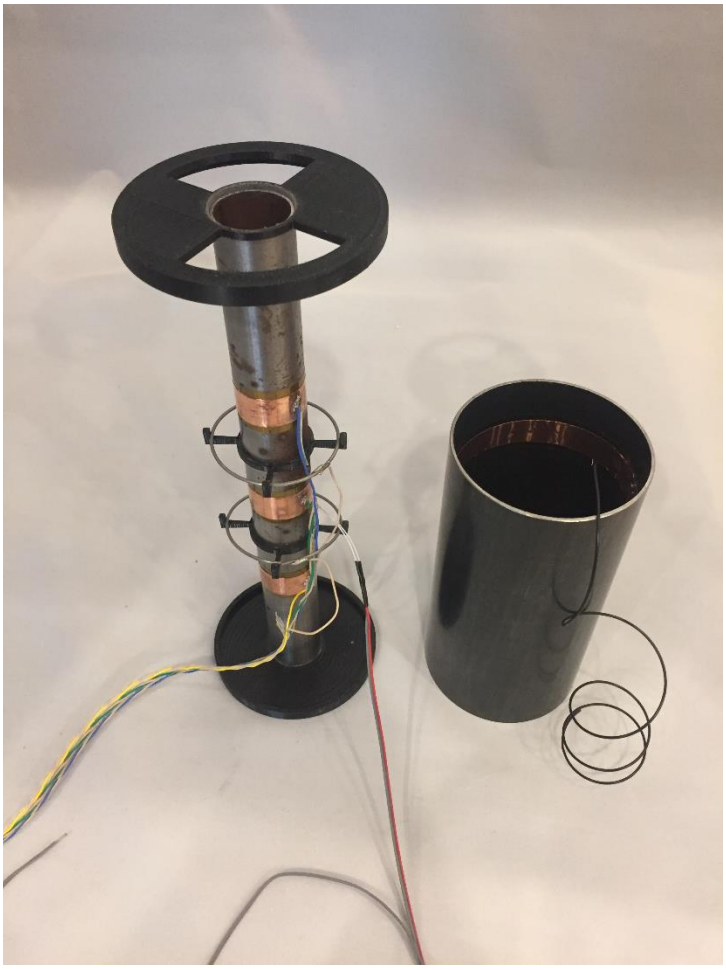

Figure 102: Fully assembled 1" pipe with electrodes and cabling ready for casting.

In parallel with the 1” pipe experiments we have designed and procured the components for a sub-scale test using pipe diameters more relevant to oil and gas well cementing (Figure 103). These test specimens consist of a 36” length of 4-inch schedule 40 steel pipe which is dimensionally close to 4 ½” API casing pipe but more readily available and shipped in small quantities. For the outer pipe a 30” length of 6” schedule 40 pipe is used. The inner pipe ends are externally threaded for use with high pressure 4” NPT female end caps. ¼” NPT threaded through holes in the end caps allow connection to the hydraulic pump and vent valve.

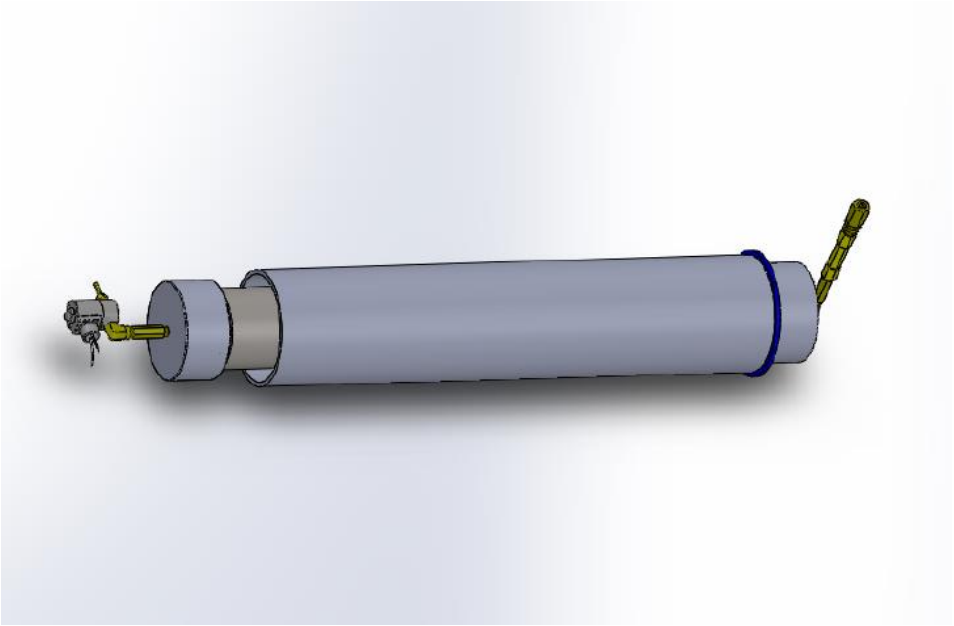

Figure 103: Rendering of the 4" hydraulic test specimen showing inner and outer pipes with attached endcaps and plumbing.

For safety considerations, this larger system will be operated by remote control with a solenoid valve used to release and bleed down the high-pressure water.

The 4” pipe will be instrumented with an array of electrodes and simulated defects. The final electrode geometries will be determined based on the upcoming results of testing the 1” pipe specimens.

Quarter 13: Period End Date December 31, 2016

In this period, we focused on the development and implementation of a test fixture and methodology for the hydraulic pressurization of an analogue casing pipe surrounded by an instrumented Nanite cement annulus.

Subscale Proof Testing

Concentric Casing Pipe Multifunctional Hydraulic Test Fixture

Following the successful testing of the hydraulic pressurization system with 1" specimens, Oceanit proceeded to design and construct a test fixture based on 4 ½" diameter steel pipe. The system has demonstrated Nanite's ability to sense radial stress applied to a ¾" thick cement annulus by a 4 ½" steel casing pipe up to 1500 psi. The demonstration system consists of a 36" long 4 ½" steel casing pipe within a 30" long 6" casing pipe. The annulus between the pipes is filled with Nanite cement and instrumented with 18 Nanite sensing electrodes for stress localization, four resistive strain gauges, and a thermocouple, Figure 104. Water is pumped into the inner pipe at rates up to 20 mL/min up to 1500 psi under computer control with a high resolution digital pressure readout. The system may be configured for remote operation to verify the maximum safe working pressures of system components.

These test specimens consist of a 36" length of 4-inch schedule 40 steel pipe which is dimensionally close to 4 ½" API casing pipe but more readily available and shipped in small quantities. For the outer pipe a 30" length of 6" schedule 40 pipe is used. The inner pipe ends are externally threaded for use with high pressure 4" NPT female end caps. ¼" NPT threaded through holes in the end caps allow connection to the hydraulic pump and vent valve.

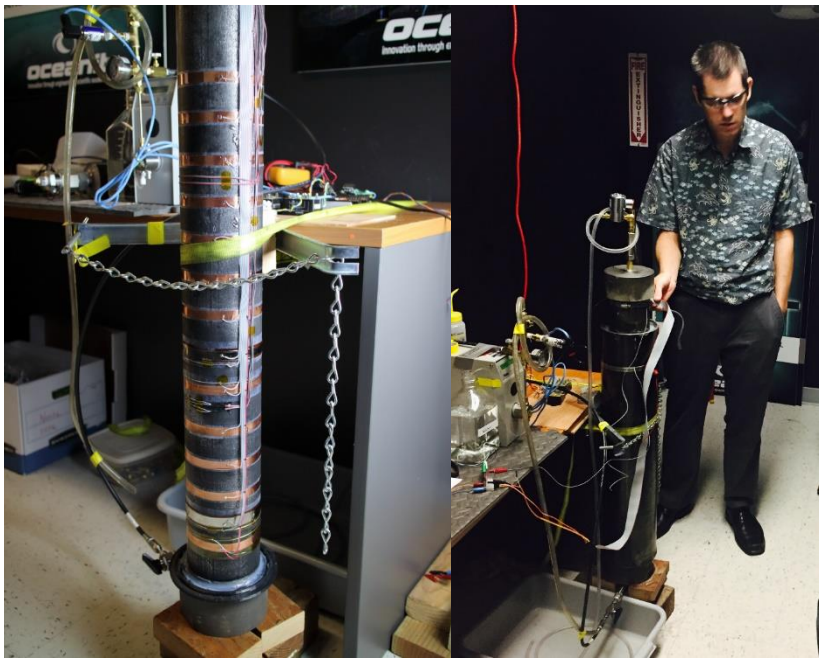

Figure 104: 4 1/2" demonstration pipe before (left) and after (right) cementing

Oceanit is using the hydraulic test fixture in conjunction with computer simulations to identify the optimal electrode configuration for deployment downhole in near-term field trials. Figure 105 shows a typical set of experimental response data for pressurization of the 4 ½" pipe with Nanite annulus.

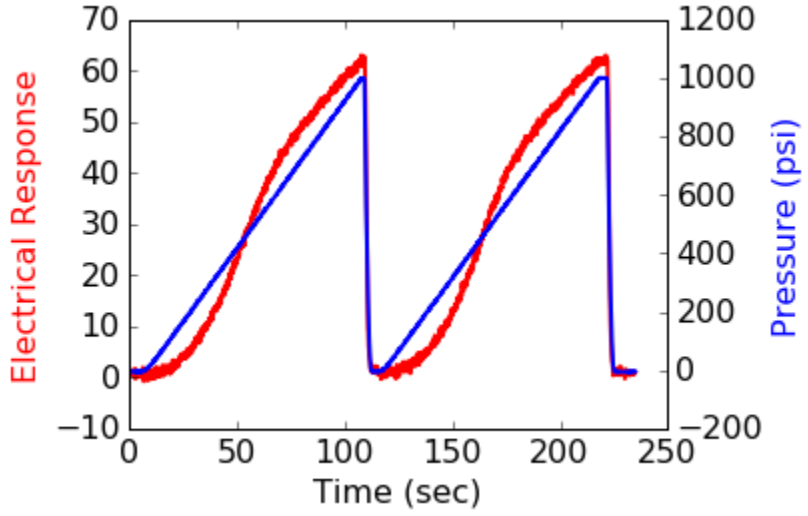

Figure 105: Typical Nanite electrical response to 4.5" casing pipe pressurization.

Electrode Geometry Optimization

The electrode configuration for the first test fixture consisted of annular strips of ½" wide copper tape layered on top of ¾" wide Kapton insulating tape. Between some adjacent pairs of copper electrodes, additional insulation and annular wire loop electrodes were placed to enable 4-wire impedance measurements between the tape electrode pair. While a response to pressure is clearly visible in the results, the impedance values measured between various electrode pairs did not agree with predictions based on the 1" pipe experiments.

COMSOL modelling of electrodes was performed to more fully understand the current density within the cement annulus. In the larger pipe configuration, the strain gradient across the cement annulus is significantly smaller than in the 1" case where the Nanite response was strongest near the inner pipe wall. As plotted in Figure 106, the hoop strain in the cement annulus exceeds the radial strain so it is important to include electrodes that provide radial and azimuthal electric fields to aid investigation of Nanite piezo-resistive anisotropy under annulus loading.

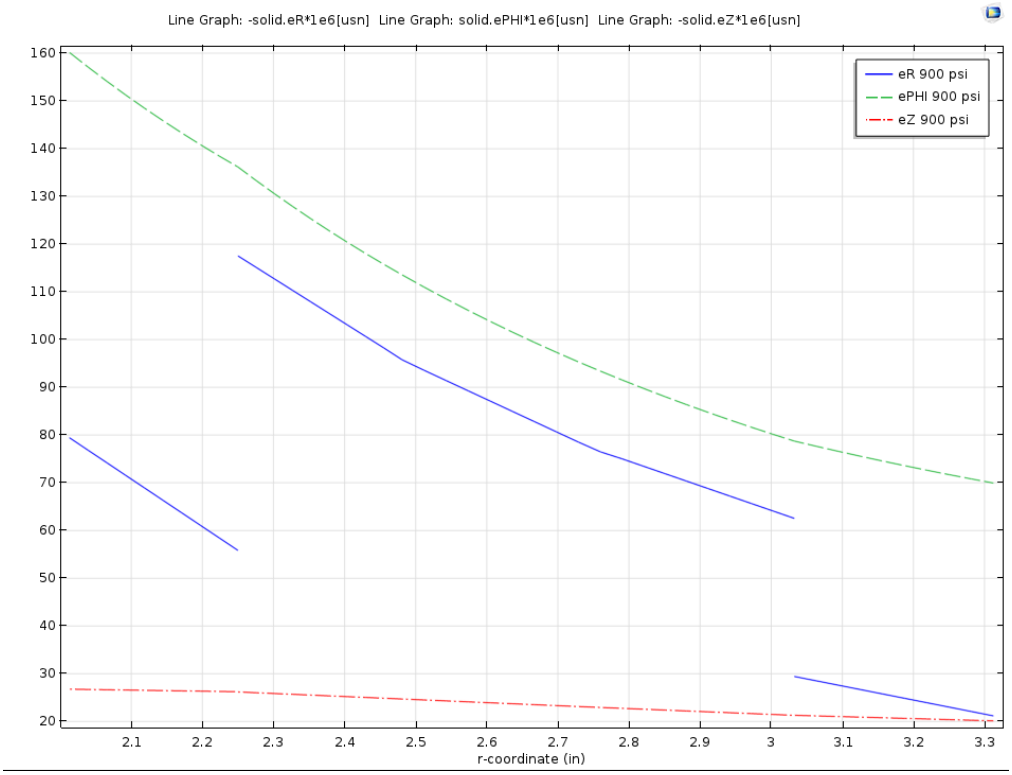

Figure 106: Radial and hoop strain in the pipe walls and cement annulus

In addition to annular tape electrodes the use of coaxial electrodes within the annulus were revisited. Modeled here is a 4" long wire placed coaxially within the cement annulus at various radial offsets. It is found that the sensitivity to applied pressure is maximized for a wire placed exactly in the middle of the annulus with decreasing sensitivity with proximity to either pipe wall. In this geometry, the current density is predominantly radial.

We also consider the use of two adjacent axial wires in the annulus. For closely spaced wires there is a substantial azimuthal component (Figure 107) yet for separation of more than 20° the two wires do not influence one another and the pipe wall becomes the dominant conductor between the two wires (Figure 108).

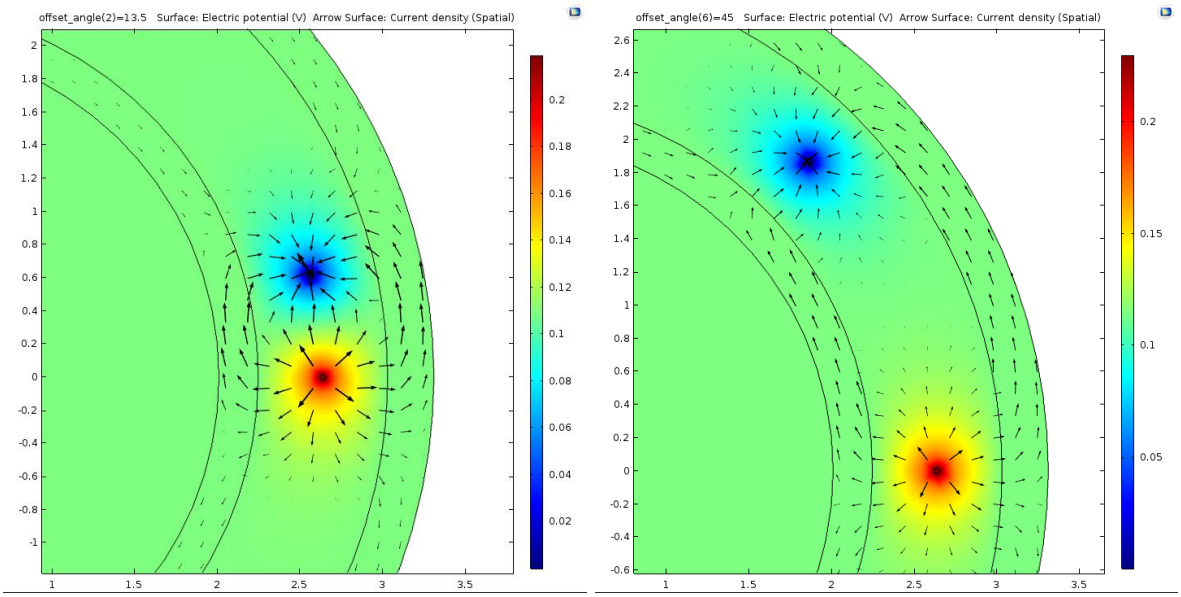

Figure 107: Effect of adjacent coaxial electrode proximity on electric field distribution.

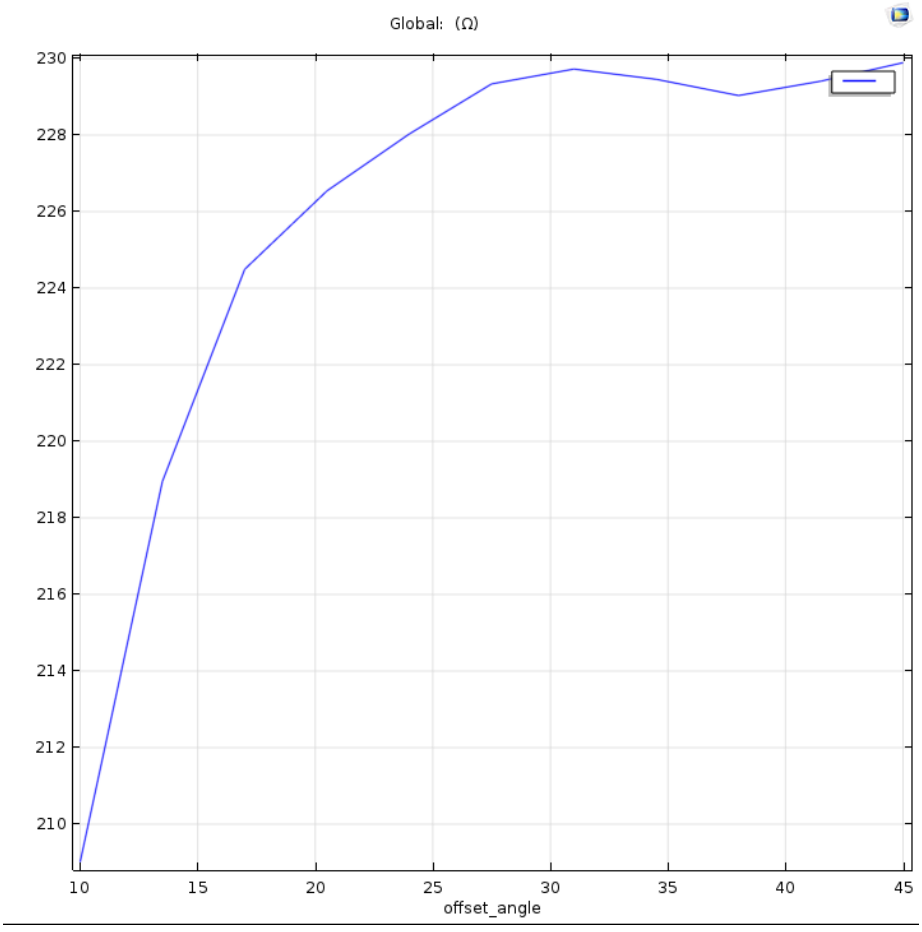

Figure 108: Adjacent wire impedance dependence on offset angle between the wires.

Nanite Piezo-resistivity Modelling

COMSOL simulations were used to optimize the electrode geometry for a 2" cube that allow precision measurement of the material anisotropy. A series of 4" wire electrodes akin to Nanite experiments performed early in the project provide a uniform current that can be applied parallel or perpendicular to applied load in laboratory testing. Future work will use this geometry to measure the transverse piezo-resistivity coefficients more accurately than previous work that did not account for non-uniform stress in the cube.

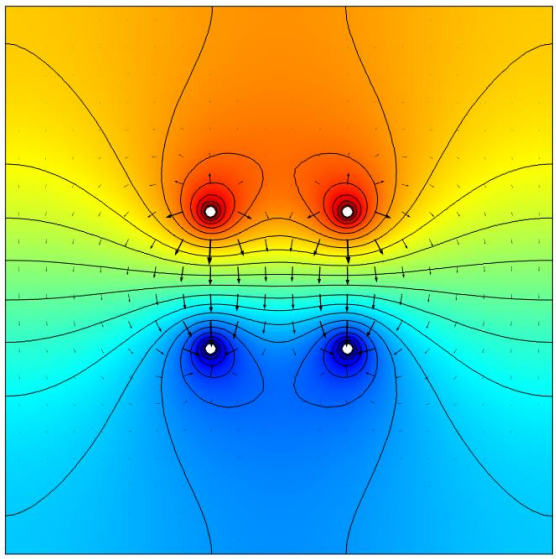

Figure 109: Nanite electric field distribution for piezo-resistivity testing

Components have been fabricated and construction is underway for a second 4 ½ " pipe specimen. The pipe will include both axial and radial electrode configurations, strain gauges, and temperature measurement. Casting of cement and testing will commence following the electrode installation.

Concentric Casing Pipe Multifunctional Hydraulic Test Fixture Part 2

A second 4 ½" pipe specimen was designed based on the experience from the first specimen. The pipe was prepared in a manner like the first experiment including test electrode configurations, temperature, and strain sensors. One again, the bottom 1/3 of the pipe was cast with base cement as a control. The primary electrodes consist of ¼" wide copper tape supported on a layer of ½" Kapton insulating tape every 2" along the length of the pipe. A secondary set of axial electrodes consists of pairs of 4" long stainless steel wires spaced 0.75" apart and help parallel to a 0.5" from the inner pipe on 3D printed plastic holders. Six pairs of axial electrodes were installed, one pair on each side of the inner pipe (180° between pairs around the pipe) at each of 3 stations at different depths along the pipe. Two of the pairs are cast in the control cement portion and the other four in Nanite with the redundancy to reduce risk of an anomalous result due to a casting defect. Each set of axial electrodes has one copper tape electrode located on the inner pipe at the center of the wire length to allow testing the impedance between the axial and tape pairs.

The 30" pipe section was cast using cement mixed in batches. The only exposed cement surface, at the top of the casting, was coated with silicone RTV after initial setting. No water is added during curing or allowed to escape to simulate downhole curing conditions.

After 14 days of curing at room temperature, electrical impedances of all electrode pairs were measured followed by cyclic pressurization to 400 psi. Figure 110 shows the average sensitivity of each of 27 electrode pair combinations measured during the test. These tests include both tape and axial electrodes in base and Nanite cement. Figure 111 summarizes these results grouping them by electrode and cement type. Nanite shows a clearly stronger response for tape electrodes as expected from past experiments, however, the axial electrodes surprisingly show very little sensitivity to pressure in all pairing arrangements. This result is attributed to the smaller effective sensing volume of the axial electrodes compared with the circumferential tape electrodes.

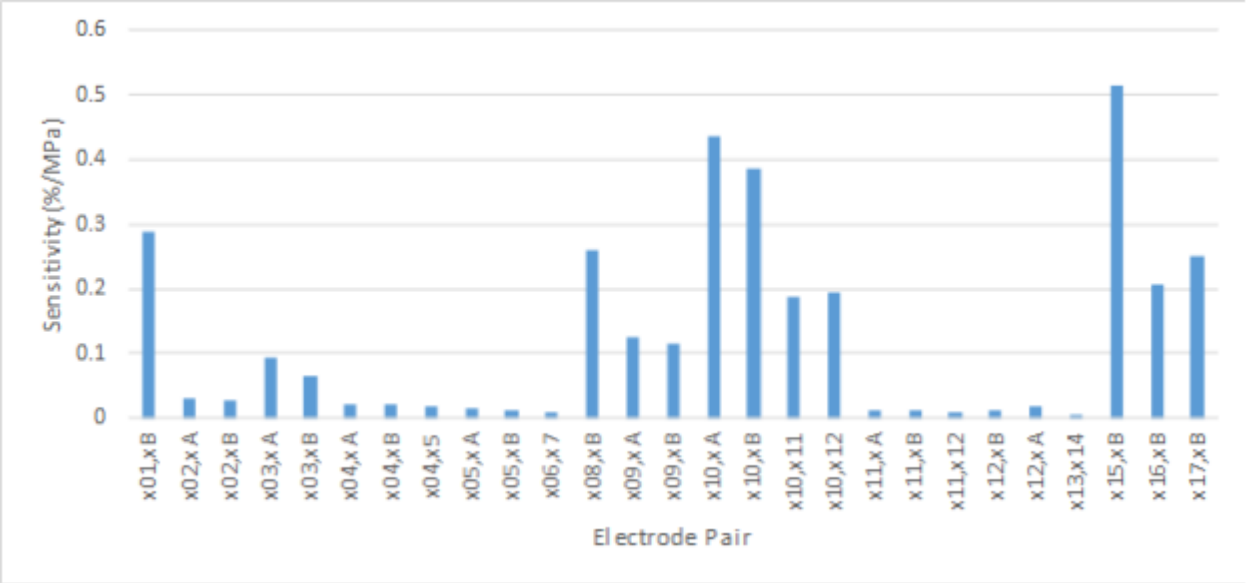

Figure 110: Nanite pipe pressurization electrode pair impedance response

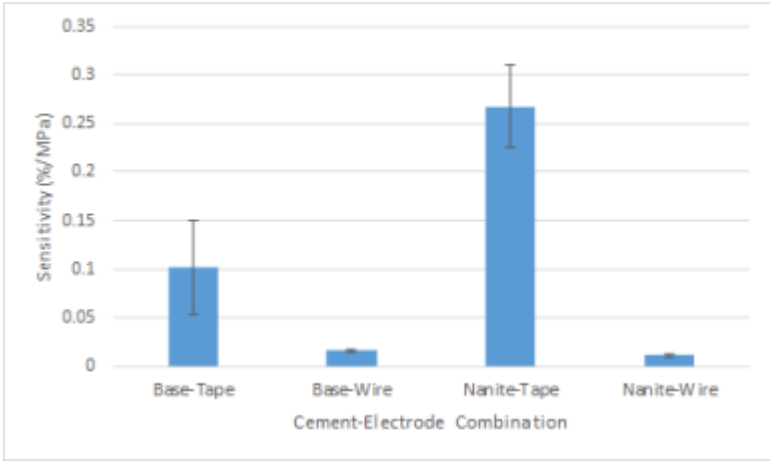

Figure 111: Nanite pipe pressurization test results

We conclude that circumferential electrodes are superior for downhole deployment scenarios, especially due to the possibility of electrode installation using layers of conductive and non-conductive pipe coatings.

CONCLUSIONS

Through this project, Oceanit has substantially improved the effectiveness and market readiness of nanomaterial enhanced cement for downhole applications. Investigations of various modalities including electric, acoustic, and nuclear have resulted in a solid approach to electrical interrogation of cement stress, curing state, and condition using a custom, low-cost, compact electrical resistivity tool. Oceanit efforts achieved the design of a cement admixture with enhanced electrical responsiveness in conduction with custom fabricated electronics and associated data processing software to reliable extract meaningful information from cement. The ability of Nanite to accurately measuring curing, damage, contamination, and mechanical load using the complex electrical impedance response was explored in detail.

Oceanit has also explored the translation of Nanite technology from the laboratory to downhole relevant form factors, such as concentric steel pipes. Nanite admixture production was scaled up to produce small specimens in statistically significant quantities and to cast larger pipe dimensions for sub-scale evaluation.

Based on the results of this project, Oceanit has identified steps forward to develop and commercialize Nanite technology in the oil and gas industry, and beyond. Through close collaboration with industry partners, additional use cases and field test opportunities have been identified. Future work includes design and deployment of interventional and continuous monitoring systems for Nanite field testing and further development of concepts for applications such as: top of cement measurement, plug and abandonment long term integrity, and behind multiple casing presence and quality assurance.

Beyond the oil and gas industry, opportunities for sensing cement and concrete abound for applications including nuclear waste isolation, vehicle weigh-in-motion overweight vehicle detection, and structural integrity monitoring, particularly in bridges and other infrastructure.

GRAPHICAL MATERIALS LIST

All graphical materials associated with this report are shown in the Table of Figures and Table of Tables.

REFERENCES

1. Evgenij Barsoukov, J. Ross Macdonald, Impedance Spectroscopy: Theory, Experiment, and Applications, 2nd Edition, March 2005, John Wiley & Sons, Inc.
2. ASTM C1202, “Standard Test Method for Electrical Indication of Concrete’s Ability to Resist Chloride Ion Penetration”
3. AASHTO T277, “Standard Method of Test for Rapid Determination of the Chloride Permeability of Concrete”
4. Whiting D ‘Permeability of Concrete,’ SP-108, American Concrete Institute, 1988, pp. 195–222.
5. Kupresan, Heathman, and Radonjic. “Experimental Assessment of Casing Expansion as a Solution to Microannular Gas Migration.” IADC/SPE 168056, 2014.

6. http://redpitaya.com/
7. Huang and Terentjev, "Dispersion of Carbon Nanotubes: Mixing Sonication, Stabilization, and Composite Properties", Polymers 2012, 4, p275-295
8. McCalister, "Gamma Ray Attenuation Properties of Common Shielding Materials," PG Research Foundation, Inc. 1955 University Lane Lisle, IL 60532, USA http://www.eichrom.com/PDF/gamma-ray-attenuation-white-paper-by-d.m.-rev-4.pdf
9. http://pandas.pydata.org/
10. http://jupyter.org/
11. K. Aulia, et al., "Resistivity behind Casing", Oilfield Review, Spring 2001
12. Federal Register, 2008, Environmental Protection Agency, Toxic Substance Control Act Inventory of Status of Carbon Nanotubes, Federal Register, Voume 73, No. 212, pp 64946-64947.
13. NIOSH, National Institute of Safety and Health, 2013. Current Intelligence Bulletin 65 Occupational Exposure to Nanotubes and Nanofibers, Department of Health and Human Services.

LIST OF ACRONYMS AND ABBREVIATIONS

AAS	Atomic Absorption Spectroscopy
AASHTO	American Association of State Highway and Transport Officials
AC	Alternating Current
ADC	Analog to Digital Converter
ANSI	American National Standards Institute
API	American Petroleum Institute
ASTM	American Section for Testing Materials
BP	Budget Period
C	Capacitive
CBL	Cement Bond Logging
CF	Carbon Fiber
CH	Calcium Hydroxide
CNT	Carbon Nano-Tube
CHFR	Cased-Hole Formation Resistivity
DC	Direct Current
DI	De-Ionized
DoD	Department of Defense
DoE	Department of Energy
DoT	Department of Transportation
EDX	Energy Dispersive X-ray
EIS	Electrical Impedance Spectroscopy
EKG	Electrocardiogram
EMAT	Electromagnetic Acoustic Transducer
EPA	Environmental Protection Agency
GOM	Gulf of Mexico
GF	Gauge Factor
GS	Gel Strength

ID	Inner Diameter
ISO	International Organization for Standardization
JIP	
LSU	Louisiana State University
MTS	Material Testing System
MWCNT	Multi-wall Carbon Nanotube
NCE	No Cost Extension
NETL	National Energy Technology Laboratory
NIOSH	National Institute for Occupational Safety and Health
NPT	National Pipe Thread
OD	Outer Diameter
O&G	Oil and Gas
OTC	Oilfield Testing and Consulting
P&A	Plug and Abandonment
PARSTAT	Potentiostat Galvanostat
PMP	Project Management Plan
R	Resistive
RF	Radio Frequency
SCP	Sustained Casing Pressure
SEM	Scanning Electron Microscopy
SNR	Signal to Noise Ratio
SOPO	Statement of Project Objectives
SWCNT	Single-wall Carbon Nanotube
TDR	Time Domain Reflectometry
TGA	Thermo-Gravimetric Analysis
TSCA	Toxic Substances Control Act
UV	Ultra-violet
WOC	Wait on Cement

APPENDICES

None.